論文 / 著書情報
Article / Book Information

題目(和文)	光反応性配向膜の光誘起異方性と重合性液晶の配向挙動に関する研究
Title(English)	Studies on photoinduced anisotropy of photoreactive materials in alignment layer and orientation behavior of polymerizable liquid crystals
著者(和文)	木村佑希
Author(English)	Yuki Kimura
出典(和文)	学位:博士(工学), 学位授与機関:東京工業大学, 報告番号:甲第10107号, 授与年月日:2016年3月26日, 学位の種別:課程博士, 審査員:扇澤 敏明,腰原 伸也,安藤 慎治,石川 謙,戸木田 雅利
Citation(English)	Degree:Doctor (Engineering), Conferring organization: Tokyo Institute of Technology, Report number:甲第10107号, Conferred date:2016/3/26, Degree Type:Course doctor, Examiner:,,,,
学位種別(和文)	博士論文
Type(English)	Doctoral Thesis

Doctoral Dissertation

Studies on photoinduced anisotropy of photoreactive materials in alignment layer and orientation behavior of polymerizable liquid crystals

Yuki KIMURA

Department of Chemistry and Materials Science

Graduate School of Science and Engineering

Tokyo Institute of Technology

March 2016

Table of contents

Chapter 1 General Introduction 1

1-1 Liquid Crystals and Liquid Crystal Displays 2

1-2 Alignment Method of Liquid Crystal 3

1-3 Objective of this thesis 9

Chapter 2 Photoalignment layer consisting of bisazides in polymer matrix 15

2-1 Abstract 16

2-2 Introduction 17

2-3 Experimental section 19

2-4 Results and Discussion 22

2-5 Conclutions 51

2-6 References 53

Chapter 3 Photoalignment layers containing bis(benzylidene)cyclohexanone unit 59

3-1 Abstract 60

3-2 Introduction 61

3-3 Experimental section 63

3-4 Results and Discussion 69

3-5 Conclusions 95

3-6 References 97

Chapter 4 Solvent-induced enrichment in PMMA/SQ-CI blend 101

4-1 Abstract..... 102

4-2 Introduction..... 103

4-3 Experimental section 106

4-4 Results and Discussion..... 109

4-5 Conclusions..... 134

4-6 References..... 136

Chapter 5 Anisotropic dewetting of polymerizable liquid crystals on a photoalignment layer. 142

5-1 Introduction..... 143

5-2 Introduction..... 144

5-3 Experimental section 144

5-4 Results and Discussion..... 147

5-5 Conclusions..... 160

5-6 References..... 161

Chapter 6 General Conclusions..... 163

Chapter 1

General Introduction

1-1 Liquid Crystals and Liquid Crystal Displays

Liquid crystals (LCs) were discovered by F. Reinitzer [1] in 1888 and identified by Lehmann.[2] The LCs are regarded as the forth state of substance, because the LCs have both a sort of crystalline order and liquidity. Liquid crystalline phases are mainly categorized into nematic, smectic and cholesteric liquid crystalline phases as shown in Figure 1. Nematic phase shows long-range order along an orientation direction (director ***n***) of LCs without order for center of mass (Figure 1 (a)). Smectic phase shows layers perpendicular to the director ***n*** and has many different varieties such as Smectic A (Figure 1 (b)), Smectic C which has a declined director ***n*** to the layer normal, Smectic B which resembles smectic A phase and has sixfold bond orientation order, and so on. Cholesteric phase (chiral nematic phase) shows nematic order in a plane and indicates that the director ***n*** changes in each layer with a helical pitch as shown in Figure (c). The LCs are also categorized as thermotropic and lyotropic LCs, which are liquid crystalline state depending on temperature and concentration of solute, respectively.

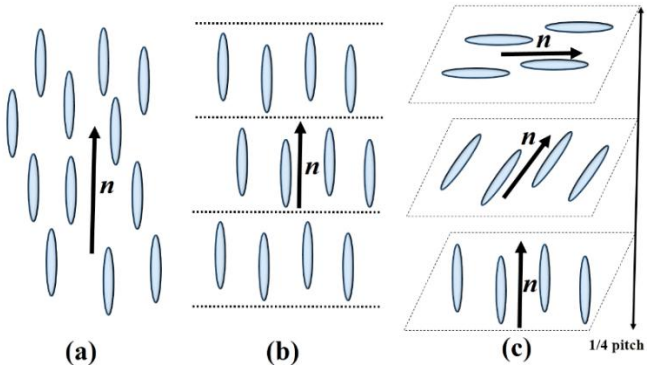

Figure 1. Schematic of liquid crystalline phases.
(a) nematic, (b) smectic (Sm A) and (c) cholesteric state.

In organic devices, liquid crystal displays (LCDs) utilizing nematic LCs are the most successful application until now. The LCDs have various display mode such as Twisted Nematic (TN), Super Twisted Nematic (STN), Multi-domain Vertical Alignment (MVA), Patterned-ITO Vertical Alignment (PVA), In-Plane Switching (IPS), Fringe-Field Switching (FFS). In addition, a lot of functional organic films are used as multi-layers in these devices such as a polarizer, a black matrix, a color filter, a protection layer, an alignment layer, a photo-spacer, an insulation layer and a retarder. Therefore, LCDs are "organic device" in the real sense of the term.

1-2 Alignment Method of Liquid Crystals

LCs spontaneously align in localized domains, but homogeneous alignment in wide area is not achieved without any treatments of substrate or external fields such as electric field, magnetic field and flow field. An uniform orientation of liquid crystals on the crystal surface was observed by Mauguin for the first time.[3-5] The substrate which contacts with LCs is usually treated by an alignment layer with a rubbing in order to give the alignment layer a sort of anisotropy. The orientation of LCs by alignment layers has been an attractive topic at least over the past 40 years. For the treatment of substrate by rubbing with soft materials [6] or by evaporated SiO_x film [7], the mechanism of aligning LCs was explained as a result of a minimization of elastic energy for LCs on the surface of alignment layer having a periodic groove by Berreman.[8] The periodic groove of alignment layer is several tens nanometers.[9, 10] Elastic energy of LCs is minimized by the orientation of LCs parallel to the groove patterns.

The rubbed polyimides have birefringence due to the orientation of polyimide chain by rubbing. The orientation of polyimide at the surface of the alignment layer was correlated to the orientation direction of LCs as reported by Geary et al. in 1987.[11]

Photoalignment of liquid crystals has also been investigated by many researchers. Ichimura et al. indicated that homeotropic-homogeneous transition of liquid crystals on azobenzene monolayer by the irradiation.[12] This fact is regarded as the first example of photo-induced alignment of liquid crystals.

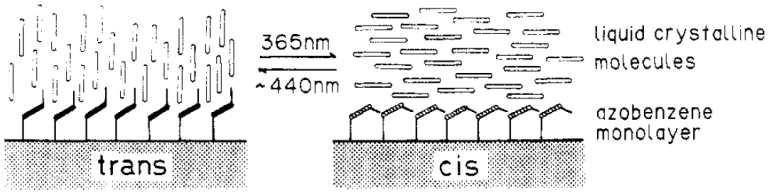

Figure 2. Schematic of homeotropic-homogeneous transition of liquid crystals by photoisomerization of azobenzene monolayer. [12]

The photoisomerization of azobenzene occurs reversibly by the irradiation of uvtraviolet-visible light. Azobenzene changes from trans-isomer to cis-isomer by the photoisomerization and the cis-isomer easily returns to the trans-isomer by visible light or thermal annealing. The trans-isomers of azobenzene lying along the direction of linearly polarized ultraviolet light (LPUVL) gradually decrease because trans-isomer parallel to the LPUVL is electronically excited repeatedly during the LPUVL irradiation. In the late stage of LPUVL irradiation, many trans-isomers are aligned to the direction perpendicular to the LPUVL by the photoisomerization as shown in Figure 3. This reorientation of azobenzne via the photoisomerization is called Weigert effect.[13-15] Many studies of azobenzene derivatives utilizing Weigert effect have been

reported.[16-24] In particular, the reorientation of liquid crystalline polymers containing azobenzene by photoisomerization and thermal annealing have been achieved without any alignment layer.[25-30] These polymers are studied as a photoalignment layer, a coatable retarder and a polarizer for LCDs.

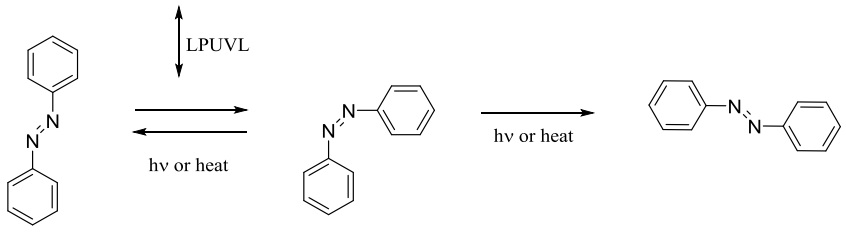

Figure 3. Schematic of Weigert effect for azobenzene.

Kvasnikov et al. have reported the anisotropy induced by the axis-selective photoreaction. They showed that birefringence was generated in poly(vinyl cinnamate) by irradiating of linearly polarized ultraviolet light (LPUVL).[31] Schadt et al. showed that the control of orientation direction of nematic LCs was performed by LPUVL-irradiated poly(vinyl cinnamate)[32] and some researches have investigated cinnamate derivatives in recent decades.[33-38] As is the case in azobenzene, the reorientation of liquid crystalline polymers containing cinnamate unit have been achieved by LPUVL irradiation and thermal annealing.[39-42]

The mechanism of photoinduced anisotropy of poly(vinyl 4-methoxy cinnamate) (PVMC) was proposed by Schadt et al. PVMC is photoreacted by the ultraviolet ray around 300 nm. Although phtoproducts of cinnamoyl group generally include photoisomerization and photodimerization in Figure 4, the photoreaction of PVMC mainly results in the dimer via [2+2] cycloaddition between cinnamoyl groups. In addition, the LPUVL give an axis-selective photodimerization as shown in Figure 5.

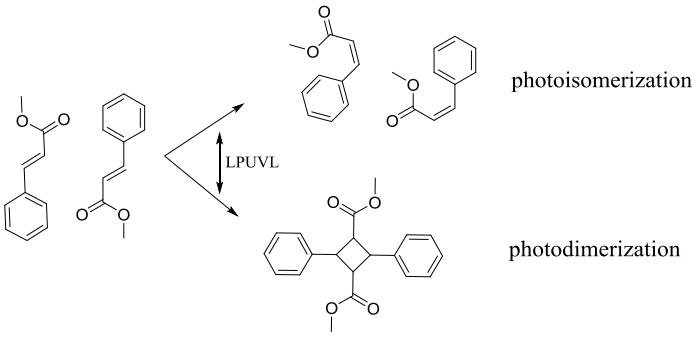

Figure 4. Schematic of photoreaction of cinnamate.

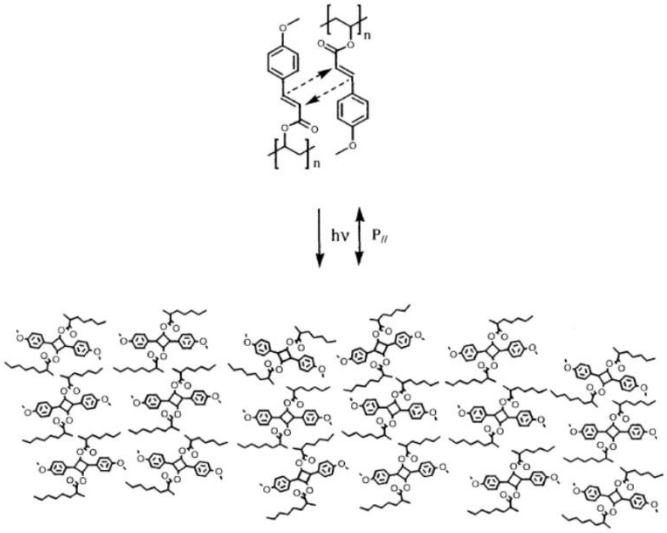

Figure 5. Schematic of axis-selective photodimerization of PVMC. [32]

Schadt et al. showed that coumarin derivatives were also able to align LCs by LPUVL irradiation.[43] The photoreaction of coumarin included only [2+2] photodimerization between coumarins (Figure 6). Coumarin derivatives have also been investigated by various authors.[44-50]

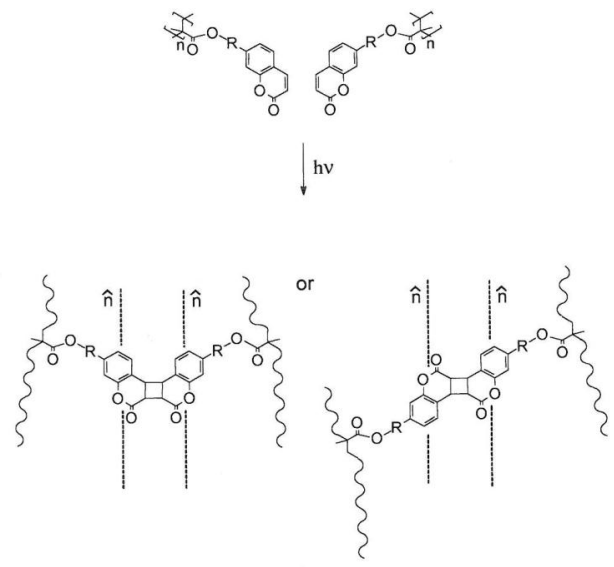

Figure 6. Schematic of photodimerization of polymer containing coumarin unit. [43]

Makita et al. investigated polymers containing chalcone unit for photoalignment layer [51], and some reports by other authors have been done.[52-56] The photoreaciton of chalcone derivatives is photoisomerization and photodimerization as with the case of cinnamate as shown in Figure 7. The photoalignment via axis-selective photodegradation has been reported for various polymers in Figure 8.[57-60] In addition to the above, the studies of other photoalignment methods exists such as polymers containing anthracene at its side chain[61] (Figure 9), polyimide containing stilbene unit in the main chain [62] and polymethacrylate containing stilbene with liquid crystalline side chains [63] (Figure 10), and the photoalignment through the use of photo-Fries rearrangement [64-67] (Figure 11).

Some helpful reviews for photoalignment method are included on a list of references.[68-74]

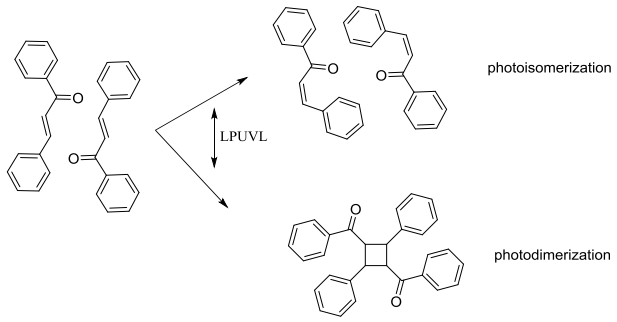

Figure 7. Schematic of photoreaction of chalcone unit.

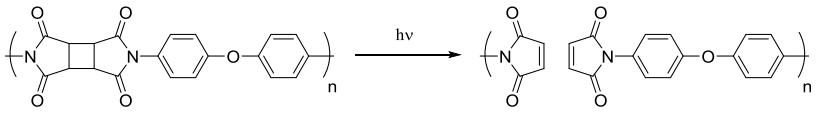

Figure 8. Schematic of photoalignment via photodegradation.

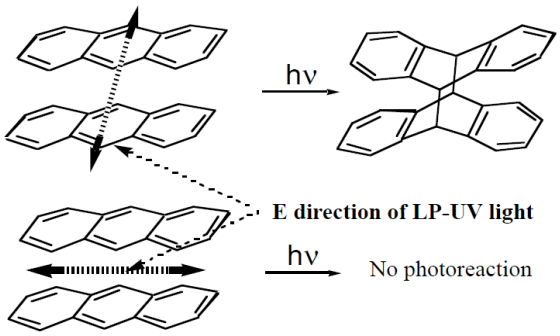

Figure 9. Schematic of photodimerization of anthracene unit. [61]

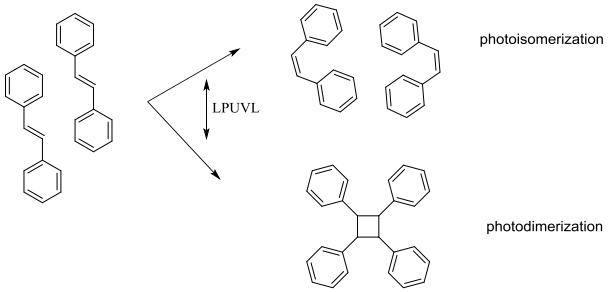

Figure 10. Schematic of photodimerization of stilbene unit.

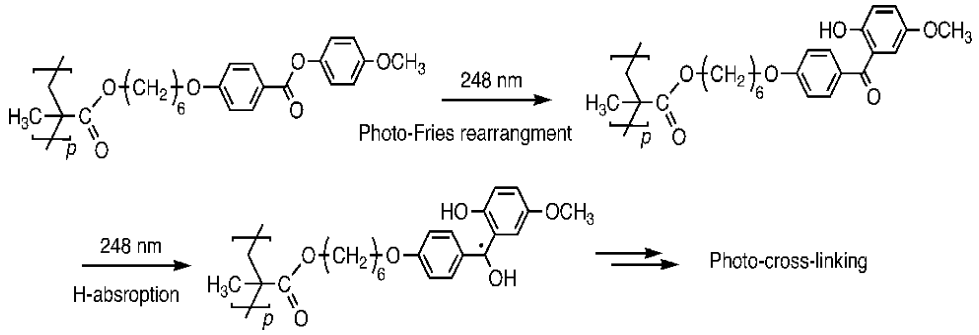

Figure 11. Schematic of photo-Fries rearrangement.[66]

1-3 Objective of this thesis

Despite much investigation, the photoalignment methods have been rarely applied to liquid crystal displays due to the insufficiency of long-term reliability and low anchoring energies, compared with alignment layer of polyimides prepared by rubbing method.

On the other hand, polymerizable liquid crystals (PLCs), such as acrylate-terminated liquid crystals, which has large birefringence derived from the oriented mesogens have been reported and investigated for use as coatable retarders and polarizers.[75-79] The thermal stability of the oriented PLCs results from the formation of three-dimensional cross-linkages by photo-radical reaction. In the applications, PLCs are cross-linked by photo-radical polymerization immediately after orientation on the alignment layer. Therefore, the photoalignment layer is not required to maintain long-term reliability and strong anchoring of the liquid crystals, but is needed to enhance photo-sensitivity i.e., short-time irradiation of LPUVL in order to achieve high-throughput in manufacturing process. From this standpoint, the photoalignment method is suitable for applications using PLCs.

In this study, we investigated the photoinduced alignment behavior of PLCs using photoreactive materials of bisazide, bis(benzylidene)cyclohexanone and citraconimide. Our purposes are to reveal the mechanism of photoalignment (Chapter 2, 3, 4), to achieve the unification of two functional layers for a photoalignment and protection layers in liquid crystal displays (Chapter 4), and to elucidate the mechanism of dewetting phenomena of PLC thin film in order to understand the stability of thin film (Chapter 5).

References

[1] F. Reintzer. *Monatshefte*. **1888**, 9, 421.

[2] O. Rehmann. Z. Physik. Chem. 1889, 4, 462.

[3] C. Mauguin. *Bull. Soc. Fr. Min.* **1911**, 34, 6-15.

[4] C. Mauguin. *Bull. Soc. Fr. Min.*, **1911**, 34, 71-117.

[5] C. Mauguin. *Phys. Z.* **1911**, 12, 1011-1015.

[6] H. E. W. Zocher, K. Cooper. *Z. Phys. Chem. Bd.* **1928**, 132, S295.

[7] J. L. Janning. *Appl. Phys. Lett.* **1972**, 21, 173.

[8] D. W. Berremann. *Phys. Rev. Lett.* **1972**, 28, 1683.

[9] H. E. W. Zocher. *Ministerio da Agricultura, Brasil Boletim* **1947**, 26, 12.

[10] J. Cognard. *Mol. Cryst. Liquid Cryst.* **1982**, A 5, 1.

[11] J. M. Geary, J. W. Goody, A. M. Kmetz et al. *J. Appl. Phys.* **1987**, 62, 4100.

[12] K. Ichimura, Y. Suzuki, T. Seki, et al. *Langmuir.* **1988**, 4, 1214 .

[13] F. Weigert. *Verh. Deutsch. Phys. Ges.***1919**, 21, 479-483.

[14] F. Weigert. *Ann. Phys.* **1920**, 63, 681-725.

[15] F. Weigert. *Z. Phys.* **1920**, 2, 1-12.

[16] W. M. Gibbons, P. J. Shannon, S-T. Sun, et al. *Nature*, **1991**, 351, 49-50.

[17] H. Akiyama, M. Momose, K. Ichimura. *Macromolecules*. **1995**, 28, 288-293.

[18] B. Park, Y. Jung, H-H. Choi, et al. *Jpn. J. Appl. Phys*. **1998**, 37, 5663-5668.

[19] C. Ruslim, K. Ichimura. *Macromolecules*. **1999**, 32, 4254-4263.

[20] K. Fukuda, T. Seki, K. Ichimura. *Macromolecules*. **2002**, 35, 2177-2183.

[21] K. Fukuda, T. Seki, K. Ichimura. *Macromolecules*. **2002**, 35, 1951-1957.

[22] E. Pozhidaev, V. Chigrinov, D. Huang, et al. *Jpn. J. Appl. Phys*. **2004**, 43, 5440-5446.

[23] S. Furumi, M. Kidowaki, M. Ogawa, et al. J. Phys. Chem. B. 2005, 109, 9245-9254.

[24] A. Bobrovsky, A. Ryabchun, V. Shibaev. *J. Photochem. Photobiol. A Chem.***2011**, 218, 137-142.

[25] J. Stumpe, L. Läsker, Th. Fischer, et al. *Thin Solids Films*. **1996**, 284-285, 252-256.

[26] L. Cui, Y. Zhao. *Macromolecules*. **2003**, 36, 8246-8252.

[27] L. Cui, Y. Zhao. *Macromolecules*. **2003**, 36, 8246-8252.

[28] N. Kawatsuki, E. Uchida, H. Ono. Chem. Lett. 2004, 33, 12-13.

[29] K. Sakamoto, K. Usami, M. Kikegawa et al. *J. Appl. Phys.* **2003**, 93, 1039.

[30] K. Sakamoto, K. Usami, T. Sasaki, et al. *Jpn. J. Appl. Phys.***2006,** 45, 2705-2707.

[31] E. D. Kvasnikov, V. M. Kozenkov, V. A. Barachevsky. *Zh.Nauchn. Prikl. Hotogr. Kinegatogr*. **1979**, 24, 222.

[32] M. Schadt, K. Schmidt, V. Koznkov, et al. *Jpn. J.Appl. Phys.***1992**, 7, 2155.

[33] T. Marusii, Y. Reznikov, D. Voloshchenko, et al. *Mol. Cryst. Liq. Cryst*. 1994, 251, 209-218.

[34] H. Tomita, K. Kudo, K. Ichimura. *Liq. Cryst*. **1996**, 20, 171-176.

[35] S. Song, M. Watabe, T. Adachi, et al. *Jpn. J. Appl. Phys.* **1998**, 37, 2620.

[36] K. Ichimura, Y. Akita, H. Akiyama, et al. *Jpn. J. Appl. Phys*. **1996**, 35, L992-L995.

[37] M. Obi, S. Morino, K. Ichimura. *Jpn. J. Appl. Phys*. **1999**, 38, L145-L147.

[38] K. Maeshima, S. Song, M. Watabe, et al. *J. Photopolym. Sci. Technol.* **1999**, 12, 249-250.

[39] N. Kawatsuki, H. Ono, H. Takatsuka, et al. *Macromolecules*. **1997**, 30, 6680-6682.

[40] N. Kawatsuki, K. Goto, T. Kawakami, et al. *Macromolecules*. **2002**, 35, 706-713.

[41] N. Kawatsuki, K. Hamano, H. Ono, et al. *Jpn. J. Appl. Phys.* **2007**, 46, 339-341.

[42] H. Ono, T. Sasaki, N. Kawatsuki. *Jpn J Appl Phys* **2008**, 47, 1642-1646.

[43] M. Shcadt, H. Seiberle , A. Schuster. *Nature*. **1996**, 381, 212-215.

[44] M. Obi, S. Morino, K. Ichimura. *Macromol. Rapid Commun.* **1998**, 19, 643-646.

[45] M. Obi, S. Morino, K. Ichimura. *Chem. Mater*. **1999**, 11, 656-664.

[46] P. O. Jachson, M. O'Neill. *Chem. Mater*. **2001**, 13, 694-703.

[47] C. Kim, A. Trajkovska, J. U. Wallace, et al. *Macromolecules*. **2006**, 39, 3817-3823.

[48] A. Trajkovska, C. Kim, K. L. Marshall, et al. *Macromolecules*. **2006**, 39, 6983-6989.

[49] C. Kim, J. U. Wallace, A. Trajkovska, et al. *Macromolecules*. **2007**, 40, 8924-8929.

[50] C. Kim, J. U. Wallace, S. H. Chen, et al. *Macromolecules*. **2008**, 41, 3075-3080.

[51] Y. Makita, T. Natsui, S. Kimura, et al. J. Photopolym. Sci. Technol. **1998**, 11, 187-192.

[52] M. Kimura, S. Nakata, Y. Makita, et al. *Jpn. J. Appl. Phys*. **2001**, 40, L352-L354.

[53] B. Chae, SW. Lee, M. Ree, et al. *Vib. Spectrosc.* **2002,** 29, 69-72.

[54] L. Zhang, Z. Peng, L. Yao, et al. *J. Mater. Chem.* **2007**, 17, 3015.

[55] T. Mihara. *Mol. Cryst. Liq. Cryst.* **2005**, 441, 185-200.

[56] X-D. Li, Z-X. Zhong, SH. Lee, et al. *Jpn. J. Appl. Phys.* **2006**, 45, 906-908.

[57] M. Hasegawa. *Jpn. J. Appl. Phys.* **2000**, 39, 1272-1277.

[58] M. Nishikawa, J. L. West, Y. Reznikov. *Liq. Cryst*. **1999**, 26, 575-580.

[59] S. Nespurek, Y. Zakrevskyy, J. Stumpe, et al. *Macromolecules* **2006**, 39, 690-696.

[60] O. Yaroshchuk, A. Kadashchuk. *Appl. Surf. Sci.* **2000**, 158, 357-361.

[61] N. Kawatsuki, T. Arita, T. Kawakami, et al. *Jpn. J. Appl. Phys.* **2000**, 39, 5943-5946.

[62] SG. Hahm, SW. Lee, TJ. Lee, et al. *J Phys Chem B.* **2008**, 112, 4900-4912.

[63] R. Giménez, M. Piñol, J. L. Serrano, et al. *Polymer*. **2006**, 47, 5707-5714.

[64] V. Kyrychenko, G. Smolyakov, V. Zagniy, et al. *Mol. Cryst. Liq. Cryst.* **2008**, 496, 278-292.

[65] L. Vretik, L. Paskal, V. Syromyatnikov, et al. *Mol. Cryst. Liq. Cryst.* **2007**, 468, 173-179.

[66] N. Kawatsuk, H. Matsushita, T. Washio, et al. *Macromolecules.* **2012**, 45, 8547-8554.

[67] N. Kawatsuki, T. Neko, M. Kurita, et al. *Macromolecules.* **2011**, 44, 5736-5742.

[68] K. Ichimura. *Chem. Rev.* **2000**, 100, 1847-1873.

[69] M. O'Neill, SM. Kelly. *J. Phys. D Appl. Phys.* **2000**, 33, R67-84.

[70] J. Hoogboom, JAAW. Elemans, T. Rasing, et al. *Polym. Int.* **2007**, 56, 1186-1191.

[71] N. Kawatsuki. *Chem. Lett.* **2011**, 40, 548-54.

[72] O. Yaroshchuk, Y. Reznikov. *J. Mater. Chem.* **2012**, 22, 286.

[73] T. Seki, S. Nagano, M. Hara. *Polymer*. **2013**, 54, 6053-6072.

[74] T. Seki. *Macromol. Rapid Commun*. **2014**, 35, 271-290.

[75] M. Schadt, H. Seiberle, A. Schuster, et al. *Jpn. J. Appl. Phys. Part 1*.**1995**, 34, 3240-3249.

[76] M. Schadt, H. Seiberle, A. Schuster, et .al. *Jpn. J. Appl.Phys. Lett.* **1995**, 34, 764-767.

[77] D. J. Broer, J. Boven, G. N. Mol, et al. *Makromol. Chem.* **1989**, 190, 2255-2268.

[78] D. J. Broer, R. A. M. Hikmet, G. Challa. *Makromol. Chem.* **1989**, 190, 3201-3215.

[79] D. J. Broer, G. N. Mol, G. Challa. *Makromol. Chem.* **1991**, 192, 59-74.

Chapter 2

Photoalignment layer consisting of bisazides in polymer matrix

2-1. Abstract

Photo-reactive bisazides in a polymer matrix containing acryloyl groups on the side chain were investigated as a photo-alignment layer for polymerizable liquid crystals (PLC). We found the thin film of polymer/bisazide blend, irradiated by linearly polarized ultraviolet light (LPUVL), was able to homogeneously align PLC. The LPUVL irradiation dose changed the orientation direction of the PLC on the thin film of 2,6-bis(4-azidobenzylidene)-4-methyl-1-cyclohexanone in the polymer matrix. Furthermore, only control of the irradiation dose achieved in-plane switching (change in the orientation direction of liquid crystals from parallel to perpendicular to the LPUVL in a plane). The direction of the slow axis for the retardation of the photo-alignment layer changed from parallel to perpendicular to the LPUVL electric field with changes to the irradiation dose. Therefore, the PLC was likely to be aligned along the slow axis of the retardation of the photo-alignment layer. We concluded that the key mechanism that changed the direction of the slow axis in a plane was the photoreaction of azide–acrylate at low irradiation doses and that of bis(benzylidene)cyclohexanone at high irradiation doses. The photo-alignment as a result of a simple photo cross-linking were previously little known, except in the case of photo-dimerization.

2-2. Introduction

The rubbing or photo-alignment process in the alignment layer is needed to control the orientation direction of liquid crystals and to align liquid crystals uniformly. In particular, studies of the photo-alignment process are required to obtain defect-free alignment of liquid crystals and achieve dust-free processing. For these reasons, a number of studies have been performed using polymers containing photo-reactive units such as cinnamate, chalcone, coumarin and azobenzene in the side or main chains of polymers.[1-7] These polymer films enable liquid crystals to align homogeneously by irradiation of linearly polarized ultraviolet light (LPUVL). Previous research has shown that photo-isomerization and photo-dimerization creates the anisotropic surface of the photo-alignment layer such as cinnamate, chalcone, coumarin and azobenzene. [1-4] In contrast, acryl-terminated liquid crystals, known as polymerizable liquid crystals (PLC), that have large birefringence derived from oriented rigid mesogens have been reported and investigated for coatable retardation and polarization.[8-12] In these applications, the photo-polymerization of the PLC using a photo-radical generator is executed directly following the orientation on the photo-alignment layer. It is not important for the photo-alignment layer to reliably achieve long-term anchoring of liquid crystals, but high sensitivity is required, i.e., only a low irradiation dose of LPUVL need be applied

to achieve high throughput in the manufacturing process. Therefore, the photo-alignment method is compatible with the applications using PLC.

In addition, several studies have considered methods for controlling the orientation direction of PLC to obtain a patterned orientation of the crystals. Initial evidence was shown of switching of the orientation direction of low molecular weight liquid crystals from homeotropic to homogeneous alignment on a mono-layer of azobenzene by irradiation at 365 nm.[13] The polymers containing azobenzene on the side-chain switched from out-of-plane to in-plane orientation.[14, 15] In-plane switching of the orientation by an irradiation dose, using photoreactive side-chain liquid crystalline polymers with cinnamoyl group by the LPUVL irradiation and an annealing of the film, has also been reported.[16, 17] Studies have also found in-plane switching of low molecular weight liquid crystals on polymer thin films containing coumarin or cinnamoyl groups by a LPUVL irradiation dose [18, 19]. In the case of side-chain liquid crystalline polymers, the polymer film must be annealed at high temperature after the LPUVL irradiation to switch the orientation direction. Although the photo-alignment layer with a coumarin or cinnamoyl group require only LPUVL irradiation to achieve in-plane switching of low molecular weight liquid crystals, these materials have a problem of a low degree of orientation of the liquid crystals.

In this study, we investigated a photo-induced alignment for PLC using photo-reactive bisazide molecules in a polymer matrix containing an acryloyl group in the side chain of the polymer. The main purpose of this study was to achieve the in-plane switching of low molecular weight liquid crystals at highly-ordered alignment on the photo-alignment layer using only an irradiation dose.

2-3. Experimental section

Materials

2,6-bis(4-azidobenzylidene)-4-methyl-1-cyclohexanone (bisABmC) and 2,6-bis(4-azidophenyl) methane (bisAPM) were obtained from TOYO GOSEI Co., Ltd (Figure 1(a)). As a polymer matrix of alignment layer, GH-1203 (Figure 1(d)) was obtained from Shin-Nakamura Chemical Co., Ltd, an acrylic polymer containing acryloyl groups on the side chain. The weight-average molecular weight of GH-1203 is 13000. 1,6-hexanediol diacrylate, cyclopentanone and toluene were purchased from Tokyo Chemical Industry Co., Ltd. Dimethyl 2,2’-azobis(2-methylpropionate) (V-601) was purchased from Wako Pure Chemical Industries, Ltd. As di-functional and mono-functional PLCs, LC242 (Figure 1(b)) and CBHA (Figure 1(c)) were obtained from BASF Japan Ltd. and JNC Petrochemical Corp., respectively. A surfactant

(Byk361N) was obtained from Big Chemie Co. Ltd. These materials were used without further purification.

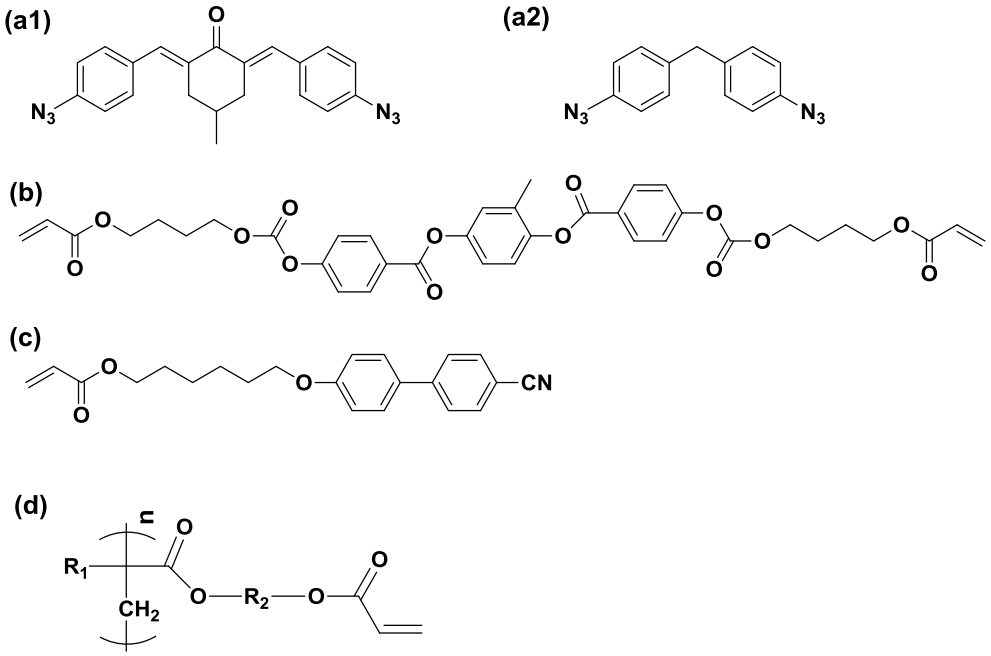

Figure 1. Chemical structures of (a1) bisABmC, (a2) bisAPM, (b) LC242, (c) CBHA, and (d) GH-1203 (R_1 and R_2 are not disclosed).

Preparation of PLC solution

The sample preparation of PLC was as follows. As PLC, a mixture of 1.000 g of LC242 (1.42 mmol) and 0.4948 g of CBHA (1.42 mmol) was diluted by 13.99 g of toluene with 0.0448 g of photo-radical generator (Irgacure 907) and 0.0149 g of surfactant (Byk-361N). The PLC solution was finally filtered through a polytetrafluoroethylene membrane filter (average pore size : 0.2 μm).

Measurements

The thin film, which consisted of photo-alignment layer and PLC layer, was prepared by a spincoater (1H-DX, Mikasa Co., Ltd.) on a glass substrate (40 mm square, 0.7 mm thickness, EagleXG, Corning Inc.). Film thicknesses were measured by an ellipsometer (SA-101, Photonic Lattice Inc.) and a profilometer (alpha-step P-16, KLA-Tencol Corp.). After spincoating, the films were dried off on a hot-plate. The LPUVL was provided by a xenon lamp (300 W) with an Al wire-grid polarizer and a cut-filter below 300 nm to irradiate the sample film.

An ultraviolet-visible-near infrared (UV-vis-NIR) spectrometer (V-7200, Jasco. Co., Ltd.) was used for evaluation of both polarized and non-polarized UV-vis spectra. A polarized optical microscope (BX60, Olympus Corp.) was used for morphological observation of samples. The changes of polymer/bisazide blend by the irradiation or the thermal treatment were measured by Infrared spectroscopy (FT/IR6110FF, Jasco. Co., Ltd.). Retardation of the thin films was measured using the photo-elastic modulation method. Gel permeation chromatography measurements were carried out on a Shimadzu prominence system equipped with polystyrene gel columns, using tetrahydrofran as an eluent after calibration with polystyrene standards.

Calculations

Density functional theory (DFT) calculations for model compounds were executed using Gaussian09 Revision D.01 (Gaussian Inc.).[20] Geometrical optimization and polarizability calculations were performed by B3LYP hybrid functional, which employs the Becke exchange and LYP correlation functions [21] and a Gaussian basis set of 6-311++G(d,p). In addition, the calculation of the excited state was executed using the time-dependent DFT (TD-DFT) method in CAM-B3LYP functional.[22]

2-4. Results and Discussion

Photo-induced alignment of PLC on bisazide thin film

To evaluate the photo-alignment behavior of PLC on bisazide itself, a 5.0 wt% solution of bis-ABmC in cyclopentanone was spincoated on a glass substrate and dried on a hot-plate at 80°C for 5 min. After the dry-baking, the film thickness of the sample measured by the profilometer was approximately 50 nm.

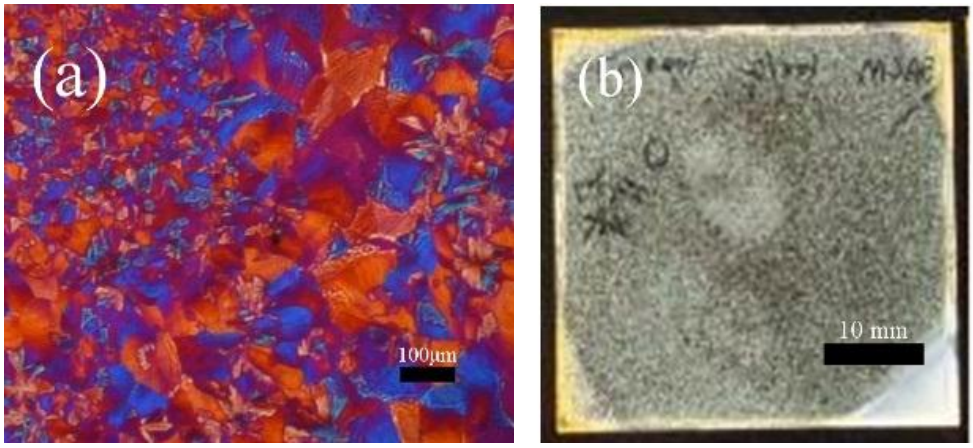

Figure 2. (a) Polarized optical microscope image of bisABmC on a glass substrate with sensitive color plate (530 nm) and (b) image of PLC on bisABmC polycrystalline thin film under crossed Nicol.

As shown in Figure 2(a), the thin film of bisABmC was polycrystalline. Irradiation of this polycrystalline thin film by LPUVL did not induce uniform orientation of PLC over a wide area. This was because a monodomain orientation of the PLC was not achieved on the localized polycrystalline domains of bisABmC with various orientation directions for each domain (Figure 2(b)).

Photo-induced alignment of PLC on polymer/bisABmC blend film

To avoid crystallization of bisABmC at room temperature, we blended bisABmC with several types of polymers (poly(methyl methacrylate), poly(butyl methacrylate), poly(2-hydroxyethyl methacrylate), or polystyrene). Although thin films composed of a

5 or 10 phr (parts per hundred resin) in GH-1203 were not cystalized, these thin films were unable to align the PLC. We next blended bisABmC with a acryloyl polymer containing an acryloyl group on the side chain (GH-1203), in expectation of a photoreaction between azide and the acryloyl group. The thin films of the GH-1203/bisABmC blend were formed in the same way as those of bisABmC. When the composition was GH-1203/bisABmC (100/5 phr), no aggregates were observed under the polarized optical microscope after dry-baking at 80°C for 2 min (Figure 3 (a) and (b)). However, the composition GH-1203/bisABmC (100/20) showed the acicular crystalline aggregates after dry-baking (Figure 3(d)). In the GH-1203 matrix, bisABmC was precipitated and crystallized at high concentrations of bisABmC.

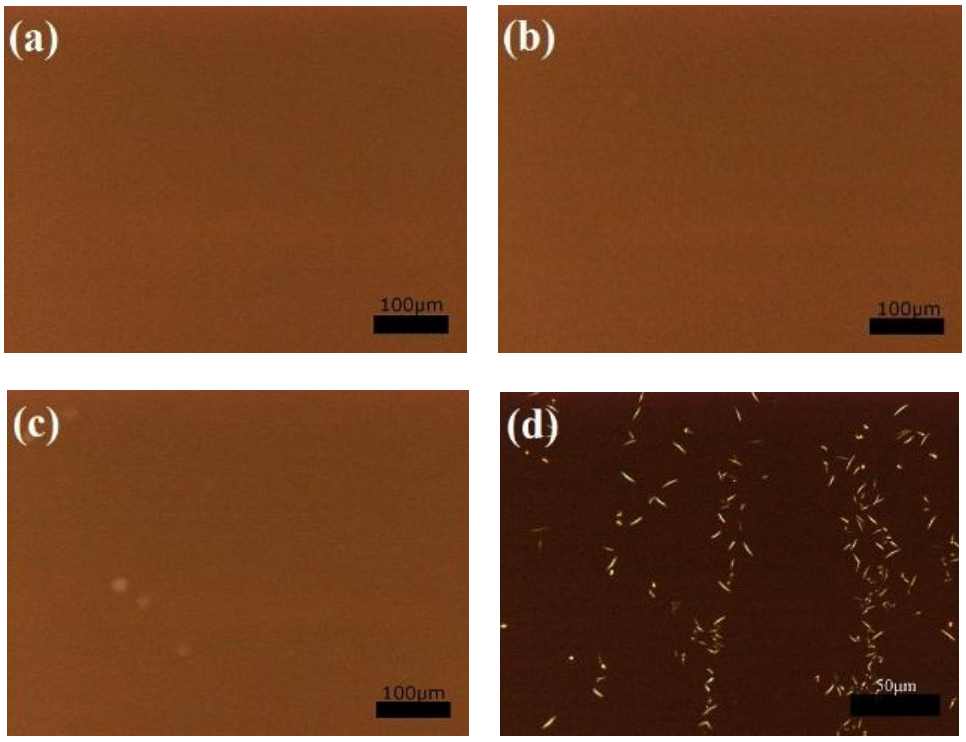

Figure 3. Polarized optical microscope images of GH-1203/bisABmC; (a) 100/5 spincoated at 1500 rpm for 20 s, (b) dry-baking at 80°C for 2 min after (a), (c) 100/20 spincoated at 1500 rpm for 20 s and (d) dry-baking at 80°C for 2 min after (c).

To evaluate the photo-induced alignment of the PLC on GH-1203/bisABmC blend film, the thin film of GH-1203/bisABmC (100/5) was formed by spin-coating and soft-baking at 80°C for 2 min to allow evaporation of the solvent. The thin film was irradiated by LPUVL for 5 s. Subsequently, PLC solution was spincoated on the photo-alignment film. The samples were soft-baked at 60°C for 1 min and quenched to room temperature. Next, the sample was photo-cured for 20 s in a nitrogen atmosphere at room temperature. Polarized optical microscope observations confirmed monodomain

homogeneous alignment of the PLC. The polarized UV-vis spectra of the PLC thin film showed a clear difference between the spectra parallel and perpendicular to the LPUVL electric field (Figure 4). The peak at 297 nm was attributed to the absorption of cyanobiphenyl group of CBHA, which was calculated by the TD-DFT and the direction of transition dipole moment was parallel to the long axis of cyanobiphenyl. At a low irradiation dose, the PLC aligned parallel to the LPUVL electric field (Figure 4(a)); however, the PLC aligned perpendicular to the LPUVL at a high irradiation dose (Figure 4(b)).

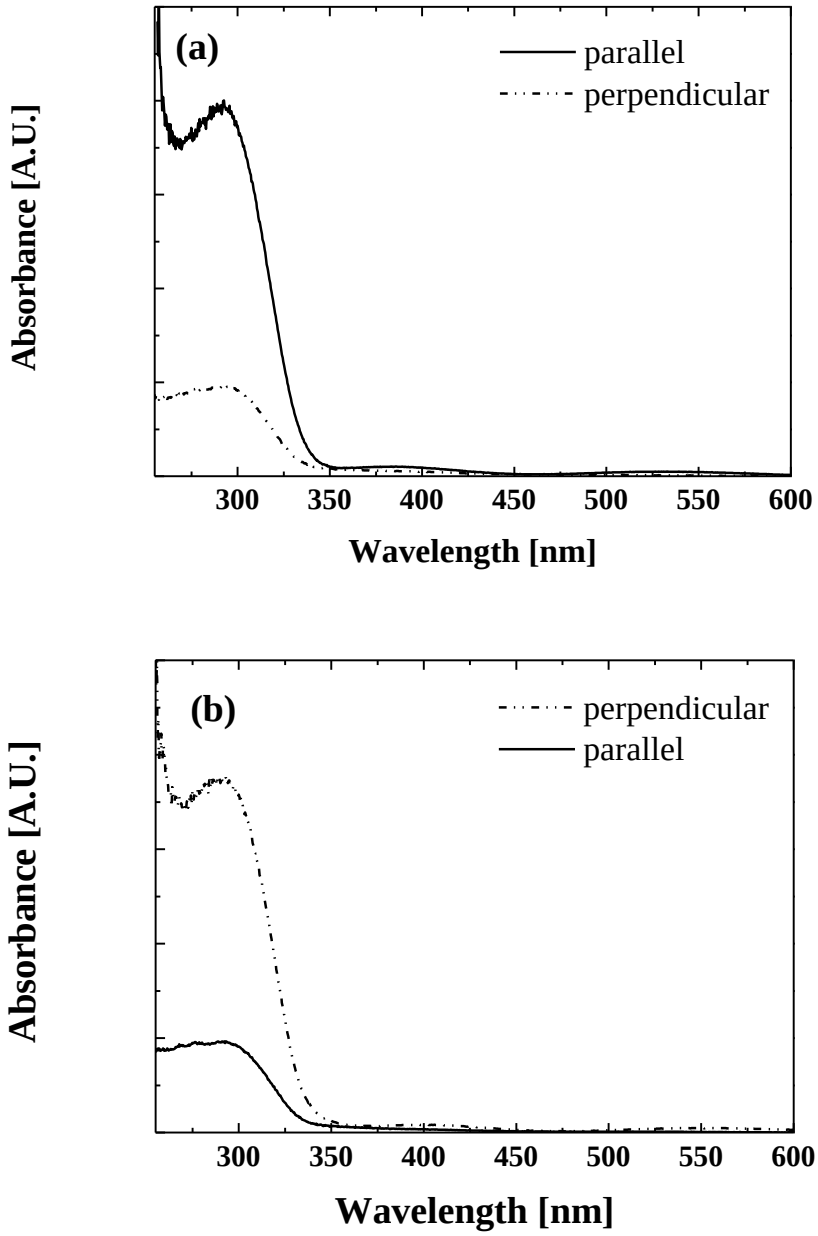

Figure 4. Polarized UV-vis spectra of PLC on the thin film of GH-1203/bisABmC (100/5) irradiated for (a) 5 s and (b) 60 s after the photo-curing of PLC.

Irradiation dose dependence of the order parameter

To clarify the irradiation dose dependence of PLC, we estimated an order parameter on the thin film of GH-1203/bisABmC (100/5) using polarized UV-vis spectroscopy. The order parameter of the PLC (S) was calculated using the peak height at 297 nm as follows:

$$S = \frac{A_{\parallel} - A_{\perp}}{A_{\parallel} + 2A_{\perp}}$$

where $A_{\parallel}$ and $A_{\perp}$ are the absorbances parallel to and perpendicular to LPUVL electric field, respectively. For GH-1203/bisABmC (100/5), we estimated the order parameter of the PLC using polarized UV-vis spectra with the irradiation dose (Figure 5). At low irradiation doses, the PLC was aligned along the direction parallel to LPUVL electric field. However, the order parameter of the PLC decreased with increasing irradiation dose, and a sign inversion of S occurred at an irradiation time between 15 and 30 s. Interestingly, at high irradiation doses, the PLC was once more well-aligned along the direction perpendicular to LPUVL electric field. This phenomenon may be considered to be in-plane switching of the PLC orientation direction.

To reveal the mechanisms behind the switching, we substituted bisABmC for a simple bisazide with no reactive unit without azide groups (bisAPM). We added 10 phr of

bisAPM into GH-1203, because the PLC on a thin film prepared by GH-1203/bisAPM (100/5) was not aligned.

The order parameter of the PLC on the thin film composed of GH-1203/bisAPM (100/10) showed a positive value throughout the irradiation (Figure 6(a)). To remove the influence of the azide group in the GH-1203/bisABmC system, the thin film composed of GH-1203/bisABmC (100/5) was thermally-cured at 80°C for 25 min before the LPUVL irradiation to complete the reaction of azide with the acryloyl group.[23] The disappearance of the azide group after baking for 25 min was confirmed by FT-IR spectroscopy. As shown in Figure 6(b), the order parameter of the PLC was negative throughout the irradiation. These results indicate that the photo-reaction of the azide group induced the orientation of the PLC parallel to the LPVUL electric field. In addition, photo-reaction of the bis(benzylidene)cyclohexanone (bisBC) unit in bisABmC also played an important role in the orientation of PLC perpendicular to the LPUVL electric field. Therefore, some competitive photo-reaction must have occurred at low irradiation regions.

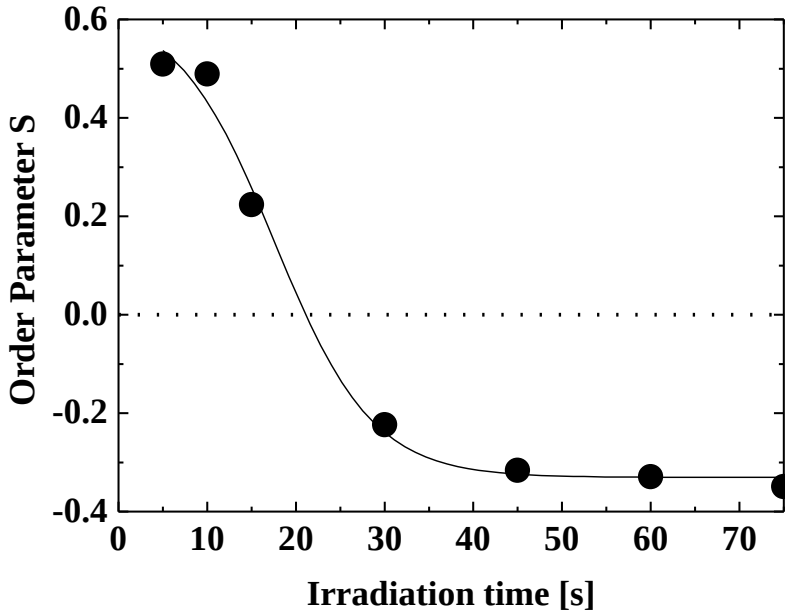

Figure 5. Irradiation dose dependence of the PLC order parameter on GH-1203/bisABmC (100/5) thin film after baking at 80°C for 2 min.

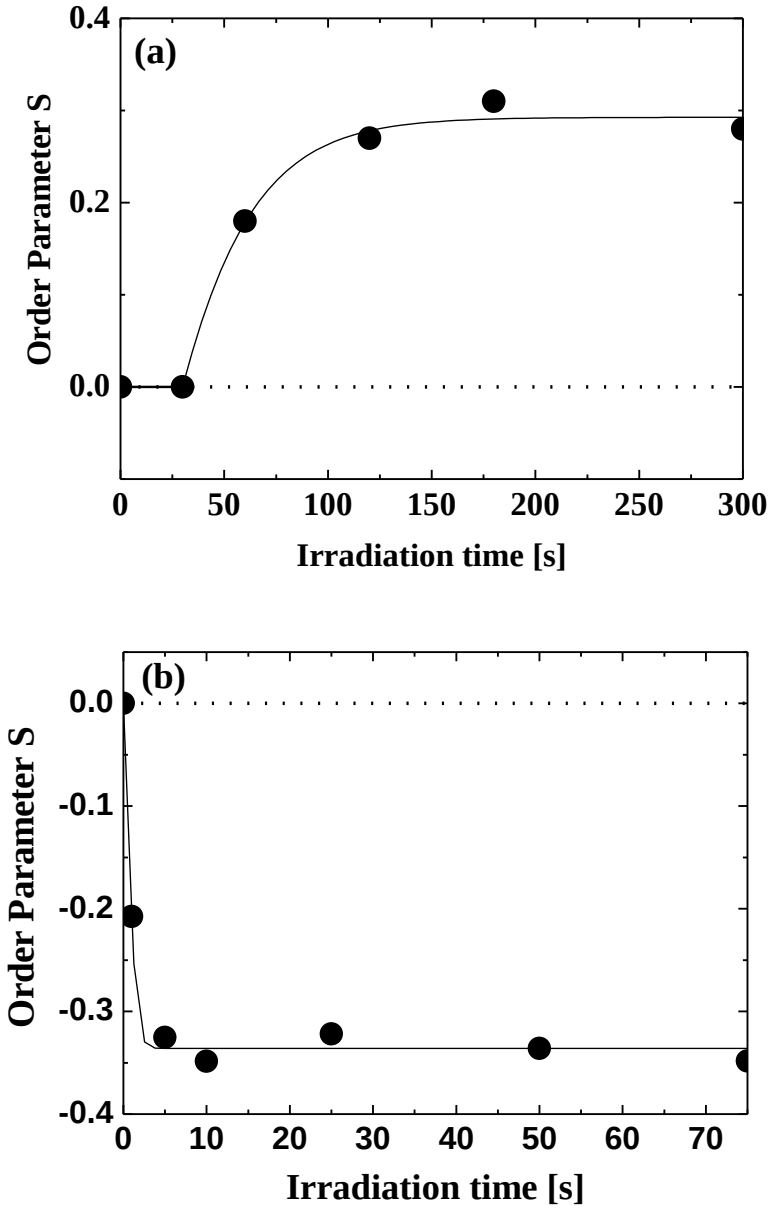

Figure 6. LPUVL irradiation dose dependence of PLC order parameter on (a) GH-1203/bisAPM (100/10) baked at 80°C for 25 min and (b) GH-1203/bisABmC (100/5) baked at 80°C for 25 min.

Thermal reaction and aggregate of bisABmC in GH-1203

To confirm the mixture state of bisABmC in GH-1203, we measured the UV-visible absorption spectrum of 1.0×10^{-3} wt% of bisABmC in acetonitrile and those of GH-1203/bisABmC (100/25, 100/20, 100/15, 100/10, and 100/5) in Figure 7. The absorption maximum of bisABmC in acetonitrile was located at 353 nm. This peak is likely to be associated with single molecule of bisABmC because the concentration of bisABmC is quite low. The absorption spectra of GH-1203/bisABmC thin films after the baking at 80°C for 2 min are shown in Figure 7 (b). The absorption maximum of bisABmC in a polymer matrix was at 374 nm in the case of GH-1203/bisABmC (100/5) baked at 80°C for 2 min. Comparison with Figure 7 (a) shows that the peak position of bisABmC shifted to longer wavelengths even at 5 phr of bisABmC.

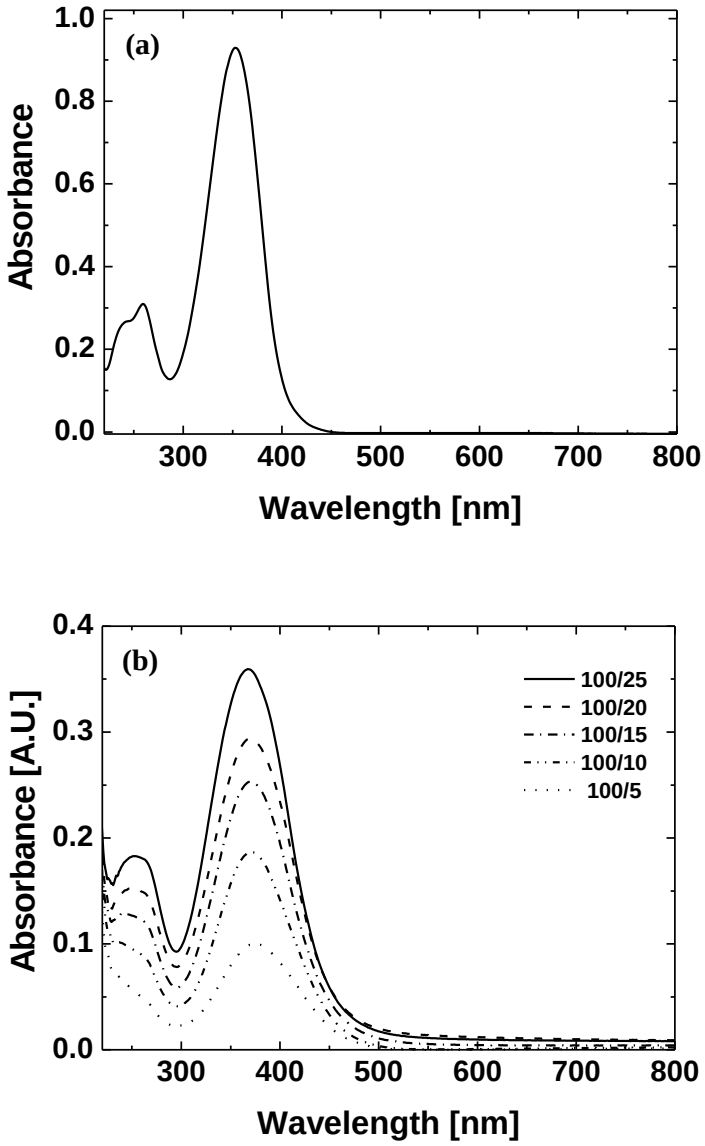

Figure 7. UV-vis absorption spectra of (a) 1.0×10^{-3} wt% of bisABmC in acetonitrile and (b) thin films of 5, 10, 15, 20, or 25 phr of bisABmC in GH-1203 baked at 80°C for 2 min.

Subsequently, we measured the change of UV-vis spectra of thin film composed of GH-1203/bisABmC (100/5) to confirm the effect of baking time. We found that the absorption maximum changed to the long wavelength with increased baking time (Figure 8).

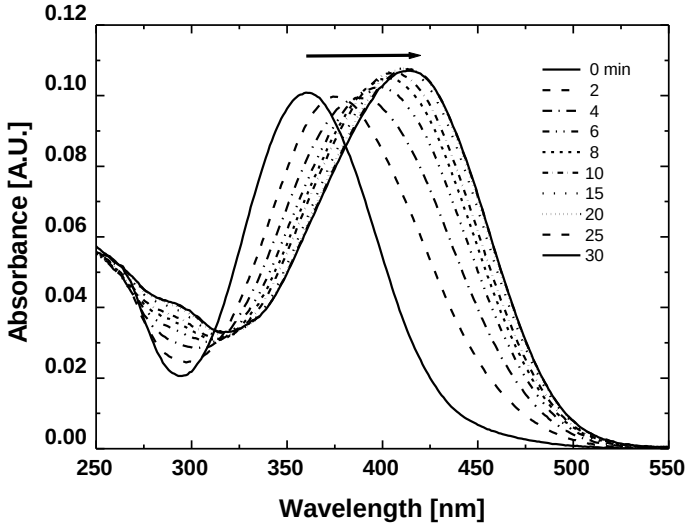

Figure 8. Baking time dependence of UV-vis absorption spectra of GH-1203/bisABmC (100/5) thin film. Baking temperature was at 80°C. Film thickness of sample was approximately 150 nm.

To clarify the reason for the change in UV-vis spectra, we next used UV-vis spectroscopy to measure bisABmC in poly(butyl methacrylate) (PBMA) and poly(2-hydroxyethyl methacrylate) (PHEMA) as model polymers without an acryloyl group. The model polymers PBMA and PHEMA are non-polar and polar, respectively. In this experiment, GH-1203 is the polar polymer because it has a hydroxyl group, which was confirmed by its FT-IR spectra. Although the absorption maximum of PBMA/bisABmC at 355 nm were constant after baking at 80°C for 25 min, the intensity and the peak position of PHEMA/bisABmC changed with increased baking time (Figure 9).

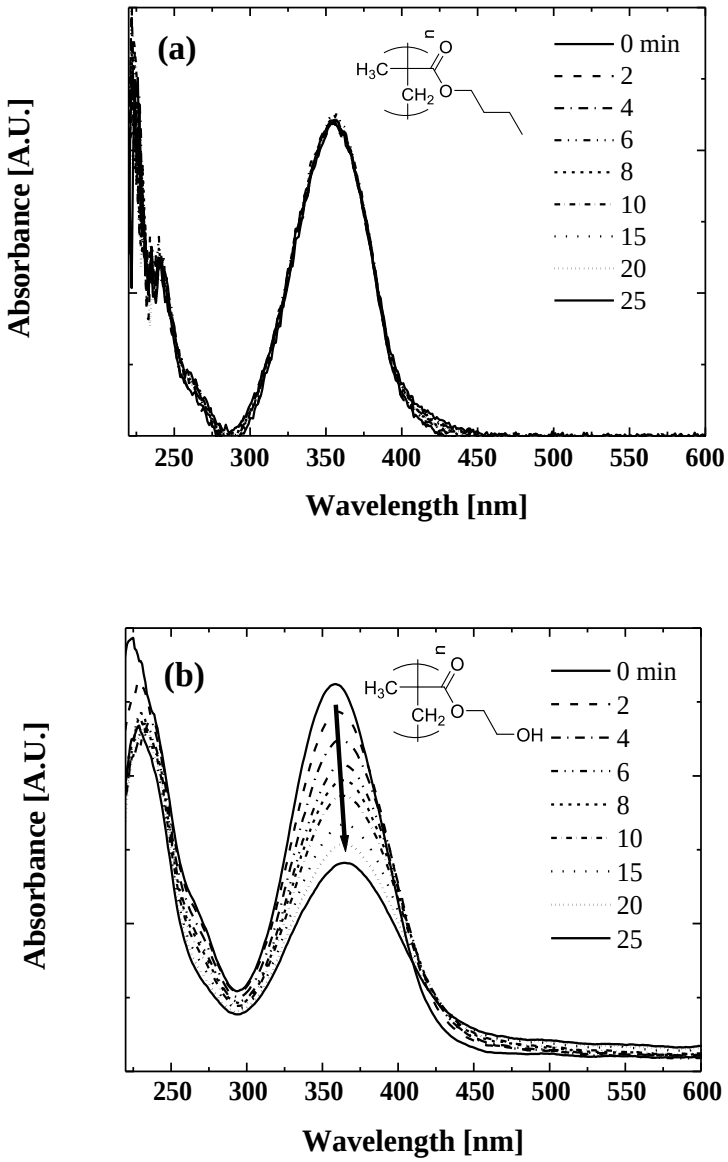

Figure 9. UV-vis absorption spectra of (a) PBMA/bisABmC (100/5) and (b) PHEMA/bisABmC (100/5) with increasing baking time at 80°C.

However, the FT-IR spectra of PHEMA/bisABmC showed no change after baking at 80°C (Figure 10 (a)). The peak of PHEMA/bisABmC at 2115 cm^{-1} was assigned to the azide group and the peak at 1598 cm^{-1} was assigned to the benzylidene cyclohexanone of bisABmC. These peaks did not change in response to baking time; therefore, bisABmC in PHEMA aggregated without any thermal reaction. In contrast, a thermal reaction at 80°C was evident for bisABmC in the GH-1203 matrix because the peak assigned to the azide group at 2115 cm^{-1} disappeared with increased baking time (Figure 10(b)).

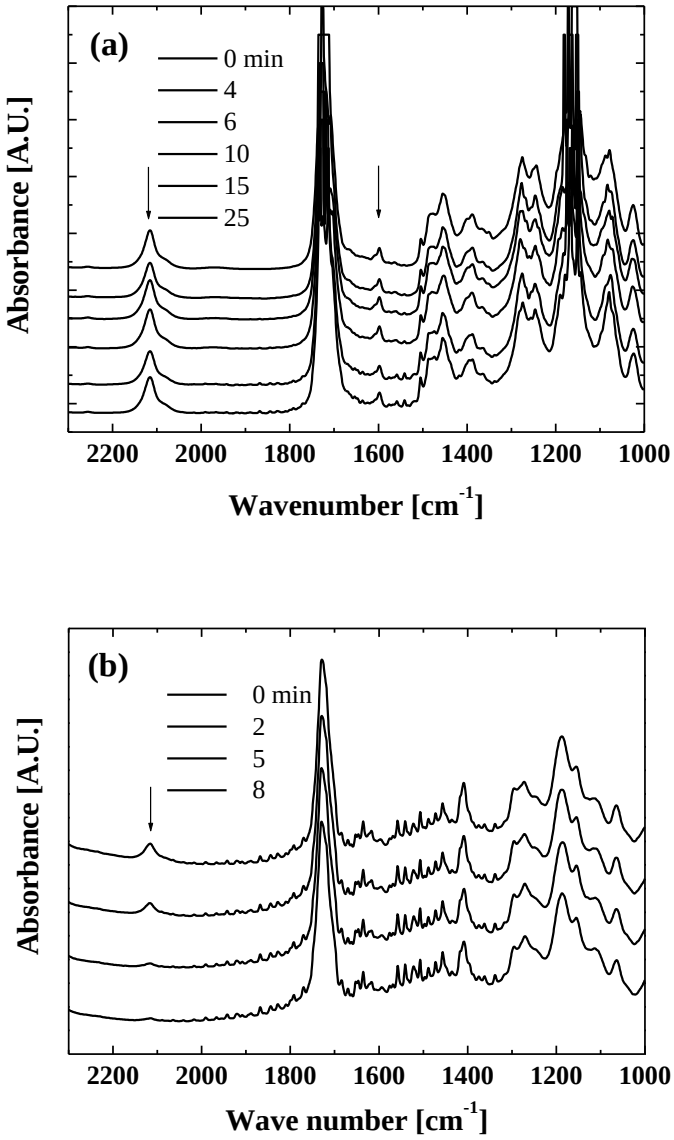

Figure 10. FT-IR spectra of (a) PHEMA/bisABmC (100/5) and (b) GH-1203/bisABmC (100/5) with increased baking time at 80°C.

These results suggest that the bisABmC aggregated in the polymer by baking and the peak derived from chromophores changed as a result of the dipole–dipole interaction between the bisABmCs in the PHEMA and in the GH-1203 matrix. However, the thermal reaction of the azide group in the GH-1203/bisABmC system also occurred simultaneously. It is generally known that the thermal reaction between the azide and acryloyl groups produces an aziridine ring via triazoline formation.[24] In the current study, the effect of this thermal reaction on absorption spectra was estimated by measuring a model polymer which was synthesized by thermal reaction of bisABmC and 1,6-hexanediol diacrylate. Because the substructure of thermally-reacted GH-1203/bisABmC and this model polymer was the same, we can estimate the effect of aziridine ring formation for absorption spectra. Figure 11 shows that the UV-vis spectrum of the model polymer had an absorption maximum at 369 nm. The position of this peak showed red-shift in comparison to that of bisABmC in acetonitrile (353 nm). However, the GH-1203/bisABmC blend showed a larger red-shift than the model polymer. This suggests that the change of absorption spectra for the GH-1203/bisABmC blend was associated with both the effect of aziridine ring formation and the aggregates of chromophores.

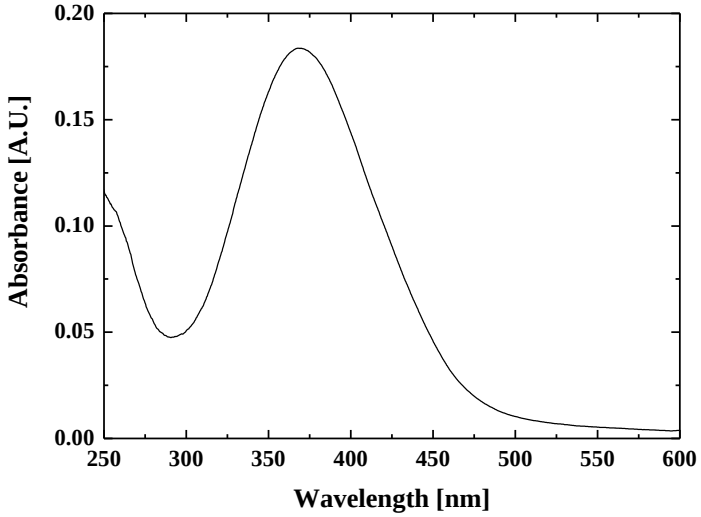

Figure 11. UV-vis spectra of the model polymer of 1,6-hexanediol diacrylate: bisABmC. 1 wt% solution in cyclopentanone was spincoated on the glass substrate. Film thickness of the sample was approximately 27 nm measured by a profilometer after baking at 80°C for 5 min on a hot-plate.

Photoreaction of GH-1203/bisABmC

The photo-reactions of azide via nitrene are generally known; for example, isomerization to imines, dimerization to azo compounds, insertion into C−H bond and addition to C=C double bond.[24] In order to separate multiple photo-reactions, the photoreaction of 1,6-hexanediol diacrylate (1,6-HDA)/bisAPM as a simple system including an azide and acryloyl group was analyzed by FT-IR spectroscopy. In Figure 12, the peaks assigned to azide group at 2115 cm^{-1} and $C=CH_2$ in the acryloyl group at

1410 cm^{-1} clearly decreased after UV-irradiation. This indicates that photo-addition of azide to the unsaturated C=C bond of the acryloyl group was the the photo-reaction in this system.

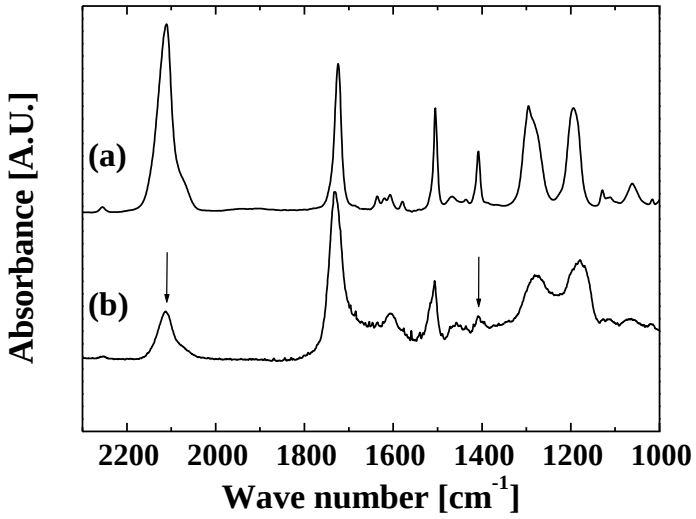

Figure 12. FT-IR spectra of (a) 1,6-HDA/bisAPM in equimolar amounts and (b) (a) after irradiation for 30 min by an Xe-lamp with cut-filter below 300 nm.

The photo-reaction of bisABmC in the GH-1203 matrix was measured by UV-vis spectroscopy. As shown in Figure 13, the absorption maximum at 369 nm decreased with the irradiation dose and the absorbance around 290 nm simultaneously increased. Our previous work with photoreactive polymers containing bisBC in main chain indicated a similar response in the UV-vis spectra.[25] The UV-vis spectrum after photo-dimerization of the photo-reactive polymers containing bisBC showed an increased absorbance around 290 nm. Therefore, the results in Figure 13 suggest the photo-reaction of the C=C bond in benzylidene. However, it remains unclear whether the bisBC unit in bisABmC reacts between bisBC and bisBC or bisBC and acrylate under LPVUL irradiation.

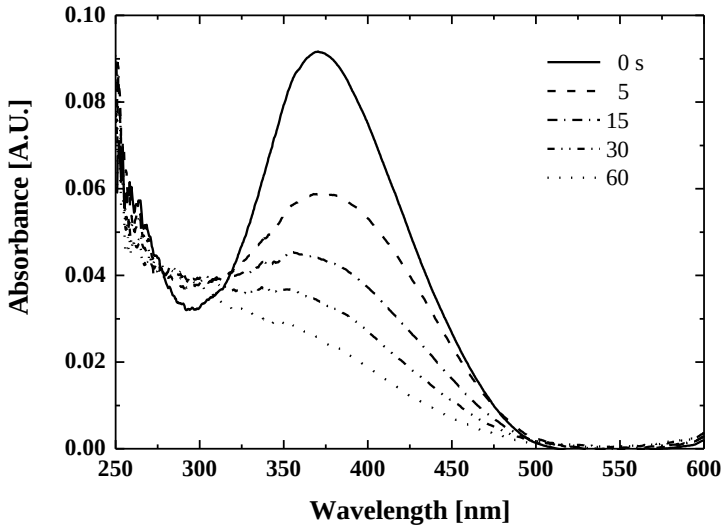

Figure 13. Irradiation dose dependence of UV-vis spectra for GH-1203/bisABmC (100/5) after baking at 80°C for 2 min.

To clarify the photo-reaction, the LPUVL irradiation dependence on FT-IR spectra were measured (Figure 14). The peak at 2115 cm^{-1} assigned to the azide group disappeared after only 5 s of LPUVL irradiation because of the photo-addition reaction between azide and acrylate. In addition, the 1598 cm^{-1} peak assigned to the C=C bond of benzylidene in bisABmC gradually decreased in amplitude with increasing time under LPUVL irradiation.

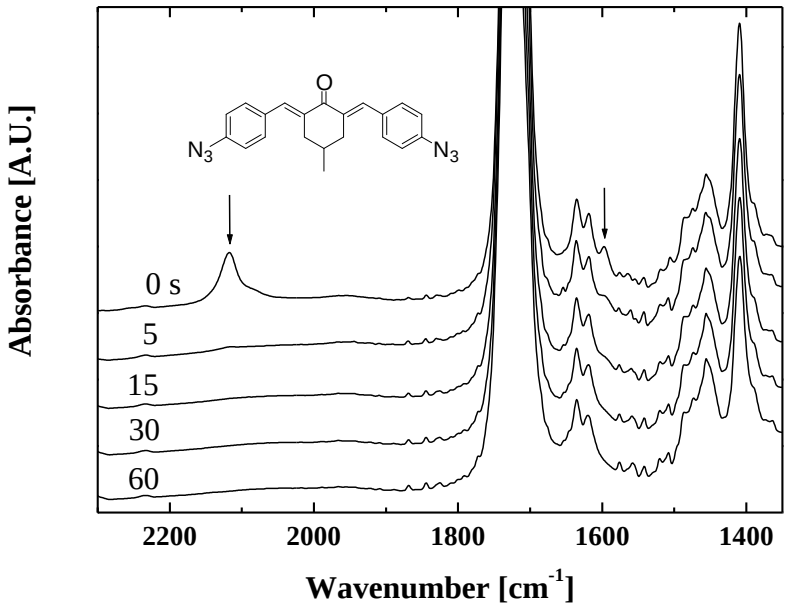

Figure 14. FT-IR spectra of GH-1203/bisABmC (100/5) after the thin film was baked at 80°C for 2 min and subsequently subjected to LPUVL irradiation for up to 60 s.

Anisotropy of GH-1203/bisABmC induced by LPUVL irradiation

The dichroic ratio (DR) was measured by polarized UV-vis spectroscopy after LPUVL irradiation because the anisotropy of photo-alignment layer itself is related to the photo-induced alignment of PLC. The DR is defined below:

$$\mathrm{DR} = \frac{\mathrm{A}_{\perp}}{\mathrm{A}_{\parallel}},$$

where $A_{\parallel}$ and $A_{\perp}$ are perpendicular and parallel absorption to the electric field of LPUVL. In a 5 phr of bisABmC in GH-1203, the absorption maximum at 374 nm was used to estimate the DR. The DR is an indicator of the orientation of chromophores, because polarized light parallel to transition dipole moment of chromophore is absorbed. The dichroic ratio of GH-1203/bisABmC (100/5) with the irradiation dose is shown in Figure 15. As the thin film of GH-1203/bisABmC irradiated by LPUVL showed dichroism, the selective photo-reaction occurred as a result of the LPUVL. The DR monotonically increased with the irradiation dose, and the behavior of the DR did not correspond to that of the PLC order parameter shown in Figure 5.

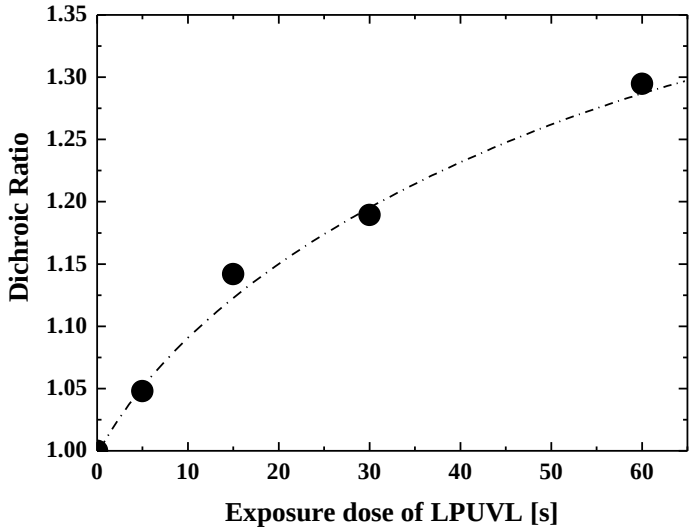

Figure 15. Dichroic ratio of thin film composed of GH-1203/bisABmC (100/5) in response to a LPUVL dose after dry-baking at 80°C for 2 min.

Irradiation dependence of retardation in GH-1203/bisABmC

The orientation direction of PLC changed in a plane from parallel to perpendicular to the electric field of LPUVL with increasing irradiation dose. The thin film of thin film composed of GH-1203/bisABmC (100/5) showed dichroism after irradiation by LPUVL. However, the DR increased monotonically (Figure 15). This suggests that the DR ratio was not related to the orientation direction of the PLC. To confirm the reason for this reversal of the PLC orientation with the occurrence of an irradiation dose, the retardation of thin film composed of GH-1203/bisABmC (100/5) was measured using the photo-elastic modulation method. Retardation (R) is defined by $R = \Delta n \cdot d$.

Anisotropic refractivity is also defined by $\Delta n = n_{\parallel} - n_{\perp}$, where $n_{\parallel}$ and $n_{\perp}$ are the refractivity parallel and perpendicular to the LPUVL electric field, respectively. Figure 16 shows that the retardation of the thin film reversed from positive to negative with increased irradiation time, corresponding to the change of order parameter of the PLC. In reference to Figure 14, the photo-addition reaction between the azide and acryloyl groups in GH-1203 was dominant at low irradiation time and the slow axis of retardation was parallel to the LPUVL electric field. Subsequently, the bisBC unit gradually photo-reacted with increased irradiation time and the slow axis changed perpendicular to the LPUVL electric field. The key reason for the monotonic increase in the DR with increase irradiation dose is assumed to be as follows. At low irradiation doses, the DR was dependent on the difference between parallel and perpendicular absorption was derived from the difference between un-reacted and reacted azide groups in bisABmC. At high irradiation doses, the DR was dominated by the difference between un-reacted and reacted bisBC units. Therefore, the DR increased monotonically because $A_{\perp}/A_{\parallel}$ was dependent only on un-reacted or reacted molecules.

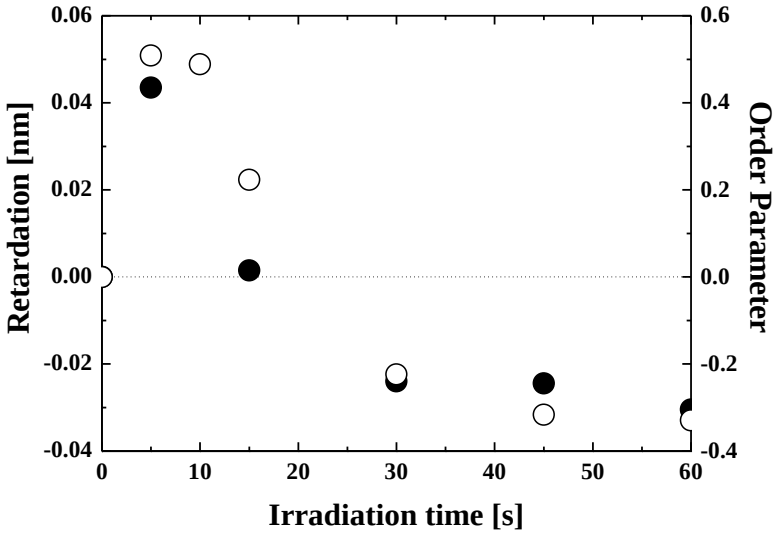

Figure 16. Irradiation dependence of retardation for GH-1203/bisABmC (100/5) and order parameter of PLC on thin film of GH-1203/bisABmC (100/5). Filled and open circles represent the retardation and order parameter, respectively.

To explain the reversion of retardation in GH-1203/bisABmC with increased irradiation dose, a molecular interpretation of the anisotropic refractive index was needed. Here, refractive index n is correlated with polarizability α by the Lorentz–Lorenz equation as follows [26, 27]:

$$\frac{n^2\text{-}1}{n^2+2}=\rho\frac{N_A\alpha}{3M}$$

where ρ is the density of the sample, N_A is Avogadro's number and M is the molecular weight. Refractive index n and polarizability α are interrelated. Therefore, the anisotropic polarizability ($\Delta\alpha$) was related to the retardation. In addition, the

photo-products of the bisBC unit are known as photo-isomers and photo-dimers.[28-33] In our previous work, we investigated photoreactive polymers containing the bisBC unit in the main chain.[25] The photoproducts of the bisBC unit were trans–cis and cis–cis isomers (bisBC-EZ, bisBC-ZZ) and a dimer (Figure 17). We calculated anisotropic polarizabilities of these photoproducts using DFT to reveal the mechanism that generates retardation of the GH-1203/bisABmC system. The magnitude of anisotropic polarizabilities for photoproducts of bisBC calculated by density functional theory were bisBC-EE (293 a.u.), bisBC-EZ (198 a.u.), bisBC-dimer (103 a.u.), and bisBC-ZZ (17 a.u.). This order indicates that the anisotropic polarizability of a rod-like structure (bisBC-EE) is larger than that of bent structures (bisBC-EZ and bisBC-ZZ) and spherical structurea (bisBC-dimer). Therefore, the unreacted bisBC unit had the largest anisotropic polarizability. These results show that anisotropic polarizability of bisABmC decreased as a result of the photo-reaction related to the bisBC unit, regardless of the photo-isomerization, photo-dimerization or other reactions accompanied by the bond cleavage of C=C. In contrast, the photo-reaction between azide and acrylate at low irradiation dose was assumed to increase the anisotropic polarizability parallel to the LPUVL electric field because the aspect ratio of the

molecule increased in response to the photo-addition reaction, retaining the structure of bisBC-EE.

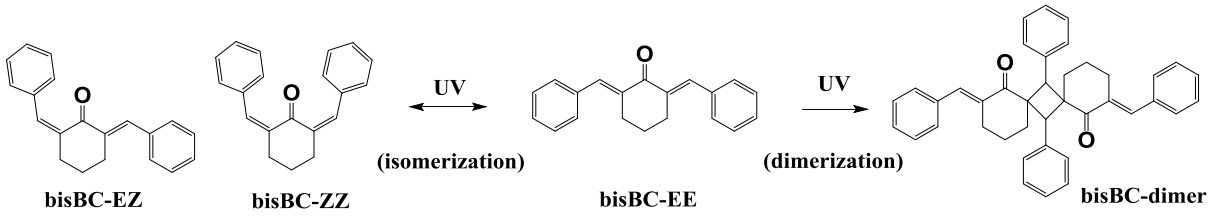

Figure 17. Photo-reaction of bisBC.

To confirm the influence of anisotropic polarizability on the conjugated length, an anisotropic polarizability of bisBC-E containing single benzylidene as a model molecule (Table 1) was calculated by DFT method according to the methods of our previous work.[25] The optimized structure of bisBC-E was slightly bent due to the lack of a C=C double bond. The anisotropic polarization of bisBC-E was smaller than that of bisBC-EE. This indicates that the photo-reaction of bisBC-EE via C=C bond cleavage produced a lower anisotropic polarizability than un-reacted bisBC-EE. Therefore, the photo-reaction of bisABmC, except for the photo-addition between azide and acrylate, may be assumed to reduce the anisotropic polarizability along the direction of LPUVL. This led to breakage of isotropy of the photo-alignment layer due to the photo-reaction

of azide–acrylate at the low irradiation dose, and that of the bisBC unit at high irradiation dose. The orientation direction of the PLC was determined by the un-reacted bisBC.

Table 1. Calculated anisotropic polarizability of bisBC-EE and bisBC-E by DFT at B3LYP/6-311++G(d,p).

	chemical structure	α_{xx}	α_{yy}	α_{zz}	$\Delta\alpha$
bisBC-EE	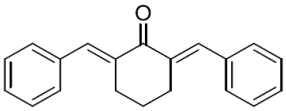	**472**	**220**	**139**	**293**
bisBC-E	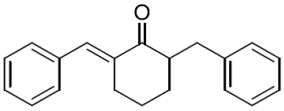	**368**	**208**	**170**	**179**

2-5. Conclusions

We evaluated the potential of photo-reactive bisazides with and without a bisBC unit in a polymer matrix containing an acryloyl group at side chain as a photo-alignment layer for liquid crystals. The PLC on the photo-alignment layer aligned homogeneously after the LPUVL irradiation to the photo-alignment layer. In the system of GH-1203/bisAPM as a simple bisazide, the PLC aligned homogeneously parallel to the LPUVL electric field. However, in the case of GH-2103/bisABmC, the PLC aligned to the direction parallel to LPUVL electric field at low irradiation doses and to the direction perpendicular to LPUVL at high irradiation doses. This system achieved the in-plane switching of the orientation direction of the PLC only by changing the irradiation dose. To confirm anisotropy of GH-1203/bisABmC system, the DR after LPUVL irradiation was measured and increased monotonically at irradiation doses up to 60 s. However, the behavior of the DR with the increase of irradiation time did not correspond to that of the order parameter of the PLC. However, the direction of slow axis of retardation for the photo-alignment layer changed from parallel to perpendicular to the LPUVL electric field with increasing irradiation dose of LPUVL. This fact indicates that the orientation direction of PLC corresponded closely to the slow axis of retardation. From the LPUVL irradiation dependence of FT-IR spectra, the azide group

of bisABmC rapidly reacted with the acryloyl group of GH-1203 and subsequently there was a gradual reaction of the bisBC unit of bisABmC. In comparison to the calculated anisotropic polarizabilities of model molecules, photo-reaction of bisBC suggested lower anisotropic polarizability regardless of the photo-isomerization, photo-dimerization or other reactions accompanied by the bond cleavage of C=C. Therefore, the reversion of the slow axis suggested that the photo-reaction of azide in the early stage of irradiation and that of bisBC unit in the late stage of irradiation dominated the slow axis of retardation. In addition, the bisBC unit irradiated by LPUVL changed to the photo-isomers or photo-dimers in GH-1203 matrix because the bisBC unit did not react with the acryloyl group in GH-1203 as a result of the irradiation. We conclude that the orientation direction of the PLC was determined by the un-reacted bisBC.

2-6. References

(1) Schadt M, Schmitt K, Kozinkov V, Chigrinov V. Surface-Induced Parallel Alignment of liquid crystals by linearly polarized photopolymers. Jpn. J. Appl. Phys. 1992;31:2155–2164.

(2) Makita Y, Natsui T, Kimura S, Nakata S, Kimura M, Matsuki Y, Takeuchi Y. Photoalignment materials with high sensitivityto near UV light. J. Photopolym. Sci. Technol. 1998;11:187–192.

(3) Schadt M, Seiberle H, Schuster A. Optical patterning of multi-domain liquid-crystal displays with wide viewing angles. Nature 1996;381:212–215.

(4) Ichimura K, Suzuki Y, Seki T. Reversible change in alignment mode of nematic liquid crystals regulated photochemically by 'command surfaces' modified with an azobenzene monolayer. Langmuir 1988;4:1214–1216.

(5) Tie W, Jeong IH, Jang IW, Han JS, Liu Y, Li X-D, Lee M-H, Jeong K-U, Lee SH. Reducing driving voltage and securing electro-optic reliability of in-plane switching liquid crystal display by applying polysulfone photoalignment layer with photo-reactive mesogens. Liquid Crystals. 2014;41:1057–1064.

(6) Kang H, Choi Y-S, Kang D, Lee J-C. Photoalignment behaviour on polystyrene films containing chalcone moieties. Liquid Crystals. 2015;42:189–197.

(7) Guo Q, Srivastava AK, Chigrinov VG, Kwok HS. Polymer and azo-dye composite: a photo-alignment layer for liquid crystals. Liquid Crystals. 2014;41:1465–1472.

(8) Schadt M, Seiberle H, Schuster A, Kelly SM. Photo-Generation of Linearly Polymerized Liquid Crystal Aligning Layers Comprising Integrated Optical Patterned Retarders and Color Filters. Jpn. J. Appl. Phys. Part 1.1995;34 :3240–3249.

(9) Schadt M, Seiberle H, Schuster A, Kelly SM. Photo-Induced Alignment and Patterning of Hybrid Liquid Crystal Polymer Films on Single Substrates. Jpn. J. Appl. Phys. Lett. 1995;34:764–767.

(10) Broer DJ, Boven J, Mol GN, Challa G. In-situ photopolymerization of oriented liquid-crystalline acrylates, 3. Oriented polymer networks from a mesogenic diacrylate. Makromol. Chem. 1989;190:2255–2268.

(11) Broer DJ, Hikmet RAM, Challa G. In-situ photopolymerization of oriented liquid-crystalline acrylates, 4. Influence of a lateral methyl substituent on monomer and oriented polymer network properties of a mesogenic diacrylate. Makromol. Chem. 1989:190:3201–3215.

(12) Broer DJ, Mol GN, Challa G. In-situ photopolymerization of oriented liquid-crystalline acrylates, 5. Influence of the alkylene spacer on the properties of the

mesogenic monomers and the formation and properties of oriented polymer networks. Makromol. Chem. 1991;192:59–74.

(13) Ichimura K, Suzuki Y, and Seki T. Reversible Change in Alignment Mode of Nematic Liquid Crystals Regulated Photochemically by "Command Surfaces" Modified with an Azobenzene Monolayer. *Langmuir*. 1988; 4:1216–1219.

(14) Meier JG, Ruhmann R, Stumpe J, Planar and Homeotropic Alignment of LC Polymers by the Combination of Photoorientation and Self-Organization. Macromolecules. 2000;33:843–850.

(15) Han M, Morino S, Ichimura K. Factors Affecting In-Plane and Out-of-Plane Photoorientation of Azobenzene Side Chains Attached to Liquid Crystalline Polymers Induced Irradiation with Linearly Polarized Light. Macromolecules. 2000;33:6360–6371.

(16) Kawatsuki N, Ono H, Taketsuka H, Yamamoto T, Sangen O. Liquid Crystal Alignment on Photoreactive Side-Chain Liquid-Crystalline Polymer Generated by Linearly Polarized UV Light. Macromolecules. 1997;30:6680–6682.

(17) Kawatsuki N, Goto K, Kawakami T, Yamamoto T. Reversion of Alignment Direction in the Thermally Enhanced Photoorientation of Photo-Cross-Linkable Polymer Liquid Crystal Films. Macromolecules. 2002;35:706–713.

(18) Obi M, Morino S, Ichimura K. The reversion of photoalignment direction of a liquid crystal induced by a polymethacrylate with coumarin side chains. Macromol. Rapid Commun. 1998;19:643–646.

(19) Obi M, Morino S, Ichimura K. Reversion of Photoalignment Direction of Liquid Crystals Induced by Cinnamate Polymer Films. Jpn. J. Appl. Phys. 1999;38:145–147.

(20) Frisch MJ, Trucks GW, Schlegel HB, Scuseria GE, Robb MA, Cheeseman JR, Scalmani G, Barone V, Mennucci B, Petersson GA, Nakatsuji H, Caricato M, Li X, Hratchian HP, Izmaylov AF, Bloino J, Zheng G, Sonnenberg JL, Hada M, Ehara M, Toyota K, Fukuda R, Hasegawa J, Ishida M, Nakajima T, Honda Y, Kitao O, Nakai H, Vreven T, Montgomery JA, Peralta JE Jr, Ogliaro F, Bearpark M, Heyd JJ, Brothers E, Kudin KN, Staroverov VN, Kobayashi R, Normand J, Raghavachari K, Rendell A, Burant JC, Iyengar SS, Tomasi J, Cossi M, Rega N, Millam JM, Klene M, Knox JE, Cross JB, Bakken V, Adamo C, Jaramillo J, Gomperts R, Stratmann RE, Yazyev O, Austin AJ, Cammi R, Pomelli C, Ochterski JW, Martin RL, Morokuma K, Zakrzewski VG, Voth GA, Salvador P, Dannenberg JJ, Dapprich S, Daniels AD, Farkas Ö, Foresman JB,

Ortiz JV, Cioslowski J, and Fox D.J.Gaussian09, Revision D.01. Gaussian, Inc., Wallingford CT, 2009.

(21) Becke AD. Density-functional thermochemistry. III. The role of exact exchange. J. Chem. Phys. 1993;98:5648–5652.

(22) Yanai T, Tew DP, Handy NC. A new hybrid exchange-correlation functional using the Coulomb-attenuating method (CAM-B3LYP). Chem. Phys. Lett. 2004;393:51–57.

(23) Sampath Kumar HM, Rao MS, Chakravarthy PP, Yadav JS. Enzymatic resolution of N-arylaziridine carboxylates. Tetrahedron: Asymmetry. 2004;15:127–130.

(24) G. L'abbe. Decomposition and addition reactions of organic azides. Chem. Rev. 1969;69:345–363.

(25) Y. Kimura, K. Kuboyama, and T. Ougizawa (submitted to Liquid Crystals)

(26) Lorentz HA. On the Relation between the Velocity of Transmission of Light and the Density of a Body. Ann. Physik Chemie. 1880;9:641–665.

(27) Lorenz L. The Index of Refraction Ann. Physik Chemie. 1880;11:70–103.

(28) Gangadhara, Kishore K. Novel Photo-Cross-Linkable Liquid Crystalline Polymers: Poly[bis(benzylidene)] Esters. Macromolecules. 1993;26:2995–3003.

(29) Gangadhara, Kishore K. Synthesis and characterization of photo-crosslinkable main-chain liquid-crystalline polymers containing bis(benzylidene)cycloalkanone units. Polymer. 1995;36:1903–1910.

(30) George H, Roth HJ. Photoisomerisierung und cyclo-1,2-addition α,β-ungesättigter cyclanone. Tetrahedron Lett. 1971;43:4057–4060.

(31) Thomas JM. Diffusionless reactions and crystal engineering. Nature. 1981;289:633–634.

(32) Sakthivel P, Kannan P. Novel thermotropic liquid crystalline-cum-photocrosslinkable polyvanillylidene alkyl/arylphosphate esters. J. Polym. Sci. A Polym. Chem. 2004;42:5215–5226.

(33) Sakthivel P, Kannan P. Thermotropic main-chain liquid-crystalline photodimerizable poly(vanillylidenealkyloxy alkylphosphate ester)s containinga cyclopentanone moiety. Polym. Int. 2005;54:1490–1497.

Chapter 3

Photoalignment layers containing bis(benzylidene)cyclohexanone unit

3-1. Abstract

Photoreactive polymers containing 2,6-bis(benzylidene)-1-cyclohexanone (bisBC) units were synthesized and investigated as a photoalignment layer for polymerizable liquid crystals (PLC) and liquid crystalline polymers (LCP). The liquid crystalline materials were aligned homogeneously on the photoalignment layers in a wide range of irradiation dose of linearly polarized UV light (LPUVL). Specifically, for the photoalignment layer baked at 80 °C, order parameters of the liquid crystalline materials were low due to the disturbance of oriented-photoreactive polymer caused by the contact with the solvent of liquid crystalline materials. However, the liquid crystalline materials were aligned homogeneously even at low irradiation doses on the thermally cured photoalignment layer baked at 180 °C. In addition, the liquid crystalline materials were aligned perpendicular to the LPUVL electric field. The alignment mechanism is discussed by comparing the retardation of photoalignment layer with anisotropic polarizabilities of model molecules calculated by density functional theory. It is suggested that the liquid crystalline materials aligned along the unreacted chromophores in the photoreactive polymer.

3-2. Introduction

In the organic devices that utilize liquid crystals, such as flat-panel displays, either rubbing or photoalignment are necessary to control the orientation of liquid crystals. In particular, studies on the use of photoreactive materials to align liquid crystals are of fundamental importance to allow the formation of defect-free, aligned liquid crystals and a dust-free process. For these reasons, a number of studies have been performed using polymers containing photoreactive units, such as cinnamate, chalcone, coumarin, and azobenzene, in the side or main chains of the polymers.[1-4] These polymer films are able to induce alignment of liquid crystals upon irradiation with linearly polarized ultraviolet light (LPUVL). Mechanisms for the anisotropic surface generation that occurs upon LPUVL irradiation have been proposed for azobenzene, cinnamate, chalcone, and coumarin.[1-4] There has been considerable interest in photoalignment of liquid crystals in recent years.[5-8]

On the other hand, polymerizable liquid crystals (PLCs), such as acrylate-terminated liquid crystals, that are birefringent because of being derived from oriented, rigid mesogens have been reported and investigated for use as coatable retarders and polarizers.[9-13] The thermal stability of the oriented PLCs results from the formation of three-dimensional cross-linkages by photoradical polymerization. In

the above mentioned applications, PLCs are cross-linked by photoradical polymerization immediately after orientation on the alignment layer. Therefore, the photoalignment layer is not required to maintain long-term, reliable anchoring of the liquid crystals, but serves to enhance sensitivity, allowing a low dose of LPUVL to be used to achieve high-throughput manufacturing. From this standpoint, the photoalignment method is suitable for applications using PLCs.

In this study, we investigated the photoinduced alignment of a PLC and a liquid crystalline polymer (LCP) using photoreactive polymers containing 2,6-bis(benzylidene)-1-cyclohexanone (bisBC) in the main chain. The polymers have been reported by Gangadhara et al. as cross-linkable liquid crystalline polymers.[14,15]

In this paper, we propose an amorphous polymer containing bisBC unit in its main chain for use as the photoalignment layer. Our polymers are easily synthesized without the use of catalysts and under mild conditions. Furthermore, they have a good solubility in organic solvents.

3-3. Experimental section

Materials

2,6-bis(4-azidobenzylidene)-4-methyl-1-cyclohexanone (bisABmC) and 2,6-bis(4-azidophenyl) methane (bisAPM) were obtained from TOYO GOSEI Co., Ltd. 1,6-hexanediol diacrylate, 1,9-nonandiol diacrylate, 1,10-decandiol diacrylate, cyclopentanone (CPN), n-heptane, and toluene were purchased from Tokyo Chemical Industry Co., Ltd. Dimethyl 2,2′-azobis(2-methylpropionate) (V-601) was purchased from Wako Pure Chemical Industries, Ltd. Di-functional and mono-functional PLCs, LC242 and *N*-*p*-cyanobenzylidene-*p*-heptylaniline (CBHA), were obtained from BASF Japan Ltd., and JNC Petrochemical Corp., respectively. Acrylic surfactant (BYK®-361-N) was provided by Big Chemie Co., Ltd. These reagents were used without further purification. The chemical structures of bisazides and PLCs are shown in Figure 1.

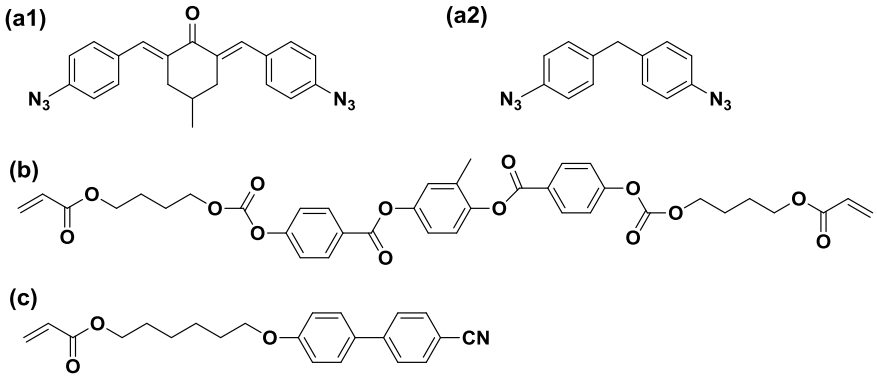

Figure 1. Chemical structures of (a1) bisABmC, (a2) bisAPM, (b) LC242, and (c) CBHA.

Synthesis of photoalignment polymers

Photoreactive polymers containing bisBC units were synthesized by thermal polymerization. The thermal reaction via 1,3-dipolar cycloaddition between azide and acrylate has been previously reported.[16] The reaction between a bi-functional azide and a bi-functional acrylate gives a linear polymer without use of a catalyst under mild conditions.

Firstly, bisABmC (10.8 mmol), the bis-azide, was dissolved in CPN (6.440 g) and was stirred in a two-necked flask with a thermometer and a Dimroth condenser at room temperature. Then, 1,6-hexanediol diacrylate (10.8 mmol) was added to the solution of the bis-azide, and this solution was heated at 80 °C for 6 h. The obtained polymer

(PbisABmC-6dA) was purified by three cycles of dissolution-reprecipitation using n-heptane. Polymerizations using 1,9-nonandiol diacrylate and 1,10-decandiol diacylate as substitutes for 1,6-hexanediol diacrylate were carried out in a similar manner. Weight-average molecular weights (M_w) of PbisABmC-6dA, -9dA, and -10dA were 35,000, 79,000, and 91,000, respectively, as determined by gel permeation chromatography (GPC). The prepared polymers were amorphous, and this was verified by differential scanning calorimetry (DSC) measurements; in contrast, the starting material, bisABmC, was crystalline. The chemical structure of PbisABmC-*i*dA is shown in Figure 2.

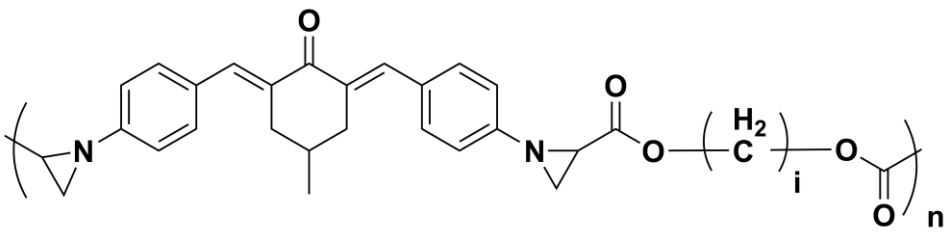

Figure 2. PbisABmC-*i*dA (*i* = 6, 9, and 10).

Preparation of polymerizable liquid crystal (PLC) solution

The weight ratio of sample was LC242/CBHA/photoradical generator/surfactant 67/33/3/1. The two PLCs were added in equimolar ratio. PLC samples were prepared as follows. As a PLC, a mixture of LC242 (1.000 g, 1.42 mmol) and CBHA (0.4948 g, 1.42 mmol) was dissolved in toluene (13.99 g) along with the photoradical generator (0.0448 g, Irgacure® 907) and the surfactant (0.0149 g, BYK®-361N). Finally, the PLC solution was filtered through a PTFE membrane (average pore size: 0.2 μm).

Preparation of LCP by polymerization of CBHA

Free-radical polymerization of CBHA was carried out to obtain a side-chain liquid crystalline polymer (Figure 3). CBHA (22.9 mmol), the monomer, was dissolved in CPN (4.308 g) and was stirred in a three-necked flask with a thermometer, a feed tube for N_2-flow, and a Dimroth condenser at room temperature. Subsequently, dimethyl 2,2′-azobis(2-methylpropionate) (0.3mmol), the radical initiator, was added to the flask, and the mixture was stirred while N_2 was bubbled through the solution. The flask temperature was maintained at 60 °C for 3 h. The obtained polymer was purified three times by dissolution-reprecipitation with n-heptane. The purified polyCBHA (PCBHA) was re-dissolved in CPN (3.5 wt%). The M_w of PCBHA was found to be 55,000 by

GPC.

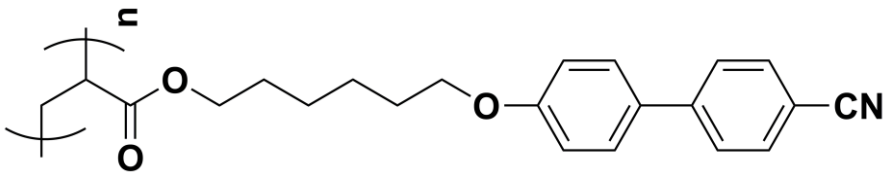

Figure 3. PCBHA (M_w=55,000).

Measurements

Thin films of the photoalignment layer and the liquid crystalline materials were prepared by a spincoating (1H-DX, Mikasa Co., Ltd.) on glass substrates (40 mm square, 0.7 mm thickness, EagleXG). The film thicknesses were measured by an ellipsometer (SA-101, Photonic Lattice Inc.) and a profilometer (alpha-step P-16, KLA-Tencol Corp.). After spincoating, the films were dried on a hot-plate. Then, the film samples were exposed with LPUVL, obtained using a xenon lamp (500 W) with an Al wire-grid polarizer and cut-filter below 300 nm.

An ultraviolet-visible-near-infrared (UV-vis-NIR) spectrometer (V-7200, Jasco. Co., Ltd.) was used to measure both UV-vis and polarized UV-vis spectra. A polarized optical microscope (BX60, Olympus Corp.) was used for morphological observations.

FT-IR measurements were performed on thin films of the polymers on Si wafers (FT/IR6110FF, Jasco., Co., Ltd.). Retardation of the thin films was measured by the photoelastic modulation method (HINDS INSTRUMENTS, Inc.). GPC measurements were carried out using SHIMADZU prominence GPC system equipped with polystyrene gel columns. Tetrahydrofuran was used as eluent after calibration with polystyrene standards.

Calculations

To find optimized molecular structures and properties such as relative energies, vibrational frequencies (IR spectra), and polarizabilities for the isomers and dimers derived from the bisBC unit, density functional theory (DFT) calculations for model compounds were carried out using Gaussian 09 Revision D.01(Gaussian Inc.).[17] Geometry optimizations, vibrational frequencies, and polarizabilities were calculated using the B3LYP hybrid functional, which employs Becke's (B88) exchange functional and the Lee, Yang, and Parr (LYP) correlation functional, and Pople's 6-311++G(d,p) Gaussian basis set.[18,19] In addition, excited state calculations were carried out using time-dependent DFT (TD-DFT) and the CAM-B3LYP functional.[20]

3-4. Results and discussion

Photoinduced alignment of PLC on PbisABmC-idA (i= 6, 9, 10)

The photoalignment ability of the synthesized polymers for liquid crystal materials were confirmed as follows: 1.0 wt% solutions of PbisABmC-*i*dA (*i* = 6, 9, and 10) in CPN were spincoated on glass substrates. Film thicknesses of all samples ranged from 23 to 27 nm and were measured using a profilometer. Thin films of PbisABmC-*i*dA (*i* = 6, 9, and 10) were baked at 100 °C for 5 min to evaporate solvent. Then, the thin films were irradiated by LPUVL for 5 s. Subsequently, the PLC solutions were spincoated onto the photoalignment layers. The samples were soft-baked at 80 °C for 1 min to evaporate solvent and quenched to room temperature. After that, the PLC thin films were photocured for 20 s under a nitrogen atmosphere at room temperature without any thermal-cure. The 'polymerized' LC obtained by photocuring is also described as 'PLC' in this paper.

As shown in Figure 4, polarized UV-vis spectra of the PLC show obvious differences between the absorbencies parallel and perpendicular to the LPUVL electric field. The PLC on the photoalignment layer showed homogeneous alignment. The peak around 297 nm was attributed to the transition dipole moment of the cyanobiphenyl group of CBHA. The absorption intensity of PLC perpendicular to the LPUVL electric

field, around 297 nm, was greater than that parallel to the LPUVL electric field. DFT calculations found that the transition dipole moment of CBHA at around 297 nm is parallel to the molecular long axis. These results indicate that the PLC orientation direction was perpendicular to the LPUVL electric field.

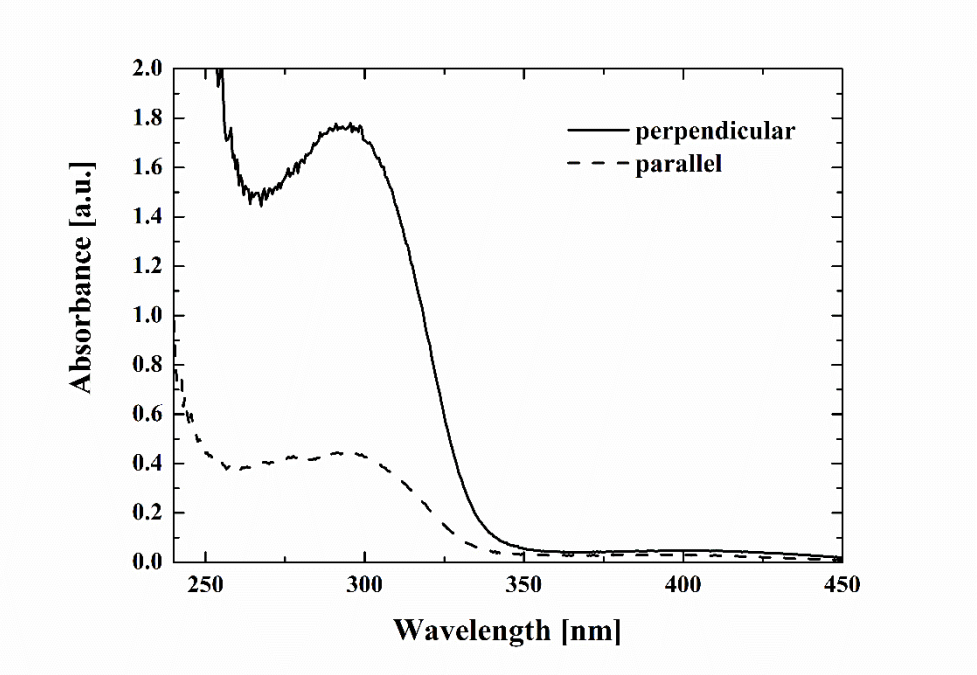

Figure 4. Polarized UV-vis spectra of PLC on PbisABmC-6dA thin film irradiated by xenon lamp for 5 s with a cut-filter below 300 nm after thermal-curing at 180 °C for 5min.

Irradiation dose and baking-temperature-dependence of PLC order parameter

To reveal the alignment behavior of the PLC regarding the dependence on the LPUVL

irradiation dose of the photoalignment layers, order parameters for the PLCs on the PbisABmC-*i*dA (*i* = 6, 9, and 10) films were measured by polarized UV-vis spectroscopy. The order parameters of the PLCs were calculated by using the peak at 297 nm. The order parameter, *S*, is defined in Equation (1).

$$S = \frac{A_{\parallel} - A_{\perp}}{A_{\parallel} + 2A_{\perp}}$$

where $A_{\parallel}$ and $A_{\perp}$ are the peak heights parallel and perpendicular to the LPUVL electric field, respectively. The value of *S* when CBHA molecules are all oriented parallel to the LPUVL electric field is 1.0. When they are all oriented perpendicularly to the LPUVL electric field, the value of *S* is – 0.5. The photoalignment layers were baked at two temperatures, 80 and 180 °C, to evaluate the effect of thermal curing of the films. As shown in Figure 5, the photoalignment layers baked at 80 °C for 5 min had different photosensitivities for PLCs with different alkyl-chain lengths, and the shorter alkyl-chain polymer (*i* = 6) was the most photosensitive. In contrast, thin films of PbisABmC-*i*dA (*i* = 6, 9, and 10) baked at 180 °C for 5 min had similar sensitivities to low LPUVL irradiation doses, as shown in Figure 6. The PLCs were aligned homogeneously on the PbisABmC-*i*dA (*i* = 6, 9, and 10) thin films irradiated for 5 s. In the case of low-temperature baking, the low sensitivity of the photoalignment layer may

be due to disturbances in the oriented photoreactive polymer caused by contact with solvent during spincoating and dry baking. In contrast, at high temperature baking, the ordered photoreactive polymer was not disturbed because the photoalignment layer was thermally cross-linked by either the reaction between the residual azide and acrylic groups or between the bisBC units in the polymer.

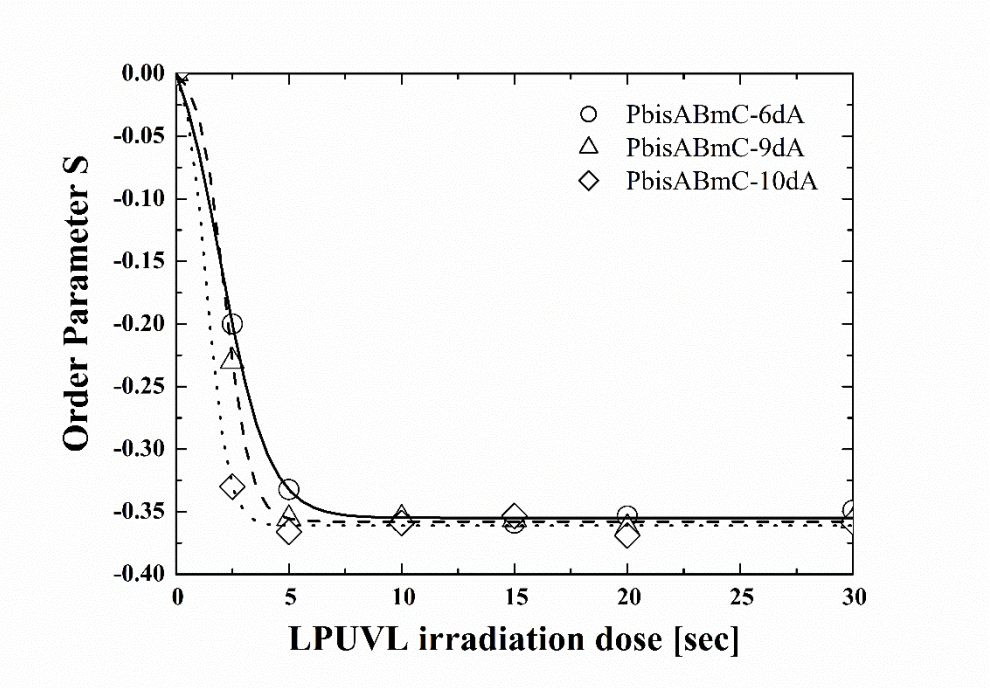

Figure 5. Order parameter of PLC on PbisABmC-*i*dA (*i* = 6, 9, 10) after baking at 80 °C for 5 min.

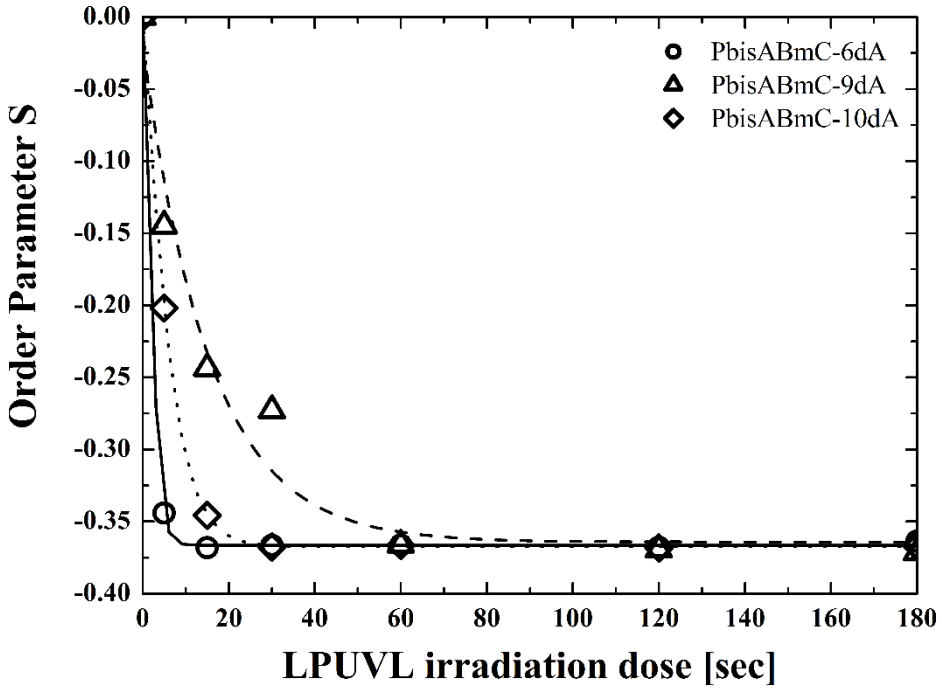

Figure 6. Order parameter of PLC on PbisABmC-*i*dA (*i* = 6, 9, and 10) after baking at 180 °C for 5 min.

Annealing temperature dependence of the LCP order parameter on PbisABmC-idA

During high-temperature baking to align the liquid crystalline materials, both the photoalignment layer and PLC were unavoidably cured; this is because of the presence of an acrylic group in the PLC. Therefore, to investigate the effect of temperature, we

replaced the PLC with an LCP without a reactive acrylic group, PCBHA. Therefore, to investigate the thermal stability of the photoalignment layer itself, the PCBHA ordering on the photoalignment layer was evaluated by means of an order parameter, which was determined under various annealing conditions.

Firstly, the photoalignment behavior of PCBHA as the LCP was evaluated at increasing irradiation doses. A 3.5 wt% solution of PCBHA (Figure 3, M_w = 55,000) in CPN was prepared. As described previously, the photoalignment layers were baked for 5 min at either 80 or 180 °C. Then, the photoalignment layers were irradiated with LPUVL. Subsequently, the PCBHA solutions were spincoated onto the PbisABmC-*i*dA (*i* = 6, 9, and 10) thin films and annealed at 120 °C for 3 min. As shown in Figure 7, for the photoalignment film baked at 80 °C, PCBHA gradually became more oriented with increasing irradiation time; however, the orientation was insufficient to be classed as nematic. PCBHA thin films on the photoalignment layers irradiated for less than 30 s were hazy and cloudy. In contrast, in the samples baked at 180 °C, PCBHA became well oriented at low irradiation doses. In the case of baking at 80 °C, the photoinduced anisotropic surface of the photoalignment layer was presumably disturbed by solvent during spincoating with PCBHA. However, the presence of cross-linked PbisABmC-*i*dA prevented solvent from disturbing the anisotropic surface significantly,

allowing PCBHA to became oriented on the surface at high LPUVL doses. In the case of baking at 180 °C, the polymer chains of the photoalignment layer were not disturbed by the PCBHA solution during spincoating, even at low irradiation doses, because the cross-linkages had already formed due to thermal reaction during baking. This suggests that photoalignment layers baked at high temperature are chemically resistant due to the thermal cross-linking between azide and acrylate in the polymer tail and also that

between bisBC units.

Secondly, the relationship between the annealing temperature and the ordering parameter of PCBHA on the PbisABmC-6dA thin films was investigated. The photoalignment layers were baked at 80 and 180 °C for 5 min. Subsequently, the alignment layers were irradiated for 20 s with LPUVL. Then, PCBHA thin films were formed on the photoalignment layer by spincoating, and they were annealed at

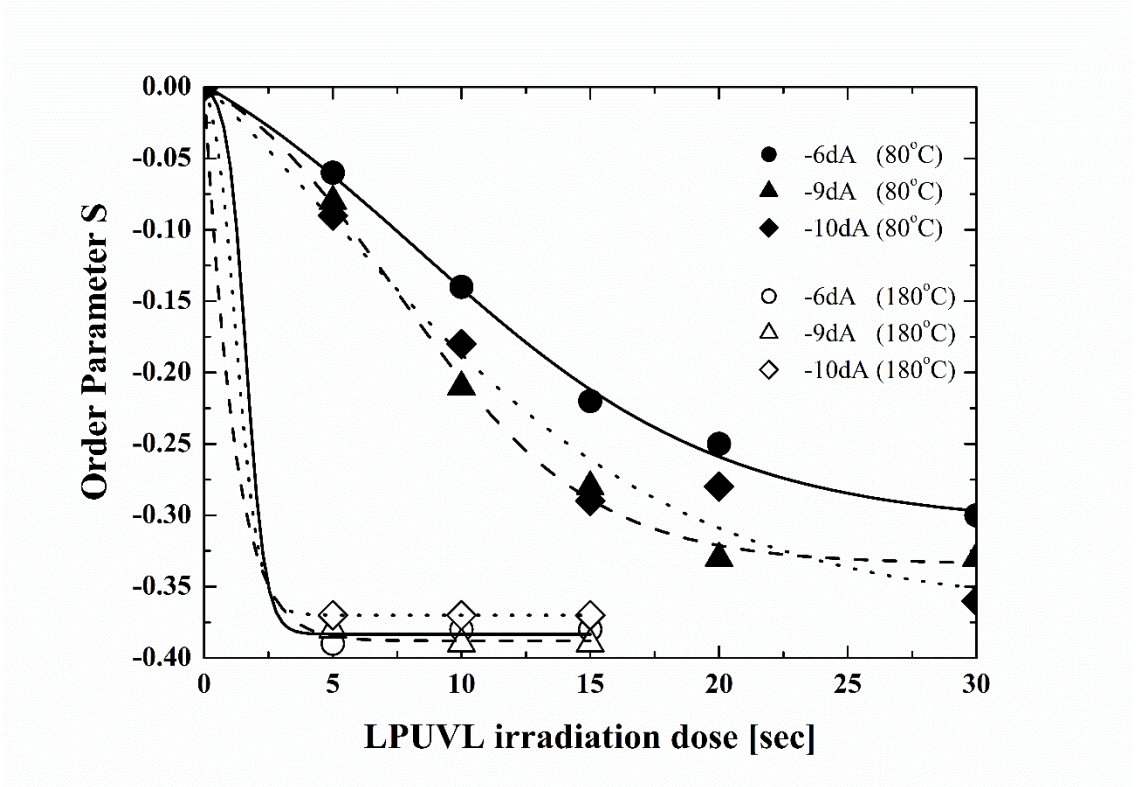

Figure 7. Order parameter of PCBHA on PbisABmC-*i*dA (*i* =6, 9, and 10) after the baking of photoalignment layers at 80 or 180 °C for 5 min. PCBHA was annealed at 120 °C for 3 min on the photoalignment layers.

temperatures ranging from 120 to 180 °C for 3 min. As shown in Figure 8, the ordering of PCBHA decreased with decreasing annealing temperature. The slope of the order parameter versus annealing temperature was nearly equal at 80 and 180°C, indicating that the orientation of PCBHA is possibly dominated by unreacted PbisABmC-6dA chromophores. In addition, the rigidity of polymers derived from thermal cross-linking did not help maintain the orientation of the LCPs against thermal fluctuations.

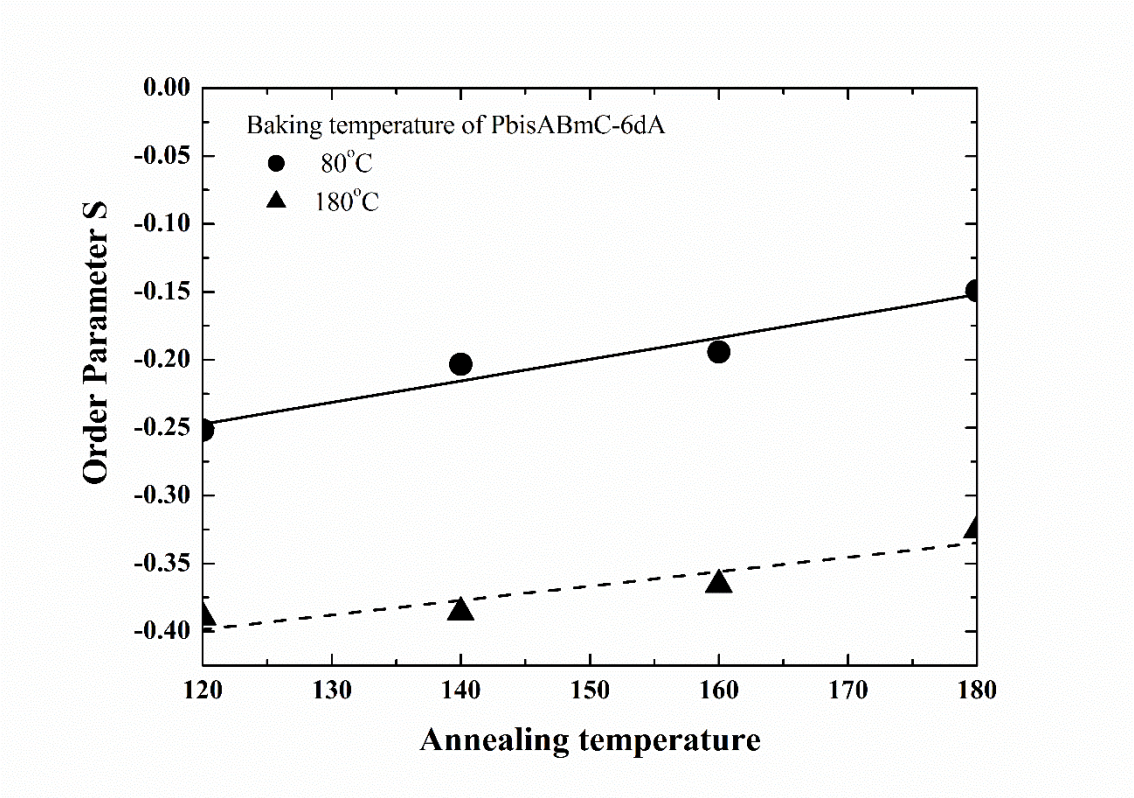

Figure 8. Annealing temperature dependence on the order parameter of PCBHA on PbisABmC-6dA after baking at 80 and 180 °C for 5 min. Annealing time was 3 min for all samples.

PbisABmC-idA anisotropy induced by LPUVL irradiation

To evaluate the anisotropy of photoalignment layer itself after LPUVL irradiation, dichroic ratios (DR) of the PbisABmC-*i*dA (*i* = 6, 9, and 10) thin films were measured by polarized UV-vis spectroscopy after LPUVL irradiation. The dichroic ratio is defined as shown in Equation (2).

$$DR = \frac{A_{\perp}}{A_{\parallel}} \quad (2)$$

where $A_{\perp}$ and $A_{\parallel}$ are the absorbencies perpendicular and parallel to the LPUVL electric field. Because polarized light parallel to the chromophore transition dipole moment is absorbed, the DR yields information on the chromophore orientation. As shown in Figure 9, the anisotropic photoreaction of the chromophores in the polymers had clearly occurred. The DR of PbisABmC-*i*dA (*i* = 6, 9, and 10) increased with increasing irradiation dose, and neither the alkylene spacer length (*i* = 6, 9, and 10) nor the baking temperature influenced the magnitude of the DR.

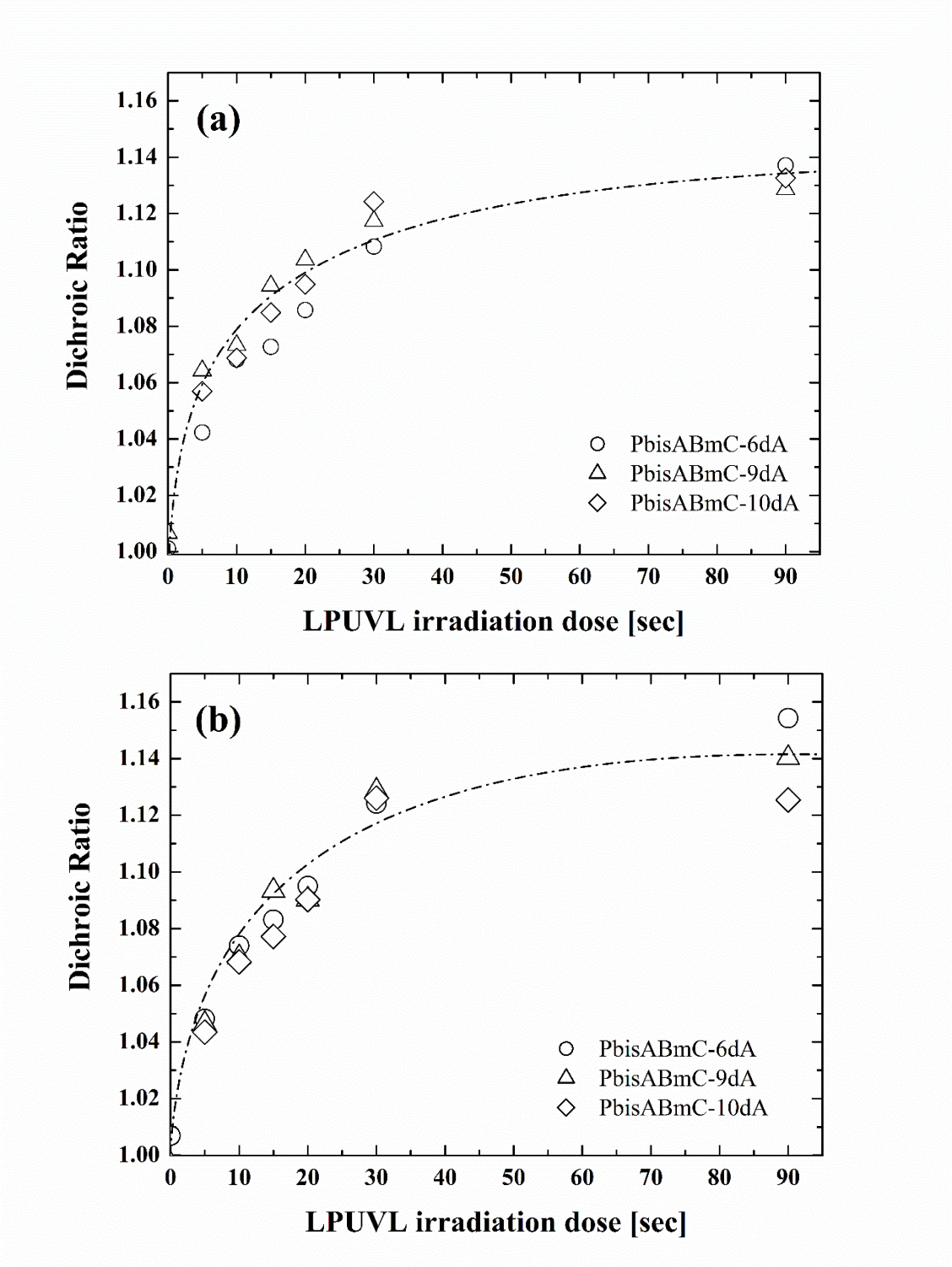

Figure 9. LPUVL irradiation dose dependence of dichroic ratio for PbisABmC-*i*dA (*i* = 6, 9, and 10) baked at (a) 80 °C for 5 min and (b) 180 °C for 5 min.

Photoreaction of PbisABmC-idA (i=6, 9, and 10)

To reveal the photoreaction of PbisABmC-*i*dA, changes in the UV-vis spectra caused by LPUVL-irradiation were measured. As shown in Figure 10, an initial peak located at 369 nm in UV-vis spectrum diminished with increasing irradiation dose; simultaneously, an absorbance around 290 nm increased.

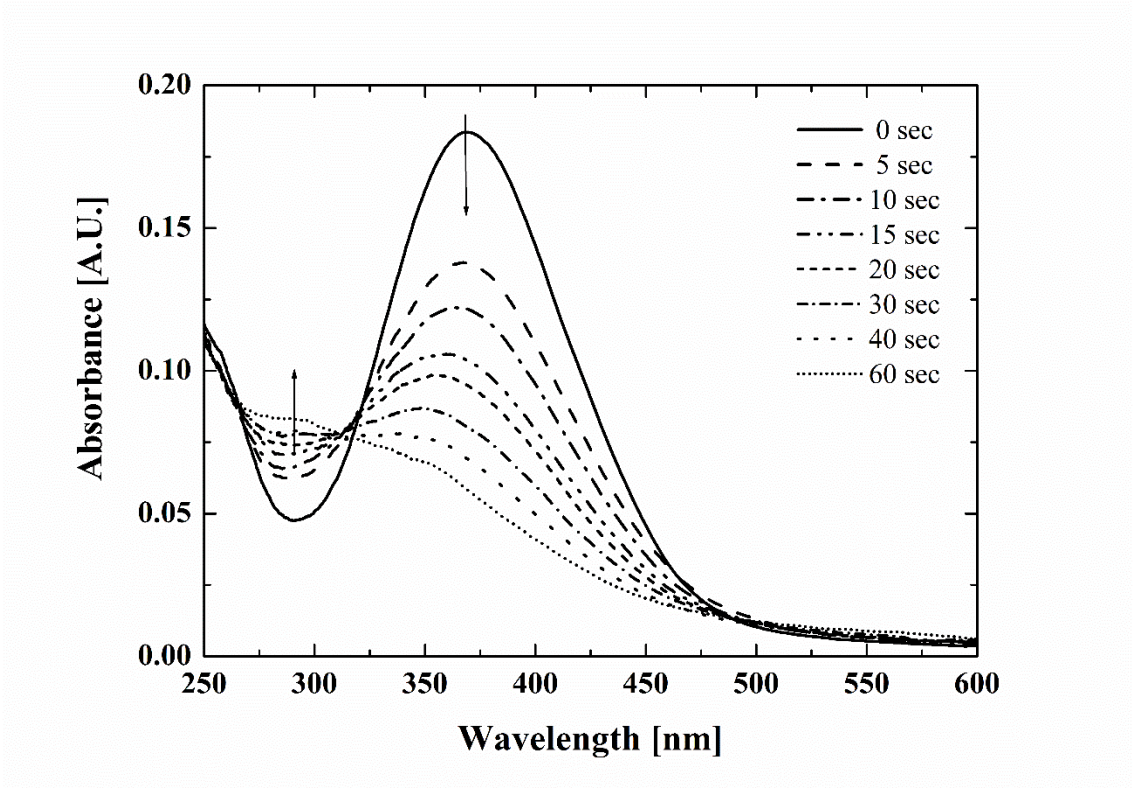

Figure 10. UV-vis absorption spectra of PbisABmC-6dA after LPUVL-irradiation from 0 to 60 s. Film thicknesses of all samples were approximately 25 nm.

The photoreactions of the bisBC units include photoisomerization and photodimerization, as shown in Figure 11.[14,15,21-24]

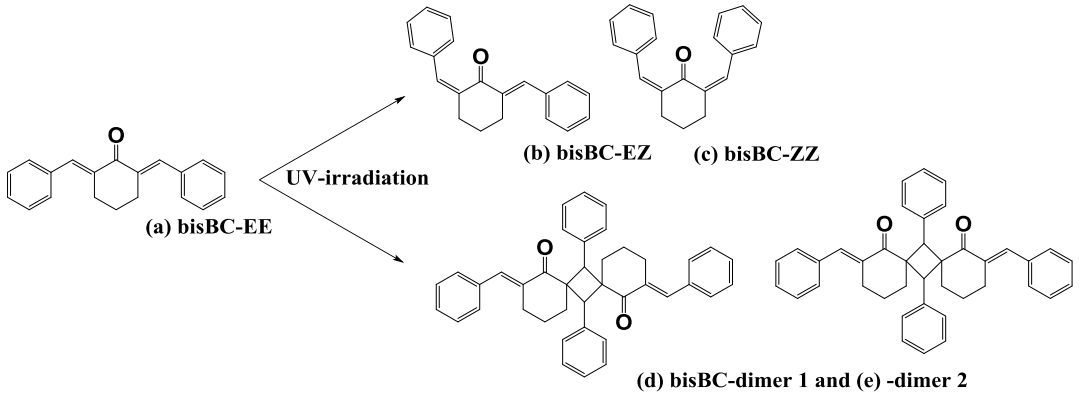

Figure 11. Photoreaction of the bisBC unit.

Calculated UV-vis spectra for model photoproducts of LPUVL irradiation are shown in Figure 11. These spectra were calculated using TD-DFT to reveal the photoreactions of PbisABmC-*i*dA (*i* = 6, 9, and 10). As shown in Figure 12, the absorption peak of the photoisomer of bisBC-EZ (Figure 11 (b)) shifted slightly to a lower wavelength; furthermore, that of bisBC-ZZ (Figure 11 (c)) shifted to much lower wavelengths than both bisBC-EE and bisBC-EZ. The photodimer absorption peaks (Figure 11 (d) and (e)) also moved to lower wavelengths. Therefore, the absorbance at around 290 nm in the spectrum shown in Figure 10 is attributed to either bisBC-ZZ, the dimers, or contributions from both.

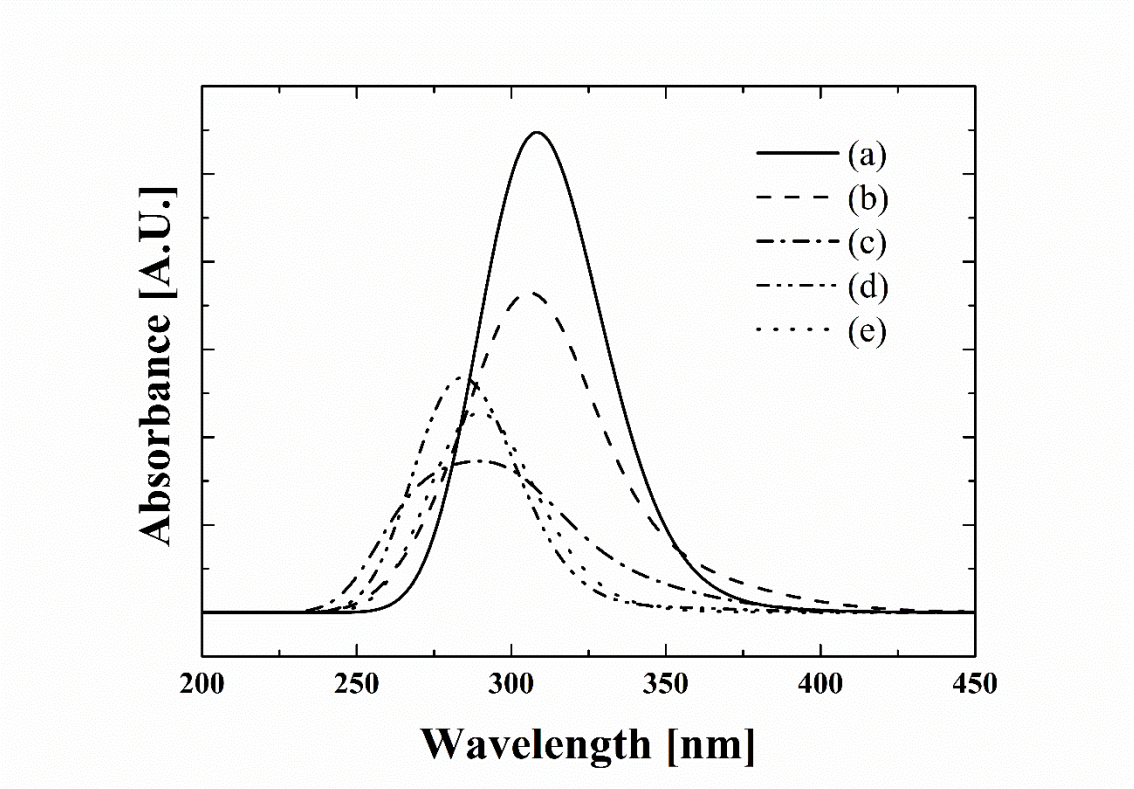

Figure 12. Calculated UV-vis spectra of model molecules using TD-DFT; CAM-B3LYP/6-311++G(d,p) level. (a) bisBC-EE, (b) bisBC-EZ, (c) bisBC-ZZ, (d) bisBC-dimer 1, and (e) bisBC-dimer 2.

To discuss the structural changes that occur in the samples on UV-irradiation, FT-IR spectra of PbisABmC-6dA were measured, and these are shown in Figure 13. The spectrum of a spincoated film after baking at 80 °C for 5 min is shown in Figure 13 (a). In addition, the FT-IR spectrum of a model monomer (Figure 14), a substructure of PbisABmC-6dA, was calculated using DFT and is shown in Figure 13 (b). From the calculated results, the vibrational modes of PbisABmC-6dA can be assigned to the ester C=O stretching at 1741 cm^{-1}, cyclohexanone C=O stretching at 1665 cm^{-1}, benzylidene

cyclohexanone C=C stretching at 1600 cm^{-1}, phenyl C=C bonds at 1507cm^{-1}, coupling of phenyl and aziridine ring stretching at 1289 cm^{-1}, coupling of phenyl and aziridine ring stretching at 1185 cm^{-1}, and coupling including bis(benzylidene)cyclohexanone) at 1149 cm^{-1}. A peak in the experimental spectrum at 2115 cm^{-1} was attributed to the terminally bonded azide in the polymer and the residual monomer. Therefore, except for the peak at 2115 cm^{-1}, the calculated infrared spectrum is consistent with the experimental results.

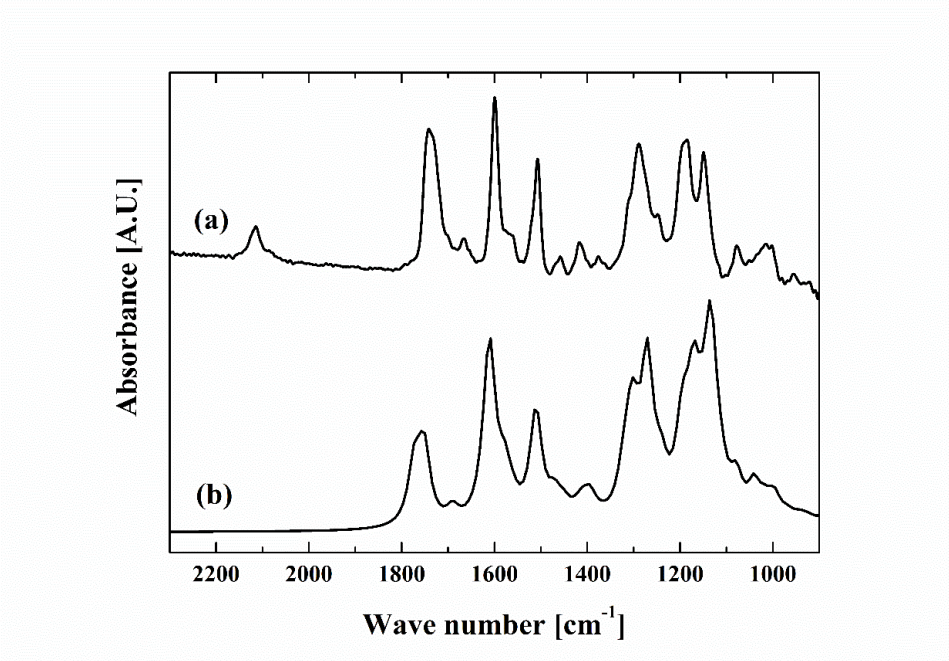

Figure 13. Infrared spectra of (a) PbisABmC-6dA as-baked at 80 °C for 5 min, and (b) that of a model molecule calculated at B3LYP/6-311++G(d,p) level of theory and scaled by 0.983.[25]

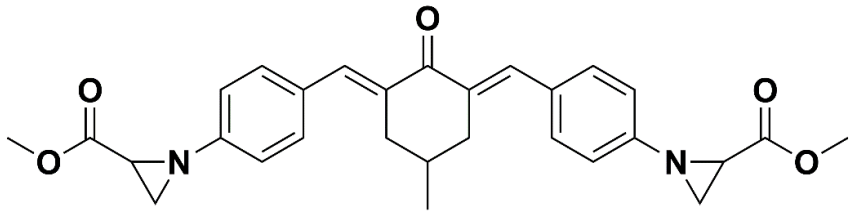

bisABmC-MA-EE

Figure 14. Model molecule for DFT calculation.

Infrared spectra of PbisABmC-6dA thin films at different irradiation doses were measured as shown in Figure 15. The peak at 2115 cm^{-1} disappeared after LPUVL irradiation for 5 s due to photoaddition between azide and C=C double bonds. In addition, the intensity of the peak at 1600 cm^{-1} slightly decreased. As shown in Figures 15 (c) and (d), the peaks at 1600 and 1149 cm^{-1} also declined on irradiation with LPUVL.

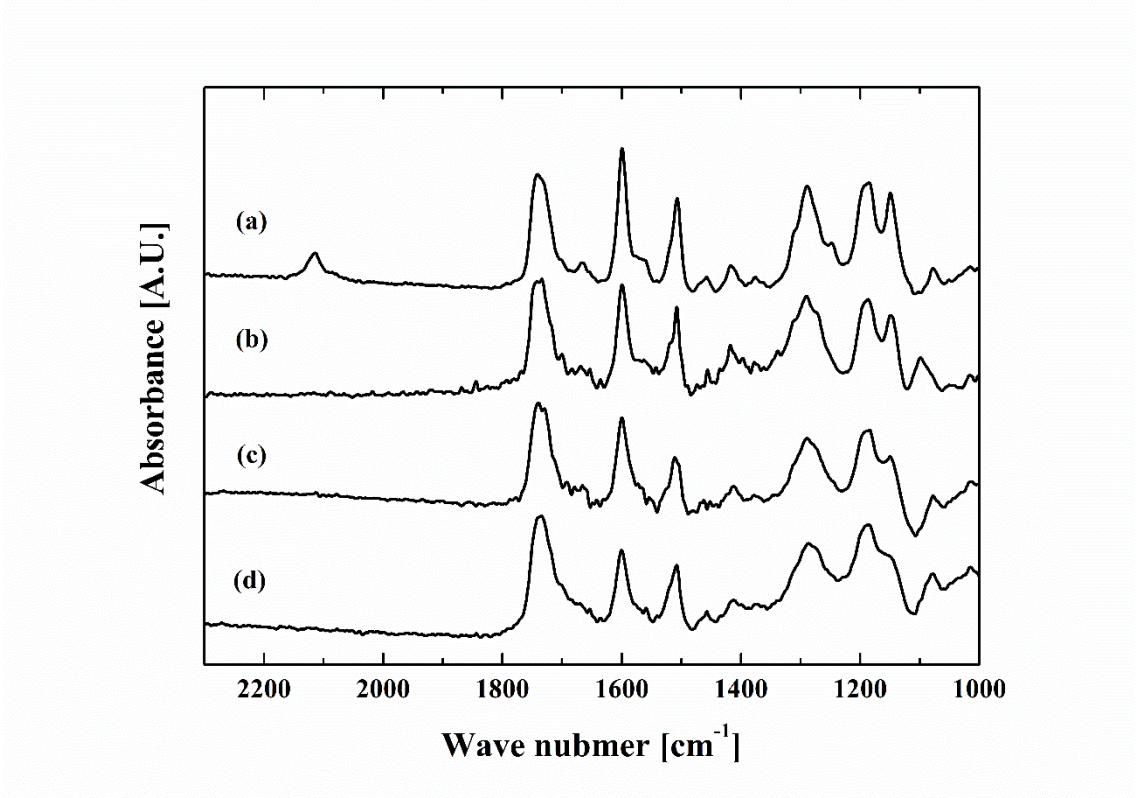

Figure 15. Infrared spectra of PbisABmC-6dA of (a) as-baked at 80 °C for 5 min, (b) LPUVL irradiation for 5 s, (c) 15 s, and (d) 30 s, respectively. Film thicknesses of all samples were about 25 nm.

To show clear experimental evidence for the photodimerization, the amount of photodimerization that occurs at low irradiation dose was estimated by measuring UV-vis spectra of PbisABmC-6dA before/after chemical etching. The photodimerized polymers do not dissolve in solvent due to the cross-linking between polymer chains. To remove the influence of the polymer azide end groups, PbisABmC-6dA without azide groups was synthesized by reaction of PbisABmC-6dA with butyl acrylate (PbisABmC-6dA-BA). FT-IR spectroscopy was used to verify that PbisABmC-6dA-BA

had no azide groups. Chemical etching tests on PbisABmC-6dA-BA thin films were then performed (Figure 16). The spincoated film had absorption maximum around 369 nm; however, this peak disappeared after the sample was dipped in CPN for 30 s at room temperature (Figure 16 (b)), indicating that the film had dissolved in the solvent. In contrast, the spincoated film, irradiated for 5 s (Figure 16 (c)), retained the absorption peak around 369 nm after submersion in CPN for 30 s (Figure 16 (d)). This fact indicates that the photoreaction of PbisABmC-6dA can be largely attributed to the photodimerization of bisBC units, even at low irradiation doses, because the solubility of the polymer to CPN does not change on photoisomerization.

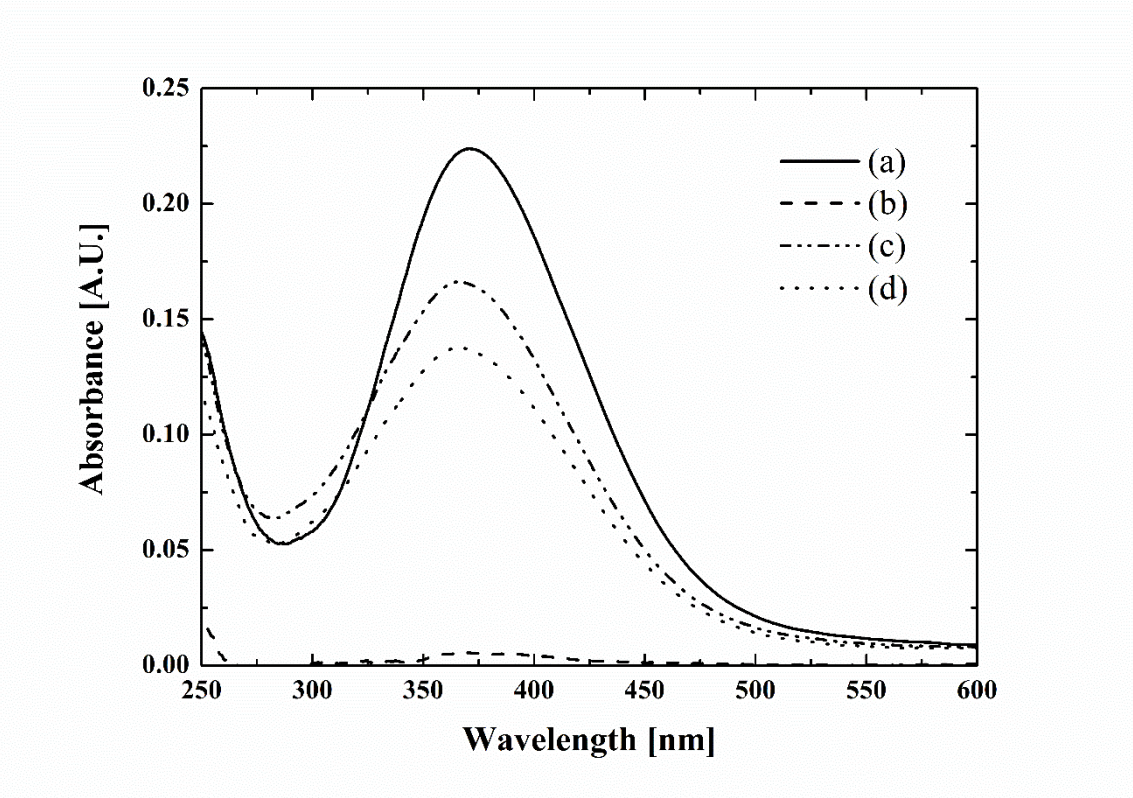

Figure 16. UV-vis spectra of PbisABmC-6dA-BA. (a) Spincoated (1500 rpm for 180 s), (b) dipped in CPN for 30 s at room temperature after (a), (c) irradiated by xenon lamp for 5 s through a wire-gird polarizer and cut-filter below 300 nm after (a), and (d) dipped in CPN for 30 s at room temperature after (c).

Refractive-index anisotropy of PbisABmC-6dA induced by irradiation with LPUVL

Thin films of PbisABmC-6dA after irradiation with LPUVL show dichroism in their UV-vis spectra, and the PLCs were aligned perpendicularly to the LPUVL electric field. Therefore, PLCs were oriented parallel to the direction of unreacted chromophores;

however, the reason for this is not obvious. Therefore, we measured the retardation of the thin films using the photoelastic modulation method to reveal the anisotropy of the refractive indexes of the PbisABmC-6dA films. When the refractive index differs depending on direction, birefringence may be observed by retardation measurements. The retardation, *R*, was calculated according to Equation (3).

$$R = \Delta n \cdot d, \quad \Delta n = n_{\parallel} - n_{\perp} \tag{3}$$

where Δn is the birefringence, and *d* is the film thickness of the sample. $n_{\parallel}$ and $n_{\perp}$ are the refractive index parallel and perpendicular to the LPUVL, respectively. As shown in Figure 17, the retardation of thin film increased negatively with increasing irradiation, and the magnitude of retardation became saturated at high irradiation doses. In this system, since the retardation shows negative values ($n_{\parallel} < n_{\perp}$), the slow axis of retardation is perpendicular to the LPUVL electric field. Therefore, the PLCs were aligned parallel to the slow axis of PbisABmC-*i*dA.

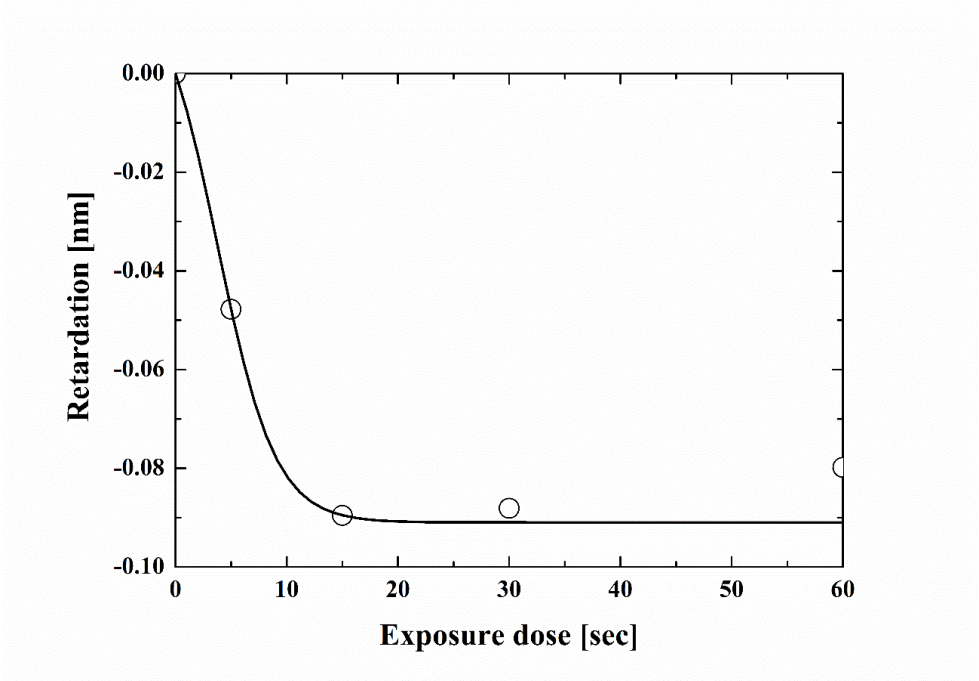

Figure 17. Retardation of PbisABmC-6dA after 80 °C for 5 min. Film thicknesses of sample were approximately 25 nm.

Anisotropic polarizability of PABmC-6dA calculated by DFT

To explain the direction of the slow axis of retardation for PbisABmC-6dA thin films after LPUVL irradiation, DFT calculations were carried out to calculate the anisotropic polarizabilities for model molecules: (a) bisBC-EE, (b) bisBC-EZ, (c) bisBC-ZZ, (d) dimer 1, and (e) dimer 2 (Figure 11). These simple structures are the minimal units related to the photoreaction. The initial ratio of bisBC-EE to the other isomers was calculated from the Boltzmann distribution (Equation (4)).

$$\frac{N_{EE}}{N_{EZ\ or\ ZZ}} = e^{\frac{-(E_{EE}-E_{EZ\ or\ ZZ})}{k_B T}} \quad (4)$$

where N_{EE}, N_{EZ}, and N_{ZZ} are the number of molecules of bisBC-EE, bisBC-EZ, and bisBC-ZZ, respectively. E_{EE}, E_{EZ}, and E_{ZZ} are total energies of bisBC-EE, bisBC-EZ, and bisBC-ZZ. k_B is the Boltzmann constant, and T is the absolute temperature. By comparison of the calculated the energies for bisBC-EE, -EZ, and -ZZ (Table 1), the most stable isomer was found to be bisBC-EE. The ratio of bisBC-EE to the other isomers at room temperature was greater than 99% before LPUVL irradiation. DFT calculations showed that bisBC-EE is the most common isomers.

Table 1. Total energies for bisBC-EE, -EZ, and -ZZ calculated by B3LYP/6-311++G(d,p)

	Total Energy [a.u.]
bisBC-EE	-848.3934
bisBC-EZ	-848.3865
bisBC-ZZ	-848.3807

The polarizabilities of each model molecule were also calculated by DFT. Anisotropic polarizabilities were calculated from Equation (5).

$$\Delta\alpha = \frac{\alpha_{xx} - \frac{(\alpha_{yy}+\alpha_{zz})}{2}}{N} \quad (5)$$

where $\Delta\alpha$ is anisotropic polarizability. α_{xx}, α_{yy}, and α_{zz} are the principal values of polarizability, and *N* is the number of molecules involved in the photoreaction.

Here, the retardation was also expressed as $R = \Delta n \times d$. Refractive index, *n*, is also correlated with polarizability, α, by the Lorentz-Lorenz equation (Equation (6)).[26,27]

$$\frac{n^2-1}{n^2+2} = \rho\frac{N_A\alpha}{3M} \quad (6)$$

where ρ is density of sample, N_A is the Avogadro constant, and *M* is molecular weight. The anisotropic polarizability ($\Delta\alpha$) calculated by DFT correlates directly with the experimental retardation results (Table 2).

Table 2. Polarizabilities and anisotropic polarizabilities.

	Polarizability [a.u.]			
	α_{xx}	α_{yy}	α_{zz}	$\Delta\alpha$
bisBC-EE	472	220	139	293
bisBC-EZ	402	249	159	198
bisBC-ZZ	262	307	184	17
dimer-1	632	461	391	103
dimer-2	608	491	397	82

From the results of the polarizability calculations, $\Delta\alpha$ of unreacted bisBC-EE was the largest of these model molecules. Based on this result, a mechanism for anisotropy generation due to LPUVL irradiation is proposed in Figure 18. Irradiation with LPUVL caused photodimerization along the LPUVL electric field, and the slow axis of retardation arose perpendicularly to the LPUVL electric field because the photoreacted dimer had lower anisotropic polarizability than that of unreacted chromophores. This corresponds to the experimental retardation results obtained by photoelastic measurements (Figure 17). Furthermore, it explains that the orientation order of PCBHA declined as the number of unreacted chromophores (bisBC-EE) decreased due to high temperature annealing (Figure 8). These results suggest that the orientation direction of PLC is mainly determined by the interaction between the PLC and

PbisABmC-*i*dA via the anisotropic van der Waals forces derived from the anisotropic polarizability of PbisABmC-*i*dA.[28,29]

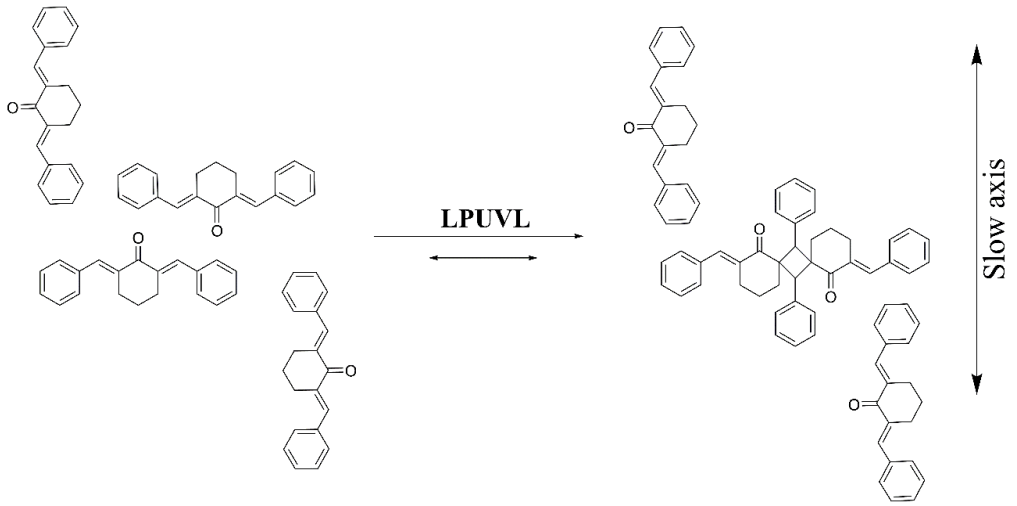

Figure 18. Schematic of photodimerization-induced anisotropy. The direction of irradiated LPUVL electric field is shown as a double-headed black arrow.

3-5. Conclusions

Three kinds of photoreactive amorphous polymers containing bisABmC were synthesized and investigated for use as the photoalignment layer for liquid crystalline materials. The PLCs and LCPs were spun cast onto the thin films and became aligned homogeneously over a wide range of LPUVL irradiation doses. The photosensitivity of the photoalignment layers depended on the baking conditions. The photoalignment layers baked at higher temperatures showed greater photosensitivity, presumably due to disturbance of the surface of the photoalignment layers baked at lower temperatures caused by solvent exposure during PLC spincoating and dry-baking. The thin films baked at high temperature were resistant to the solvent in the PLC solution because the photoalignment layer was thermally cross-linked. Cross-linking occurred between the residual azide and acrylic groups at the polymer tails or between bisBC units in the polymer. In the case of substituting LCP for the PLC, the orientation order of the LCP, decreasing with increasing annealing temperature, did not change on baking at low or high temperatures. This indicates that the orientation of LCP may be dominated by unreacted PbisABmC-6dA chromophores. In addition, the rigidity of polymer due to thermal cross-linking did not aid in the maintenance of the orientation of the LCP against thermal fluctuations at high annealing temperatures.

The liquid crystalline materials on the photoalignment layers were oriented perpendicularly to LPUVL electric field. The slow axis of retardation for the photoalignment layer was determined using the photoelastic modulation method, and the slow axis was found to be perpendicular to LPUVL electric field. In addition, the PLC and LCP were also aligned perpendicular to LPUVL electric field. A generation mechanism for optical retardation was proposed by comparing experimental and calculated anisotropic polarizabilities for model bisBC molecules, calculated using density functional theory. The calculated structures of the photoproducts (photodimers and photoisomers) had small anisotropic polarizabilities. In contrast, the unreacted chromophores showed large anisotropic polarizabilities. Therefore, the polarizability along to LPUVL electric field decreased on LPUVL irradiation. Therefore, the direction perpendicular to the LPUVL became the slow axis of retardation. The calculated anisotropies of polarizability in model molecules explained the experimental retardation results. These results suggest that the PLC orientation direction is mainly determined by the interaction between the PLC and PbisABmC-*i*dA via anisotropic van der Waals forces.

In summary, the polymers containing bisBC had high thermal stabilities, chemical resistance to solvents, and high sensitivities for photoalignment.

3-6. References

(1) Schadt M, Schmitt K, Kozinkov V, Chigrinov V. Surface-Induced Parallel Alignment of liquid crystals by linearly polarized photopolymers. Jpn. J. Appl. Phys. 1992;31:2155-2164.

(2) Makita Y, Natsui T, Kimura S, Nakata S, Kimura M, Matsuki Y, Takeuchi Y. Photo alignment materials with high sensitivityto near UV light. J. Photopolym. Sci. Technol. 1998;11:187-192.

(3) Schadt M, Seiberle H, Schuster A. Optical patterning of multi-domain liquid-crystal displays with wide viewing angles. Nature 1996;381:212-215.

(4) Ichimura K, Suzuki Y, Seki T. Reversible change in alignment mode of nematic liquid crystals regulated photochemically by 'command surfaces' modified with an azobenzene monolayer. Langmuir 1988;4:1214-1216.

(5) Tie W, Jeong IH, Jang IW, Han JS, Liu Y, Li X-D, Lee M-H, Jeong K-U, Lee SH. Reducing driving voltage and securing electro-optic reliability of in-plane switching liquid crystal display by applying polysulfone photoalignment layer with photo-reactive mesogens. Liquid Crystals. 2014;41:1057-1064.

(6) Kang H, Choi Y-S, Kang D, Lee J-C. Photoalignment behaviour on polystyrene films containing chalcone moieties. Liquid Crystals. 2015;42:189-197.

(7) Sheremet N, Kurioz Y, Senenko A, Trunov M, Reznikov Y. Photoalignment in the isotropic phase of liquid crystal on chalcogenide glass film. Liquid Crystals. 2015;42:81-86.

(8) Guo Q, Srivastava AK, Chigrinov VG, Kwok HS. Polymer and azo-dye composite: a photo-alignment layer for liquid crystals. Liquid Crystals. 2014;41:1465-1472.

(9) Schadt M, Seiberle H, Schuster A, Kelly SM. Photo-Generation of Linearly Polymerized Liquid Crystal Aligning Layers Comprising Integrated Optical Patterned Retarders and Color Filters. Jpn. J. Appl. Phys. Part 1.1995;34 :3240-3249.

(10) Schadt M, Seiberle H, Schuster A, Kelly SM. Photo-Induced Alignment and Patterning of Hybrid Liquid Crystal Polymer Films on Single Substrates. Jpn. J. Appl. Phys. Lett. 1995;34:764-767.

(11) Broer DJ, Boven J, Mol GN, Challa G. In-situ photopolymerization of oriented liquid-crystalline acrylates, 3. Oriented polymer networks from a mesogenic diacrylate. Makromol. Chem. 1989;190:2255-2268.

(12) Broer DJ, Hikmet RAM, Challa G. In-situ photopolymerization of oriented liquid-crystalline acrylates, 4. Influence of a lateral methyl substituent on monomer and oriented polymer network properties of a mesogenic diacrylate. Makromol. Chem. 1989:190:3201-3215.

(13) Broer DJ, Mol GN, Challa G. In-situ photopolymerization of oriented liquid-crystalline acrylates, 5. Influence of the alkylene spacer on the properties of the mesogenic monomers and the formation and properties of oriented polymer networks. Makromol. Chem. 1991;192:59-74.

(14) Gangadhara, Kishore K. Novel Photo-Cross-Linkable Liquid Crystalline Polymers: Poly[bis(benzylidene)] Esters. Macromolecules. 1993;26:2995-3003.

(15) Gangadhara, Kishore K. Synthesis and characterization of photo-crosslinkable main-chain liquid-crystalline polymers containing bis(benzylidene)cycloalkanone units. Polymer. 1995;36:1903-1910.

(16) Sampath Kumar HM, Rao MS, Chakravarthy PP, Yadav JS. Enzymatic resolution of N-arylaziridine carboxylates. Tetrahedron: Asymmetry. 2004;15:127-130.

(17) Frisch MJ, Trucks G.W, Schlegel HB, Scuseria GE, Robb MA, Cheeseman JR, Scalmani G, Barone V, Mennucci B, Petersson GA, Nakatsuji H, Caricato M, Li X, Hratchian HP, Izmaylov AF, Bloino J, Zheng G, Sonnenberg JL, Hada M, Ehara M, Toyota K, Fukuda R, Hasegawa J, Ishida M, Nakajima T, Honda Y, Kitao O, Nakai H, Vreven T, Montgomery JA, Peralta JE Jr, Ogliaro F, Bearpark M, Heyd JJ, Brothers E, Kudin KN, Staroverov VN, Kobayashi R, Normand J, Raghavachari K, Rendell A, Burant JC, Iyengar SS, Tomasi J, Cossi

M, Rega N, Millam JM, Klene M, Knox JE, Cross JB, Bakken V, Adamo C, Jaramillo J, Gomperts R, Stratmann RE, Yazyev O, Austin AJ, Cammi R, Pomelli C, Ochterski JW, Martin RL, Morokuma K, Zakrzewski VG, Voth GA, Salvador P, Dannenberg JJ, Dapprich S, Daniels AD, Farkas Ö, Foresman JB, Ortiz JV, Cioslowski J, and Fox D.J.Gaussian09, Revision D.01. Gaussian, Inc., Wallingford CT, 2009.

(18) Becke AD. Density-functional thermochemistry. III. The role of exact exchange. J. Chem. Phys. 1993;98:5648-5652.

(19) Stephens PJ, Devlin JF, Chabalowski CF, Frisch MJ. Ab initio calculation of vibrational absorption and circular dichroism spectra using density functional force fields. J. Phys. Chem. 1994; 98:11623-11627.

(20) Yanai T, Tew DP, Handy NC. A new hybrid exchange-correlation functional using the Coulomb-attenuating method (CAM-B3LYP). Chem. Phys. Lett. 2004;393:51-57.

(21) George H, Roth HJ. Photoisomerisierung und cyclo-1,2-addition α,β-ungesättigter cyclanone. Tetrahedron Lett. 1971;43:4057-4060.

(22) Thomas JM. Diffusionless reactions and crystal engineering. Nature. 1981;289:633-634.

(23) Sakthivel P, Kannan P. Novel thermotropic liquid crystalline-cum-photocrosslinkable polyvanillylidene alkyl/arylphosphate esters. J. Polym. Sci. A Polym. Chem. 2004;42:5215-5226.

(24) Sakthivel P, Kannan P. Thermotropic main-chain liquid-crystalline photodimerizable poly(vanillylidenealkyloxy alkylphosphate ester)s containing a cyclopentanone moiety. Polym. Int. 2005;54:1490-1497.

(25) Sundaraganesan N, Ilakiamani S, Saleem H, Wojciechowski PM, Michalska D. FT-Raman and FT-IR spectra, vibrational assignments and density functional studies of 5-bromo-2-nitropyridine. Spectrochim. Acta A. 2005;61:2995-3001.

(26) Lorentz HA. On the Relation between the Velocity of Transmission of Light and the Density of a Body. Ann. Physik Chemie. 1880;9:641-665.

(27) Lorenz L. The Index of Refraction Ann. Physik Chemie. 1880;11:70-103.

(28) Iimura Y, Saitoh T, Kobayashi S. Liquid crystal alignment on photopolymer surfaces exposed by linearly polarized UV light. J. Photopolym. Sci. Technol. 1995;8:257-262.

(29) Okano K, Matsuura N, Kobayashi S. Alignment of a liquid crystal on an anisotropic substrate. Jpn. J. Appl. Phys. 1982;21:109-110.

Chapter 4

Solvent-induced Surface Enrichment in PMMA/SQ-CI blend

4-1. ABSTRACT

Photo-reactive polymer of silsesquioxane containing citraconimide (SQ-CI) was synthesized and evaluated as a photoalignment layer for polymerizable liquid crystals (PLC). The PLC was aligned on the SQ-CI thin film which is irradiated by linearly polarized ultraviolet light (LPUVL). A generation mechanism of the anisotropy by the LPUVL-irradiation was discussed by comparing the optical retardation of SQ-CI with anisotropic polarizabilities of model molecules calculated by density functional theory. In addition, the SQ-CI and poly(methyl methacrylate) were blended for a model of unification of a photoalignment and a protection layers in liquid crystal display. The orientation of PLC was dominated by the solvent used for the sample preparation of PMMA/SQ-CI. We found that the SQ-CI was enriched at surface of the blend film prepared from the γ-butyrolactone solution, while not in the film prepared from cyclopentanone solution. The surface enrichment in the film prepared from γ-butyrolactone solution does not follow the conventional mechanism in which the lower surface free energy component segregates to the blend surface, because the surface free energy of SQ-CI is higher than that of PMMA.

4-2. Introduction

In liquid crystal displays, the rubbing or photo-alignment process is needed for controlling the orientation direction of liquid crystals. Particularly, the studies of photoalignment method to align liquid crystals have industrial importance in both defect-free alignment of liquid crystals and dust-free process. A number of studies have been performed using the photo-reactive polymers containing cinnamate, chalcone, coumarin and azobenzene at their side chain or main chain of the polymers.[1-7] In addition, the photoalignment by low molecular weight bismaleimides has been also reported.[8] The thin films composed of these photo-reactive materials are able to align liquid crystals by irradiation of linearly polarized ultraviolet light (LPUVL). The generation mechanisms of anisotropy in thin films after the LPUVL irradiation have been proposed for azobenzene, cinnamate, chalcone and coumarin due to photo-dimerization or photo-isomerization.[1-4] On the other hand, polymerizable liquid crystals (PLC) as represented by acryloyl-terminated liquid crystals have been reported for a coatable retarder and a polarizer.[9-13] The cross-linked PLC is thermally-stable due to the formation of three-dimensional cross-linkage via photo-radical polymerization. In these applications, long-term durability of the

photoalignment layer is not required because the PLC is cross-linked by photo-radical polymerization following the orientation on the photoalignment layer. Alternatively, the photoalignment layer for the PLC requires high sensitivity because of high productivity in the manufacturing process. From this aspect, photoalignment method is compatible with the applications utilizing the PLC.

In liquid crystal displays, various functional layers are used such as a black matrix, a color filter, an interlayer insulation film, a protection layer, and an alignment layer.[14-16] The process of coating, drying, thermal curing, and photo-curing are repeated in order to form each layers. The complicated processes have a potential to reduce the yield of products. Therefore, unification of the functional layers is important industrially owing to the reduction of process cycles. In the conventional framework consisting of the photoalignment and protection layer as shown in Figure 1 (a), each layer have to be prepared separately by repeating the process including spin-coating, drying and thermal curing. Furthermore, to modify the surface of first layer for the improvement of wetting, an additional process of UV-ashing on the surface of the first layer is needed before the second layer is spincoated. To avoid the complicated processes, the unification of two layers have been attempted for an antireflection coating.[17] This work was based on the mechanism of segregation of lower surface

free energy component at the surface.[18-23] However, it is difficult to recoat the other layer on the film formed via such a mechanism due to its low surface free energy. To avoid this problem, the UV-ashing at the surface of underlayer is required. The UV-ashing tends to give a serious damage to the photo-induced anisotropy of the photoalignment layer.

In this study, we synthesized a novel photoalignment material of silsesquioxane containing citraconimide (SQ-CI) and investigated unification of a photo-alignment layer for the PLC and a protection layer using a polymer blend having small difference of surface free energy as shown in Figure 1 (b).

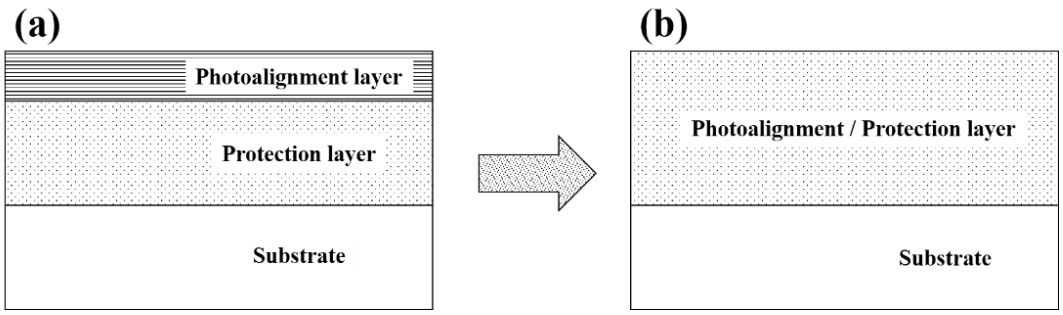

Figure 1. Schematic of unification of two functional layers. (a) conventional framework and (b) new framework consisted of unified one layer of photoalignment and protection layer.

4-3. Experimental section

Materials

Citraconic anhydride, cyclopentanone, γ-butyrolactone, ethanol, n-heptane and toluene were purchased from Tokyo Chemical Industry Co., Ltd. 3-aminopropyltriethoxysilane was obtained from JNC Corp.

As a PLC, LC242 and CBHA were obtained from BASF Japan Ltd. and JNC Petrochemical Corp., respectively. The chemical structures of PLC were shown in Figure 2. Acrylic surfactant (Byk361N) was provided from Big Chemie Co. Ltd. These reagents were used without further purification.

Synthesis of SQ-CI

Photo-reactive SQ-CI was synthesized by a simple method. At first, 50 wt% cyclopentanone solution of citraconic anhydride and 3-aminopropyltriethoxysilane are mixed at equimolar ratio in a flask with a thermometer, a Dimroth condenser at room temperature. Subsequently, the flask was heated up to 80 °C in an oil bath and refluxed for 5 h. The obtained polymer (SQ-CI) was purified by the three cycles of the dissolution-reprecipitation technique using n-heptane. Weight-average molecular weight

of SQ-CI was 3500 as determined by gel permeation chromatography. The chemical structure of SQ-CI is shown in Figure 2 (c).

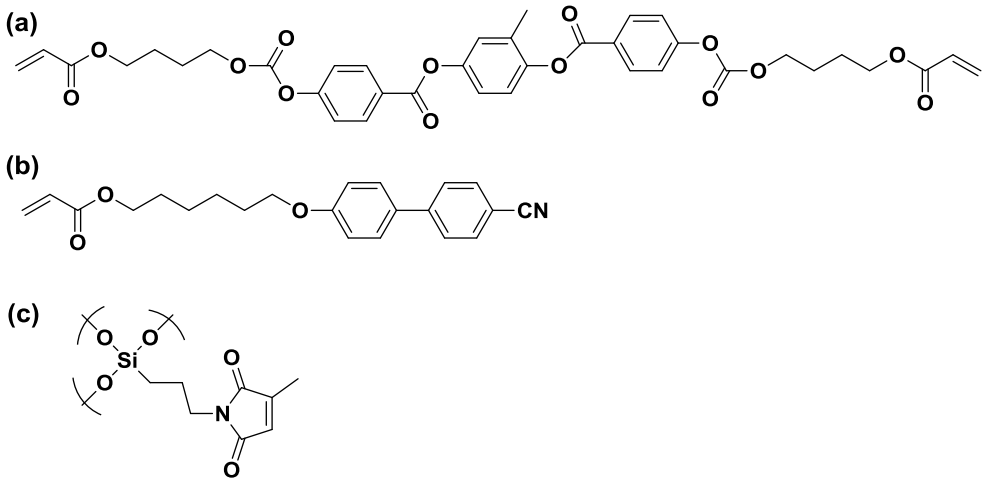

Figure 2. Chemical structures of (a) LC242, (b) CBHA and (c) SQ-CI

Preparation of PLC solution

The composition of PLC sample was LC242 / CBHA / photo-radical generator / surfactant (67/33/3/1) in weight. Two PLCs were blended in equimolar ratio. The detail of the procedure of PLC was as follows. As PLCs, the mixture of 1.000 g of LC242 (1.42 mmol) and 0.4948 g of CBHA (1.42 mmol) was diluted by 13.99 g of toluene with 0.0448 g of photo-radical generator (Irgacure 907) and 0.0149 g of surfactant (Byk-361N). The solution of PLC was finally filtrated through a PTFE membrane filter (average pore size : 0.2 μm).

Measurements

The thin films of the photoalignment layer and the liquid crystalline materials were prepared by a spin-coater (1H-DX, Mikasa Co., Ltd.) on a glass substrate (40 mm square, 0.7 mm thickness (EagleXG), Corning Inc.). Film thicknesses of the thin films were measured by an ellipsometer (SA-101, Photonic Lattice Inc.) and a profilometer (alpha-step P-16, KLA-Tencol Corp.). The LPUVL was obtained by xenon lamp (300W) with Al wire-grid polarizer and cut-filter below 300nm was exposed to the sample film.

An ultraviolet-visible (UV-vis) spectrometer (V-7200, Jasco. Co., Ltd.) was used for evaluation of UV-vis spectra and polarized UV-vis spectra. A polarized optical microscope (BX60, Olympus Corp.) was used for morphology observation of samples. FT-IR measurement was performed by FT/IR6110FF (Jasco. Co., Ltd.). Contact angle measurement was performed by contact angle meter (DM 300, Kyowa Interface Science Co. Ltd.) using water and diiodomethane. Retardation of thin films was measured by photo-elastic modulation method (HINDS INSTRUMENTS, Inc.). Gel permeation chromatography (GPC) measurement was carried out on a SHIMADZU prominence GPC system equipped with polystyrene gel columns, using tetrahydrofran as an eluent after calibration with polystyrene standards.

Calculations

To estimate the optimized structures and the properties of infrared spectra and polarizabilities for the model molecules of photo-products, density functional theory (DFT) calculations were executed by Gaussian09 Revision D.01(Gaussian Inc.).[24] Geometry optimization, vibrational absorption and polarizability were calculated by B3LYP hybrid functional, which employs the Becke exchange and LYP correlation functions and Gaussian basis set of 6-311++G(d,p).[25,26] In addition, the calculations of excited states were executed by time-dependent DFT (TD-DFT) method in CAM-B3LYP functional.[27]

4.4. Results and discussion

4.4.1 Photoalignment of PLC using SQ-CI single layer

Polarized UV-vis spectra of PLC on SQ-CI thin film

At first, to confirm the photoalignmentability of the SQ-CI single layer, the thin films of the PLC were formed on the SQ-CI after the LPUVL irradiation in the following manner. The 3.0 wt% solution of SQ-CI in cyclopentanone was spin-coated on a glass substrate. The film thicknesses of the sample was approximately 80 nm measured by the ellipsometry. Thin films of SQ-CI were thermally treated from 100 to 230°C for 5

minutes, respectively. The thin films were LPUVL-irradiated for 5 s. Subsequently, PLC solution was spincoated on the SQ-CI thin film, dried at 80°C for 1 min for evaporating the solvent and quenched to room temperature. After that, the ordered PLC thin film was photo-cured for 20 s in nitrogen atmosphere at room temperature. In Figure 3, polarized UV-vis spectra of the PLC thin film showed the obvious difference between absorbances parallel and perpendicular to the direction of LPUVL electric field. The fact suggests homogeneous alignment of the PLC. The peak at 297 nm is attributed to the CBHA from a result of dilute solution of CBHA in acetonitrile. The absorbance of CBHA perpendicular to the LPUVL at 297 nm was larger than that of CBHA parallel to the LPUVL. Transition dipole moment of CBHA at 297 nm was parallel to the molecular long axis in consequence of the calculation result by TD-DFT. Therefore, this indicates that the orientation direction of the molecular long axis, i.e. the direction of mesogen was perpendicular to the LPUVL. Therefore, the order parameter of the PLC thin film is able to be estimated by the polarized UV-vis spectra.

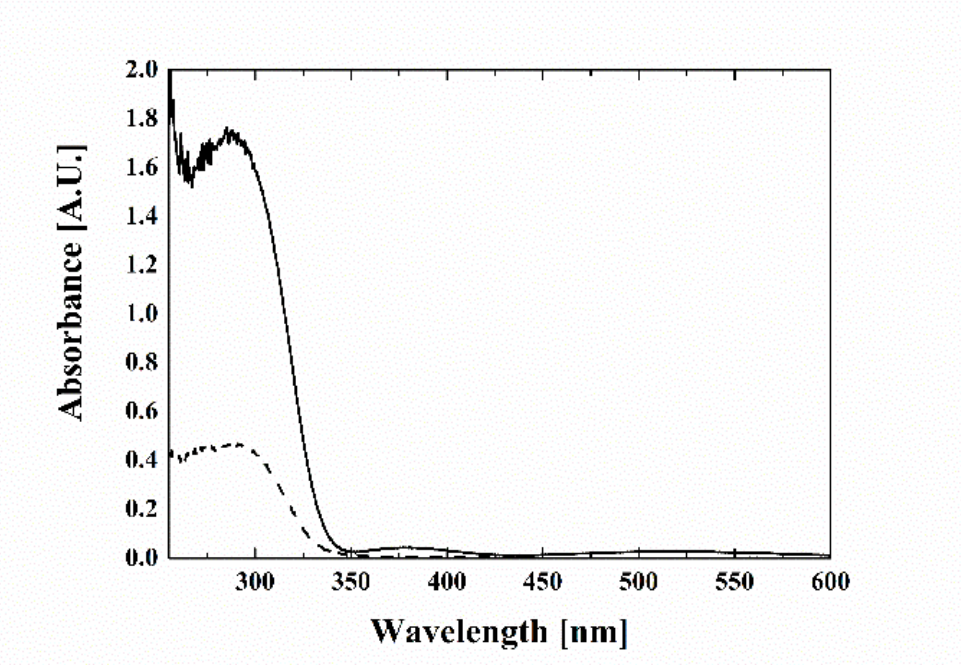

Figure 3. Polarized UV-vis spectra of PLC on SQ-CI thin film irradiated by xenon lamp for 5 seconds with cut-filter below 300 nm after the baking at 130 °C for 5 min. Solid and dashed lines show the absorbance perpendicular and parallel to LPUVL, respectively.

Thermal treatment and irradiation dose dependence on order parameter of PLC

Irradiation time dependence of an order parameter of the PLC thin film was estimated by polarized UV-vis spectrscopy. The order parameter of the PLC was calculated by the absorption peak at 297 nm attributed to CBHA. The order parameter S was defined as below.

$$S = \frac{A_{\parallel} - A_{\perp}}{A_{\parallel} + 2A_{\perp}},$$

where $A_{\parallel}$ and $A_{\perp}$ are absorbances parallel and perpendicular to the LPUVL electric field, respectively. S value at complete orientation of CBHA parallel to the LPUVL electric field is 1.0 and that of CBHA perpendicular to the LPUVL electric field is -0.5. The thermal treatment temperature of the SQ-CI thin film was from 100 °C to 230 °C, in order to evaluate the influence on photoalignmentability of PLC for the SQ-CI thin film. In Figure 4, the PLC aligned homogeneously on the SQ-CI thin film in the wide range of the LPUVL-irradiation. The orientatoin direction of the PLC was perpendicular to the LPUVL electric field, because the order parameter of the PLC was constantly negative.

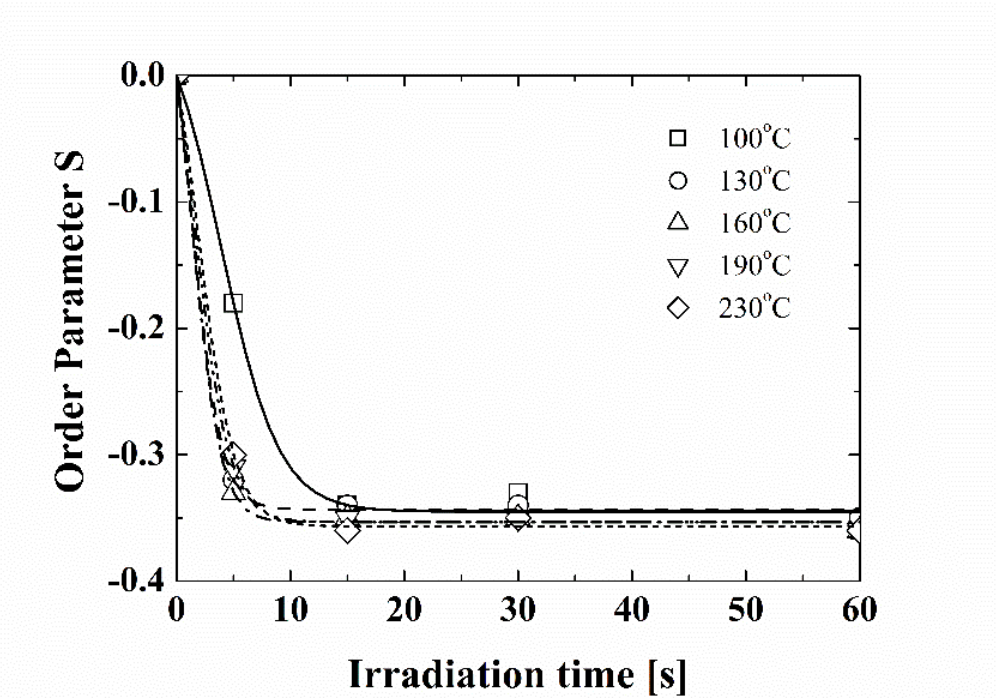

Figure 4. Thermal treatment temperature and irradiation time dependences on order parameter of PLC on SQ-CI thin film.

Photoreaction of SQ-CI single layer

To reveal photoreaction of the SQ-CI, the change of UV-vis spectra caused by LPUVL-irradiation were measured. As shown in Figure 5 (a) and (b), the SQ-CI thin film showed a strong peak at 217 nm and a weak peak around 300 nm in UV-vis spectrum before the irradiation. Both peaks diminished with the irradiation time. The photoreaction of SQ-CI occured by an electronic excitation contributed to the peak around 300 nm because the wavelength of LPUVL-irradiation is above 300 nm by a xenon lamp with the cut-filter below 300 nm.

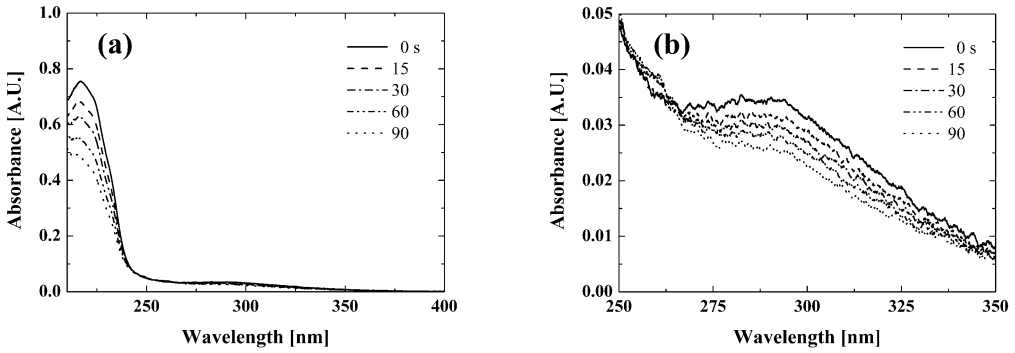

Figure 5. LPUVL-irradiation time dependence of UV-vis spectra of SQ-CI thin film. (a) Wavelength is ranging from 210 nm to 400 nm, and (b) from 250 nm to 350 nm, respectively. LPUVL was irradiated through a cut-filter below 300 nm.

In Figure 6, FT-IR spectra of SQ-CI with the increase of LPUVL irradiation were measured in order to reveal the change of molecular structure in SQ-CI by the irradiation. In comparison to the DFT calculation of model molecules of SQ-CI, the

peak at 1407 cm^{-1} was assigned to C=C and C-N coupling vibration of citraconimide. The C=C double bond decreased by the irradiation and the peaks at 1366 cm^{-1} and 1352 cm^{-1} arose simultaneously.

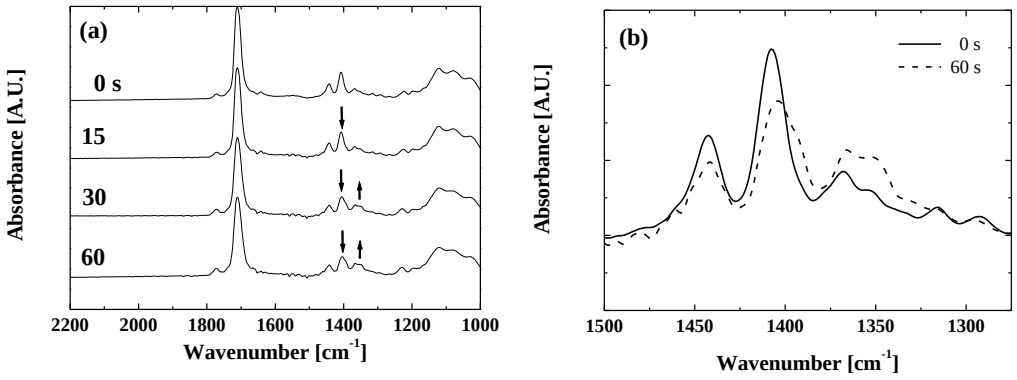

Figure 6. LPUVL-irradiation time dependence of FT-IR spectra of SQ-CI. (a) Irradiation time is 0 s, 15 s, 30 s, and 60 s, respectively. (b) Enlarged drawing of irradiation time for 0 s and 60 s is ranging from 1275 cm^{-1} to 1500 cm^{-1}.

The photoproducts of maleimide are well-known, and it is a photo-dimer and a photoproduct derived from radical reaction.[28-30]

FT-IR spectra of the model molecules (n-propyl citraconimide, n-propyl citraconimide dimer, n-propyl and citraconimide radical product) were calculated by the DFT method to assign the molecular vibrations of SQ-CI. The calculated infrared spectra in Figure 7 (a) was scaled by 0.967, to compare with the experimental result. The experimental result after the irradiation for 60 s (Figure 7 (b)) was fitted by gaussian functions based on the peak positions obtained by the DFT calculations in Figure 7 (a). The fitting

succeeded in light of the contribution of both model molecules. As a result, the photoreaction of SQ-CI presumably contained photodimerization and photoradical reaction.

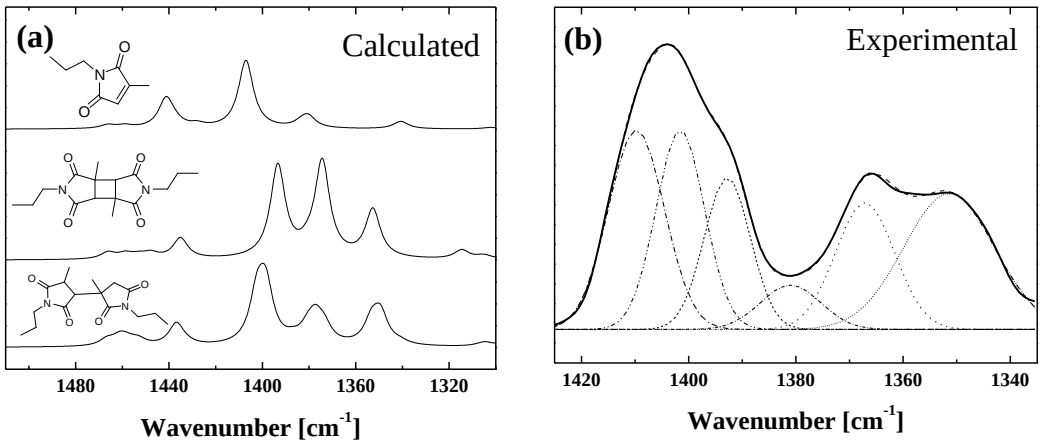

Figure 7. Identification of infrared spectrum for irradiated SQ-CI using DFT calculation. (a) Calculated spectra of model molecules using CAM-B3LYP/6-311++G(d,p) level and (b) peak separation of FT-IR spectrum for SQ-CI after irradiation for 60 s. Peaks were fitted by gaussian functions based on the calculated results.

Photo-induced anisotropy of SQ-CI

To confirm the photo-induced anisotropy of the SQ-CI after irradiation by LPUVL, an optical retardation of the SQ-CI thin film were measured by photo-elastic modulation method. When threre is the difference of refractive index depending on the direction, the birefringence may be observed by retardation measurement. The retardation R was expressed as below.

$$\mathrm{R} = \Delta n \cdot d, \quad \Delta n = n_{\parallel} - n_{\perp},$$

where Δn is birefringence and d is film thickness of the sample. $n_{\parallel}$ and $n_{\perp}$ are the refractive index parallel and perpendicular to the LPUVL respectively. As shown in Figure 8, the retardation of SQ-CI thin film increased negatively with the irradiation and the magnitude of retardation was saturated at high irradiation dose. In this system, the slow axis of retardation is perpendicular to the irradiated LPUVL electric field because the retardation shows negative values ($n_{\parallel} < n_{\perp}$). Therefore, the PLC aligned parallel to the slow axis of SQ-CI.

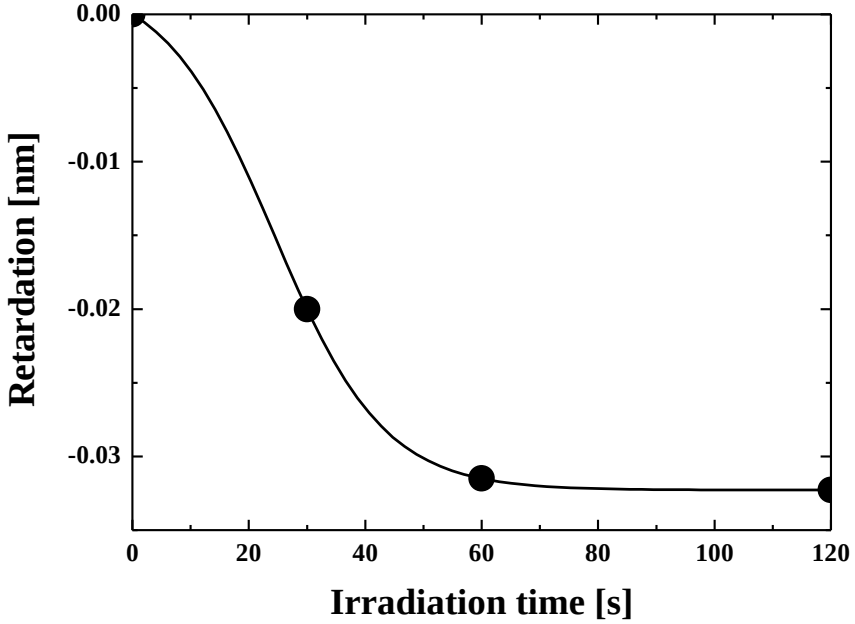

Figure 8. Retardation of SQ-CI thin film after the drying at 80°C for 5min. Film thickness of sample was approximately 80 nm.

Anisotropy of SQ-CI calculated by DFT

To explain the direction of slow axis of retardation for SQ-CI thin film after LPUVL-irradiation, the DFT calculation of anisotropic polarizability was performed for model molecules of (a) methyl citraconimide, (b) methyl citraconimide dimer, and (c) methyl citraconimide radical product. These simple structures were the minimal unit related to the photo-reaction. Polarizabilities of each model molecules were calculated by B3LYP/6-311++G(d,p) level. Anisotropic polarizability was given by following expression.

$$\Delta\alpha = \frac{\alpha_{xx} - \frac{(\alpha_{yy} + \alpha_{zz})}{2}}{N}$$

where $\Delta\alpha$ is anisotropic polarizability. α_{xx}, α_{yy} and α_{zz} are the polarizabilities along x-, y- and z-axis, respectively. The x-axis of molecule is along the long axis of molecule and is corresponding to the direction of transition dipole moment in methyl citraconimide determined by time-dependent DFT method. The y-axis is along the short axis of the molecule. *N* is number of molecules involved in the photoreaction.

Here, refractive index *n* is also correlated with polarizability α by Lorentz-Lorenz equation below.[31,32]

$$\frac{n^2 - 1}{n^2 + 2} = \rho \frac{N_A \alpha}{3M}$$

where ρ is density and N_A is Avogadro number. *M* is molecular weight. The anisotropic polarizability ($\Delta\alpha$) calculated by DFT was regarded as correlating with the experimental results of retardation. The calculated results of $\Delta\alpha$ were summarized in Table 1. The difference of dimer 1, 2, and 3 is the position of methyl and hydrogen group chemically bonded to cyclobutane of the dimer. Although other isomers exist for the dimerization of the model molecule, other isomers had larger bended-shape and lower anisotropic polarizability than dimer 1, 2, and 3. The model molecule of radical product also showed lower anisotropic polarizability than unreacted monomer. Therefore, the $\Delta\alpha$ of unreacted citraconimide was largest than the other photo-products.

These results indicated that the slow axis of retardation was perpendicular to the LPUVL electric field due to the difference between unreacted and reacted anisotropic polarizability of citraconimide.

Table 1. Anisotropic polarizabilities calculated by DFT method at B3LYP/6-311++G(d,p) level for model molecules of SQ-CI.

	Molecular structure **xz-plane**	**Anisotropic polarizability (atomic unit)** $\frac{\alpha_{xx} - \frac{(\alpha_{yy} + \alpha_{zz})}{2}}{N}$
Methyl citraconimide monomer 	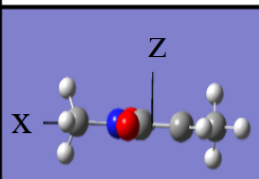	**28.1**
Methyl citraconimide dimer 1 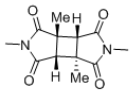		**17.3**
Methyl citraconimide dimer 2 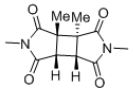	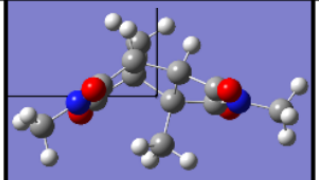	**17.3**
Methyl citraconimide dimer 3 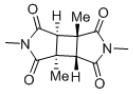	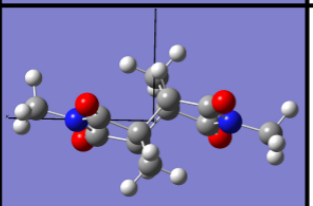	**18.4**
Methyl citraconimide radical product 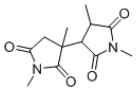	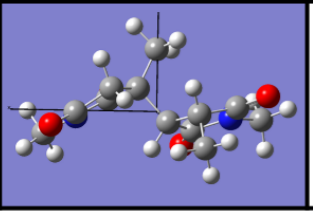	**18.1**

4.4.2 Unification of protection layer and photoalignment layer

The unification of a protection layer and a photoalignment layer for liquid crystal displays were investigated by polymer blend as shown in Figure 1. Poly(methyl methacrylate) (PMMA) as a simple model polymer for the protection layer and the SQ-CI as a photoalignment layer were blended. The 5 wt% of PMMA/SQ-CI (95/5) in cyclopentanone solution was prepared. PMMAs with different weight-average molecular weight (114k, 396k, and 821k) were used for the sample preparation. The sample solution was spin-coated and dried at 80 °C for 5 min. Subsequently, to confirm the influence on thermal treatment temperature for photoalignmentability, the blend film was thermally treated at 130, 160, 190 and 230 °C for 5 min, respectively. The blend film was irradiated by the LPUVL for 30 s and the PLC solution was spin-coated on the irradiated blend film. The PLC thin film was dried at 80 °C for 1 min to evaporate the solvent. However, the PLC was not aligned under all experimental conditions as shown in Figure 9.

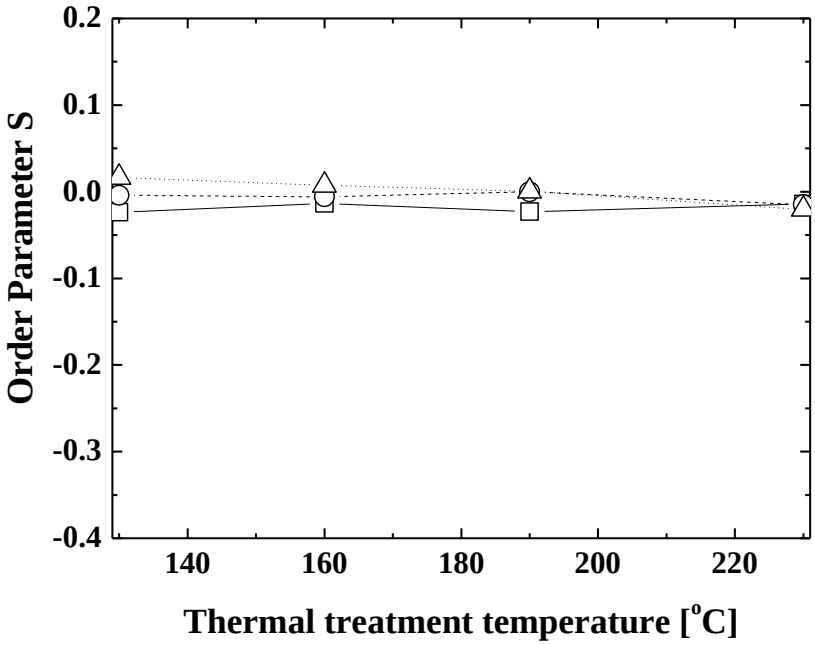

Figure 9. Thermal treatment temperature dependence on order parameter of the PLC on PMMA/SQ-CI (95/5) thin film prepared from 5 wt% solution of cyclopentanone. Open square, circle, and triangle show the result of Mw =821k, 396k and 114k for PMMA, respectively.

The composition dependence of photoalignmentability for PMMA/SQ-CI blend was investigated as shown in Figure 10. The PLC was finally aligned at least more than 20 wt% of SQ-CI in PMMA/SQ-CI system.

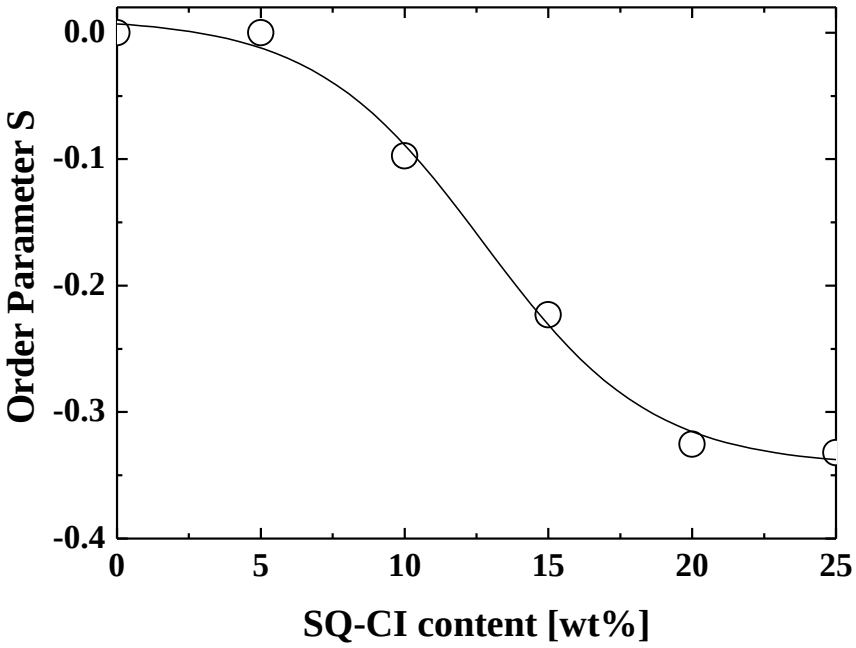

Figure 10. SQ-CI content dependence on order parameter of the PLC. Cyclopentanone solutions of PMMA/SQ-CI (95/5, 90/10, 85/15, 80/20, 75/25) were evaluated in the same manner as shown in Figure 9.

However, a lesser content of the SQ-CI than 20 wt% is preferable because the photoalignment layer is required only at surface of the film to align liquid crystals. Here, we assumed that the surface composition of PMMA/SQ-CI was enabled to change via the drying process of solvent, because the solvent evaporates through the surface of the film along the thickness direction. The difference of affinity between the polymer and solvent possibly affect the surface composition. A solution of γ-butyrolactone as substitute for cyclopentanone was prepared for the composition of PMMA/SQ-CI (95/5),

to evaluate the solvent effect. The 5 wt% of the blend in γ-butyrolactone solution was spincoated on the glass substrate and dried at 80 °C for 5 min. Subsequently, the film was thermally treated at 130, 160, 190, and 230 °C for 5 min, respectively. The PLC solution was spin-coated on the film after the LPUVL-irradiation for 30 s. As shown in Figure 11, the PLC was aligned under all of the experimental conditions.

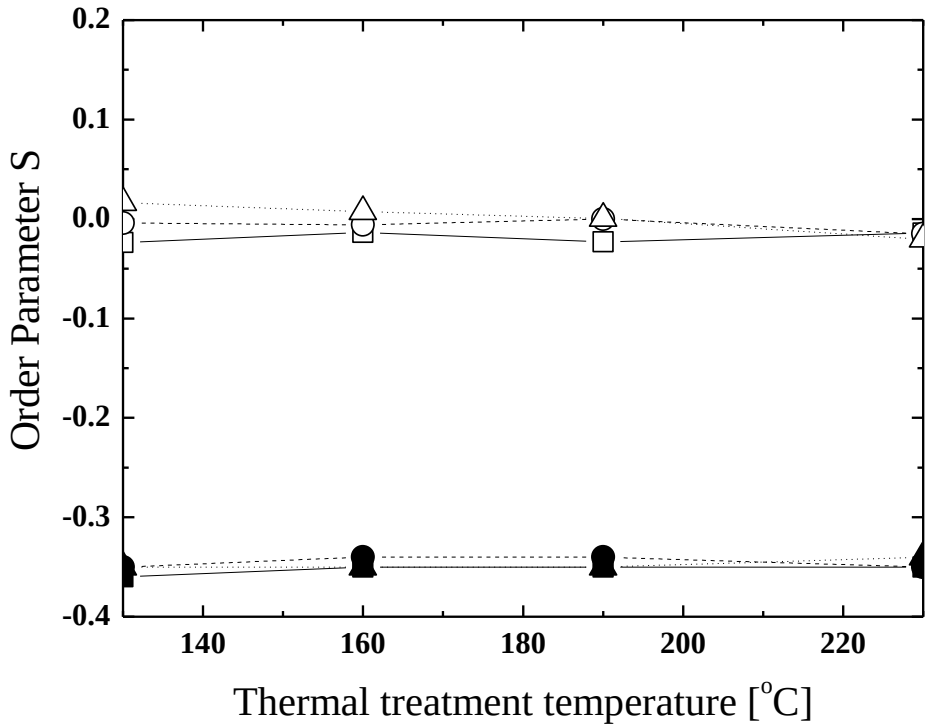

Figure 11. Thermal treatment temperature dependence on order parameter of PLC on PMMA/SQ-CI (95/5) thin film prepared from 5 wt% solution of γ-butyrolactone. Filled square, circle, and triangle show the results in the case of Mw=821k, 396k, and 114k for PMMA prepared from γ-butyrolactone solution and open square, circle, and triangle show the results prepared from cyclopentanone solution, respectively.

The surface composition of the blend film was estimated by surface free energy of PMMA, SQ-CI and PMMA/SQ-CI blend. As shown in Figure 12, surface free energy of SQ-CI was larger than PMMA for the thin films prepared by both cyclopentanone and γ-butyrolactone solution. In addition, surface free energy of PMMA/SQ-CI blend was larger than that of PMMA. Assuming an additivity of composition for surface free energy of PMMA and SQ-CI, we were able to estimate the surface composition of PMMA/SQ-CI blend. As shown in Figure 13, the estimated surface composition of SQ-CI was 7.5 wt% for the film prepared from cyclopentanone solution and that of SQ-CI was 25 wt% for the film prepared from γ-butyrolactone solution. Considering the thin film of PMMA was not able to align the PLC after the LPUVL irradiation, the results of surface composition estimated by surface free energy and the photoalignmentability of the PLC indicated that the SQ-CI was enriched to the surface of thin film prepared from γ-butyrolactone solution. Therefore, the solvent played an important role of surface composition of PMMA/SQ-CI blend.

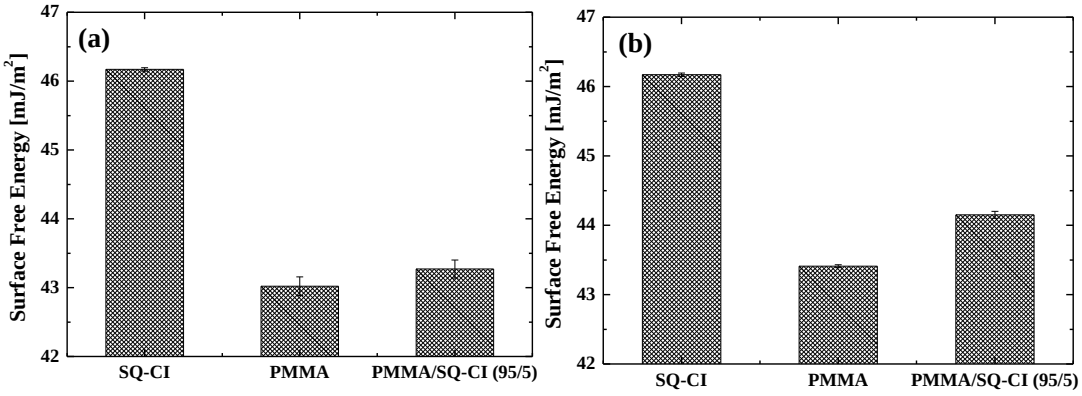

Figure 12. Surface free energy of PMMA, SQ-CI, and PMMA/SQ-CI (95/5). Thin films were prepared by (a) cyclopentanone solution, and (b) γ-butyrolactone solution. The thin films were thermally treated at 190 °C for 5 min, respectively.

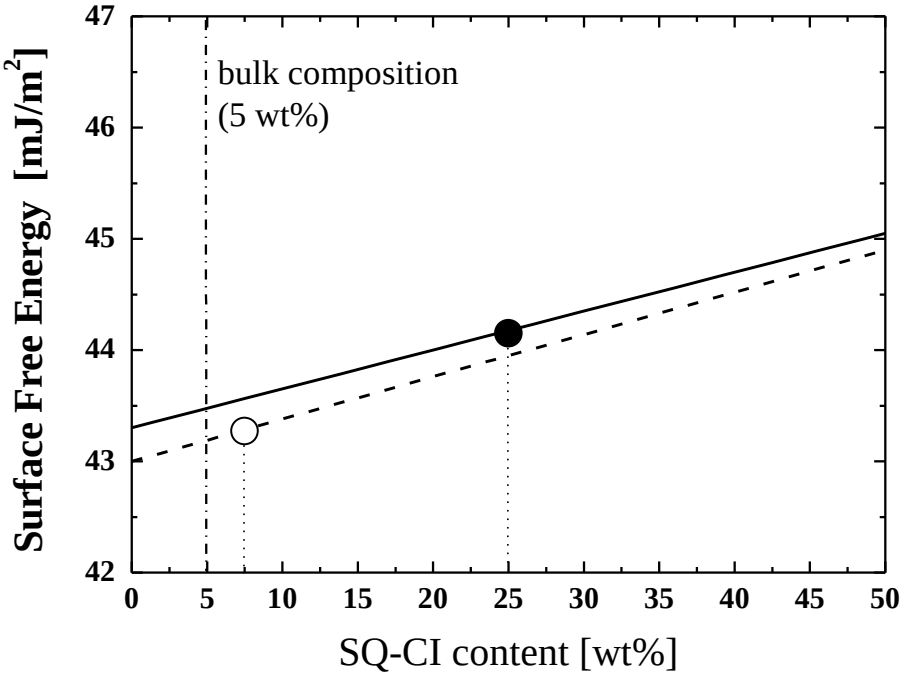

Figure 13. Surface composition of PMMA/SQ-CI estimated by surface free energy. Filled and open circle show the experimental value of surface free energy for the film prepared from γ-butyrolactone and cyclopentanone,

The surface free energy dependence on the content of SQ-CI in PMMA/SQ-CI blends was shown in Figure 14. This result indicated the SQ-CI segregated at the surface in the film prepared from γ-butyrolactone solution even at low content of the SQ-CI.

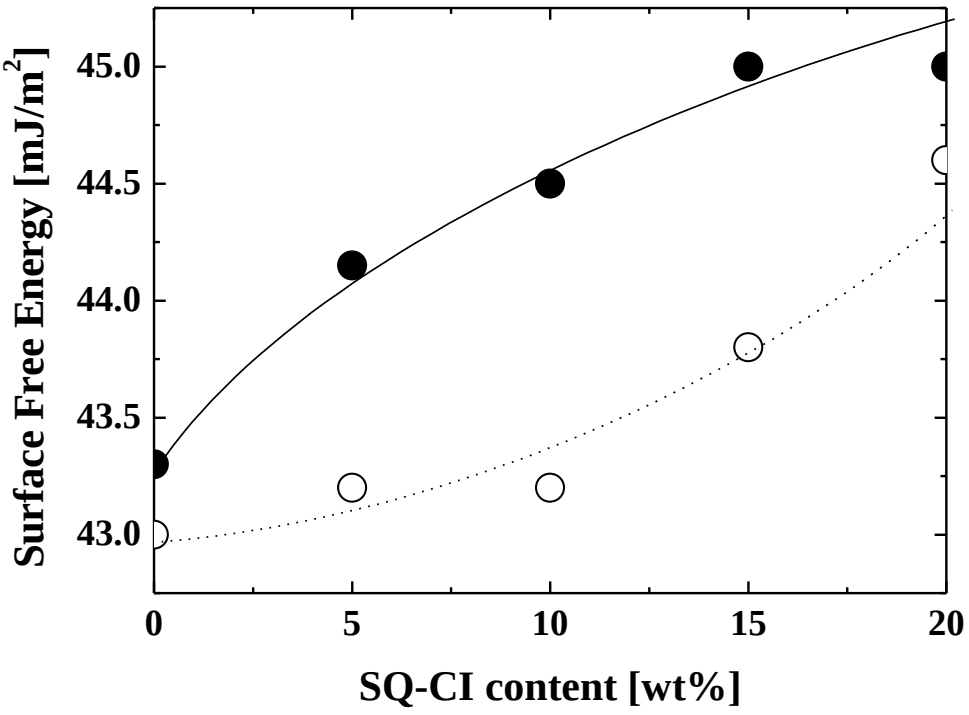

Figure 14. SQ-CI dependence of surface free energy for PMMA/SQ-CI. Open and filled circle show thin films prepared by γ-butyrolactone and cyclopentanone solution, respectively.

In general, surface enrichment in polymer blends due to the difference of surface free energy have been reported.[17-23] In the case, a polymer component having low surface free energy thermodynamically segregated to the surface of the film. However, our result as shown in Figure 11 cannot be explained by using this mechanism. The SQ-CI had low weight-average molecular weight (Mw=3.5k) and flexible structure and was easily soluble to both γ-butyrolactone and cyclopentanone. Thus, solubility of PMMA into the solvent was confirmed by estimating overlap concentration of PMMA in γ-butyrolactone or cyclopentanone as shown in Figure 15. According to scaling theory, an overlap concentration C^* for the solution is related to gyration of radius of a polymer as follows.[33]

$$C^* \cong \frac{N}{{R_g}^3} = 6a^{-3}N^{1-3\nu}$$

where N, R_g, a, and ν are degree of polymerization, radius of gyration, monomer length, and universal exponent, respectively. The C^* is correlated to the R_g, and the R_g of the polymer in the solvent reflects the solubility of the polymer in the solvent. The Rg of the polymer is enlarged in good solvent and then C^* becomes small. The result in Figure 15 indicated that PMMA in γ-butyrolactone had lower solubility than PMMA in cyclopentanone. In addition, the result in Figure 15 agreed with the prediction by solubility parameter because the value of cyclopentanone close to that of PMMA as

shown in Table 2.[34]. In the aspect of solubility parameter, PMMA has lower solubility in γ-butyrolactone in comparison to cyclopentanone because of large difference between solubility parameter of PMMA and γ-butyrolactone.

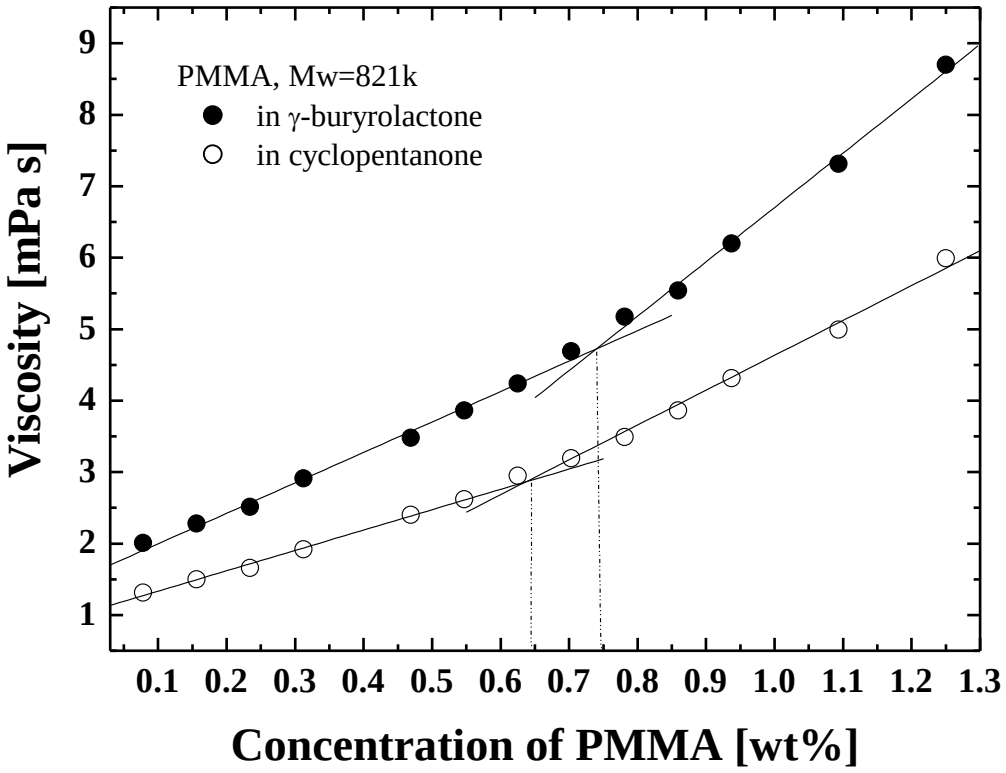

Figure 15. Overlap concentration of PMMA. Open and filled circle show results of PMMA (Mw = 821k) in cyclopentanone and in γ-butyrolactone, respectively.

Table 2. Hansen solubility parameter of PMMA, cyclohexanone, and γ-butyrolactone.[34]

	HSP $(MPa)^{1/2}$			
	δ_d	δ_p	δ_h	δ^a
Poly(methyl mathacrylate)	**18.6**	**10.5**	**7.5**	**22.6**
cyclopentanone	**17.9**	**11.9**	**5.2**	**22.1**
γ-butyrolactone	**19**	**16.6**	**7.4**	**26.3**

a $\delta = (\delta_d^2 + \delta_p^2 + \delta_h^2)^{1/2}$

To confirm solvent-induced enrichment from the other point of view, solvent-vapor annealing method for the thin film prepared from cyclopentanone solution was performed. Experimental procedure is as follows. The 5 wt% solution of PMMA/SQ-CI (95/5) in cyclopentanone was spin-coated on a glass substrate. The drying of the blend film was executed at 80 °C for 1 min to remove solvent from the film. The film was exposed by the vapor of γ-butyrolactone or cyclopentanone for 8 min. Subsequently, the film dried at 80 °C for 5 min and then treated with heat at 190 °C for 5 min. The result of surface free energy analysis for the thin film after solvent-vapor annealing was shown in Figure 16. The surface free energy of non-annealed PMMA/SQ-CI (95/5) film and PMMA film were also measured for comparison. Non-annealed film of

PMMA/SQ-CI (95/5) prepared from cyclopentanone solution did not show the large difference of surface free energy, compared with the PMMA film. Therefore, SQ-CI was not enriched at the surface of the film. However, it was suggested that SQ-CI was enriched at the surface of the film for γ-butyrolactone-annealed film because the film indicated that higher surface free energy than non-annealed film. In addition, the surface free energy of cyclopentanone-annealed film showed a value between non-annealed film and γ-butyrolactone-annealed film. This shows lower surface enrichment of SQ-CI than the film annealed by γ-butyrolactone. On the other hand, the result of ethanol-annealed film showed an interesting result. PMMA and SQ-CI do not dissolve in ethanol. However, ethanol-annealed film indicated larger surface free energy than the film annealed by cyclopentanone. The SQ-CI has high affinity for ethanol because total Hansen solubility parameter of ethanol (26.5 $MPa^{1/2}$ [34]) is close to γ-butyrolactone. This fact suggested that the affinity for solvent controlled surface composition of the blend. To confirm the surface enrichment of SQ-CI, we next examined the photoalignmentability of PLC on the LPUVL-irradiated film after the solvent-vapor annealing. As shown in Figure 17, the film without the solvent-vapor annealing (Non-annealed) was not able to align the PLC homogeneously (S ~ 0). However, the film with solvent-vapor annealing by γ-butyrolactone was able to align the PLC (S =

-0.33). In addition, the blend film of solvent-vapor annealing by cyclopentanone slightly enhanced the aligning of the PLC. These results indicated that the SQ-CI strongly segregated to the surface of the blend film during the solvent-vapor annealing of γ-butyrolactone. From the results, the mechanism of the surface enrichment of the SQ-CI by solvent-vapor annealing can be described as follows. In the solvent-vapor annealing, γ-butyrolactone exists in the gas phase adjacent to the surface of blend film. In addition to that, the surface of the blend film was plasticized by γ-butyrolactone vapor. Therefore, it is considered that both the situations induced the surface enrichment of the SQ-CI which has higher affinity with γ-butyrolactone.

Based on the result of solvent vapor annealing, we concluded as follows.

In the case of the blend film prepared from γ-butyrolactone solution by spin-coating, it was suggested that γ-butyrolactone vapor exists near the surface of blend film through the spin-coating and drying process as with the solvent-vapor annealing process. The surface enrichment was caused by the difference of affinity between the components in the blend and the solvent during the spin-coating and drying processes.

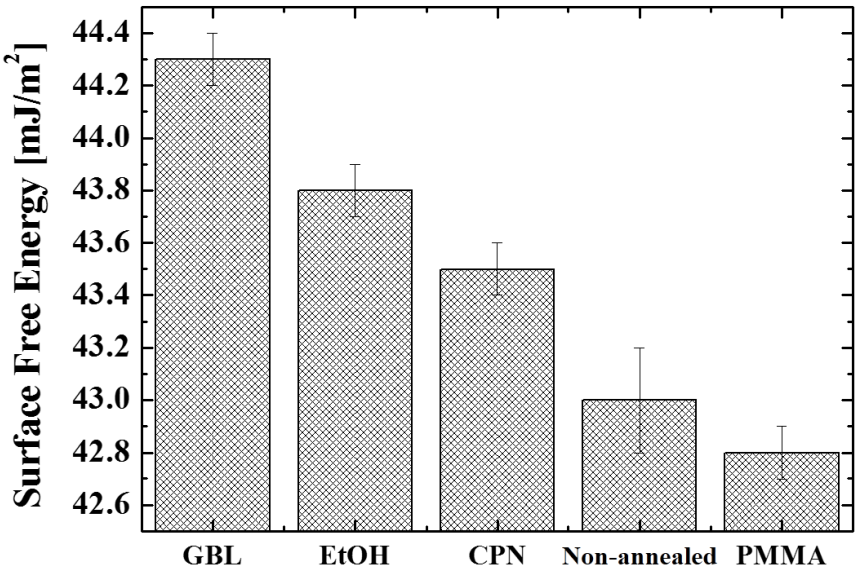

Figure 16. Solvent-vapor annealing effect on surface free energy for PMMA/SQ-CI (95/5) thin film prepared from cyclopentanone solution. GBL, EtOH and CPN show results of solvent-vapor annealing by γ-butyrolactone, ethanol and cyclopentanone, respectively. As references, non-annealed blend film and PMMA film were also shown (Non-annealed, PMMA).

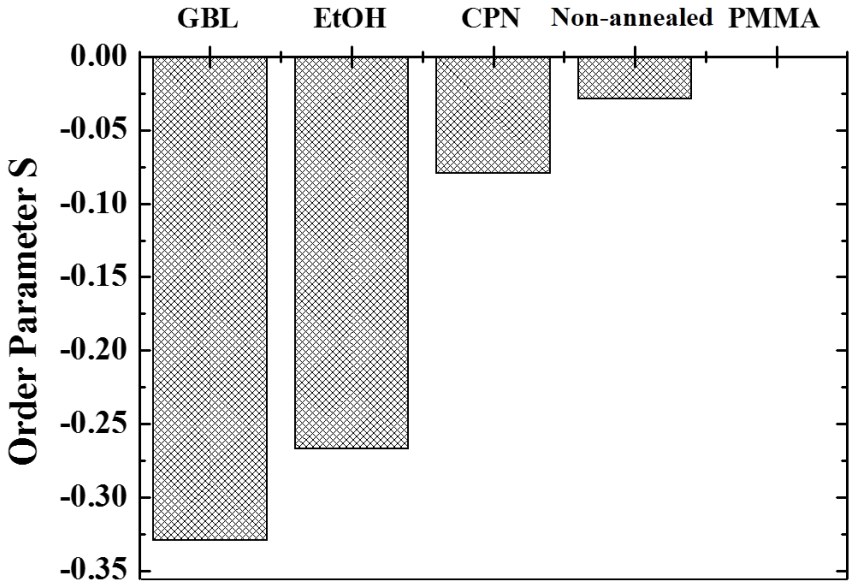

Figure 17. Solvent-vapor annealing effect of order parameter of PLC on PMMA/SQ-CI (95/5) thin film prepared from cyclopentanone solution. GBL, EtOH and CPN show results of solvent-vapor annealing by γ-butyrlactone, ethanol and cyclopentanone, respectively. As references, non-annealed blend film and PMMA film were also shown (Non-anneal, PMMA).

4.5 Conclusions

The silsesquioxane containing citraconimide (SQ-CI) was synthesized and investigated as a photoalignment layer for liquid crystals and as a model for the unification of two layers of a photoalignment and a protection layer. The PLC on the thin film of the SQ-CI single layer was aligned homogeneously in the wide range of LPUVL irradiation dose. The orientation direction of the PLC on the photoalignment layer was perpendicular to the LPUVL electric field. The slow axis of retardation for the photoalignment layer was perpendicular to LPUVL electric field. As a result of the calculations of anisotropic polarizability for model molecules using DFT, The unreacted citraconimide showed larger anisotropic polarizability than the photodimers and photo-radical product. Therefore, the polarizability along the LPUVL electric field decreased by LPUVL irradiation and the direction perpendicular to the LPUVL became the slow axis of the retardation.

Moreover, the unification of the photoalignment and protection layer was investigated by using PMMA/SQ-CI blend. The thin film prepared from γ-butyrolactone solution even in the composition of 95/5 was able to align the PLC in the wide range of thermal treatment temperature, while that prepared from cyclopentanone solution did not work as a photoalignment layer. We found that the surface enrichment of the SQ-CI in our

system was not able to explain the difference of surface free energy because the SQ-CI having higher surface free energy than PMMA. From the solvent-vapor annealing effect for surface enrichment of SQ-CI, the difference of affinity between the solvent and polymer played an important role to enrich SQ-CI to the surface during the spin-coating and drying processes. The fact is significant for both academic interests and industrial applications because the technique is quite easy and useful to control the surface component in a multicomponent system.

4-6. References

(1) Schadt M, Schmitt K, Kozinkov V, et al. Surface-Induced Parallel Alignment of liquid crystals by linearly polarized photopolymers. Jpn. J. Appl. Phys. 1992;31:2155-2164.

(2) Makita Y, Natsui T, Kimura S, et al. Photoalignment materials with high sensitivityto near UV light. J. Photopolym. Sci. Technol. 1998;11:187-192.

(3) Schadt M, Seiberle H, Schuster A. Optical patterning of multi-domain liquid-crystal displays with wide viewing angles. Nature 1996;381:212-215.

(4) Ichimura K, Suzuki Y, Seki T. Reversible change in alignment mode of nematic iquid crystals regulated photochemically by ‘command surfaces’ modified with an azobenzene monolayer. Langmuir 1988;4:1214-1216.

(5) Tie W, Jeong IH, Jang IW, et al. Reducing driving voltage and securing electro-optic reliability of in-plane switching liquid crystal display by applying polysulfone photoalignment layer with photo-reactive mesogens. Liquid Crystals. 2014;41:1057-1064.

(6) Kang H, Choi Y-S, Kang D, et al. Photoalignment behaviour on polystyrene films containing chalcone moieties. Liquid Crystals. 2015;42:189-197.

(7) Guo Q, Srivastava AK, Chigrinov VG, et al. Polymer and azo-dye composite: a photoalignment layer for liquid crystals. Liquid Crystals. 2014;41:1465-1472.

(8) Murai H, Nakata T, Goto T. Liquid crystal photoalignment layers made from aromatic bismaleimides. Liquid Crystals, 2002;29:669-673.

(9) Schadt M, Seiberle H, Schuster A, et al. Photo-Generation of Linearly Polymerized Liquid Crystal Aligning Layers Comprising Integrated Optical Patterned Retarders and Color Filters. Jpn. J. Appl. Phys. Part 1.1995;34 :3240-3249.

(10) Schadt M, Seiberle H, Schuster A, et al. Photo-Induced Alignment and Patterning of Hybrid Liquid Crystal Polymer Films on Single Substrates. Jpn. J. Appl. Phys. Lett. 1995;34:764-767.

(11) Broer DJ, Boven J, Mol GN, et al. In-situ photopolymerization of oriented liquid-crystalline acrylates, 3. Oriented polymer networks from a mesogenic diacrylate. Makromol. Chem. 1989;190:2255-2268.

(12) Broer DJ, Hikmet RAM, Challa G. In-situ photopolymerization of oriented liquid-crystalline acrylates, 4. Influence of a lateral methyl substituent on monomer and oriented polymer network properties of a mesogenic diacrylate. Makromol. Chem. 1989:190:3201-3215.

(13) Broer DJ, Mol GN, Challa G. In-situ photopolymerization of oriented liquid-crystalline acrylates, 5. Influence of the alkylene spacer on the properties of the mesogenic monomers and the formation and properties of oriented polymer networks. Makromol. Chem. 1991;192:59-74.

(14) Sabnis RW. Color filter technology for liquid crystal displays. Displays. 1999;20:119-129.

(15) Song JH, Lim YJ, Lee MH, et al. Electro-optic characteristics and switching principle of a single-cell-gap transflective liquid-crystal display associated with in-plane rotation of liquid crystal driven by a fringe-field. Appl. Phys. Lett. 2005;87:011108-011110.

(16) Jeong YH, Lim YJ, Jeong E, et al. Optimal pixel design for low driving, single gamma curve and single cell-gap transflective fringe-field switching liquid crystal display. Liquid Crystals. 2008;35:187-194.

(17) Chuang WP, Sheen YC, Wei SM, et al. Phase Segregation of Polymethylsilsesquioxane in Antireflection Coatings. Macromolecules. 2011;44:4872-4878.

(18) Prigogine I, Marechal J. The Influence of Differences in Molecular Size on the Surface Tension of Solutions. IV. J. Colloid Sci. 1952;7:122-127.

(19) Gaines Jr GS. Surface tension of polymer solutions. I. Solutions of poly(dimethylsiloxanes). J. Phys. Chem. 1969;73:3143-3150.

(20) Pan DH-K, Prest Jr WM. Surfaces of polymer blends: X-ray photoelectron spectroscopy studies of polystyrene/poly(vinyl methyl ether) blends. J. Appl. Phys. 1985;58:2861-2870.

(21) Geoghegan M, Jones RAL, Payne RS, et al. Lamellar structure in a thin polymer blend film. Polymer. 1994;35:2019-2027.

(22) Ton-That C, Shard AG, Daley R, et al. Effects of Annealing on the Surface Composition and Morphology of PS/PMMA Blend. Macromolecules. 2000;33:8453-8459.

(23) Ton-That C, Shard AG, Teare DOH, et al. XPS and AFM surface studies of solvent-cast PS/PMMA blends. Polymer. 2001;42:1121-1129.

(24) Frisch MJ, Trucks GW, Schlegel HB, et al. Gaussian09, Revision D.01. Gaussian, Inc., Wallingford CT, 2009.

(25) Becke AD. Density-functional thermochemistry. III. The role of exact exchange. J. Chem. Phys. 1993;98:5648-5652.

(26) Stephens PJ, Devlin JF, Chabalowski CF, et al. Ab initio calculation of vibrational absorption and circular dichroism spectra using density functional force fields. J. Phys. Chem. 1994; 98:11623-11627.

(27) Yanai T, Tew DP, Handy NC. A new hybrid exchange-correlation functional using the Coulomb-attenuating method (CAM-B3LYP). Chem. Phys. Lett. 2004;393:51-57.

(28) Put J, Schryver FC. Photochemistry of Nonconjugated Bichromophoric Systems. J. Am. Chem. Soc. 1973;10:137-145.

(29) Sonntag J, Knolle W, Naumov S, et al. Deprotonation and Dimerization of Maleimide in the Triplet State: A Laser Flash Photolysis Study with Opticaland Conductometric Detection. Chem. Eur. J. 2002;8:4199-4209.

(30) Decker C, Bianchi C. Photocrosslinking of a maleimide functionalized polymethacrylate. Polym. Int. 2003;52:722-732.

(31) Lorentz HA. On the Relation between the Velocity of Transmission of Light and the Density of a Body. Ann. Physik Chemie. 1880;9:641-665.

(32) Lorenz L. The Index of Refraction Ann. Physik Chemie. 1880;11:70-103.

(33) de Gennes PG. Scaling Concept of Polymer Physics. Ihaca:NY;1979.

(34) Hansen, CM. Hansen Solubility Parameters: A User's Handbook, Second Edition. Boca Raton:Florida;2007.

Chapter 5

Anisotropic dewetting of polymerizable liquid crystals on a photoalignment layer

5-1. Abstract

Dewetting phenomenon of thin film of polymerizable liquid crystals (PLC) on a photo-alignment layer was investigated. The dewetting behavior of thin films changed with the film thickness of the PLC. At thinner film, the dewetting proceeded isotropically with a round-shape. However, at thicker film, the dewetting pattern of the PLC changed to anisotropic shape like an elongated ellipse with large aspect ratio. The long axis of dewetting pattern linearly evolved with time. In addition, a rim of dewetting pattern thickened at the edge of long axis. However, an edge thickness of the film at the short axis did not change and comb-like structures along the short axis were formed. These features suggested that the flow direction of PLC molecules was approximately axis-selective in the case of anisotropic dewetting. Based on the results of dewetting behavior of simple liquid crystals which have nematic and smectic phase (5CB, 8CB) at room temperature, we concluded that anisotropic dewetting of thin film occurs in smectic phase of liquid crystals.

5-2. Introduction

Dewetting phenomenon of thin solid or liquid films consisting of various materials have been well reported. The stability of thin film is important for both industrial applications and fundamental interests. Although a thicker film is stabilized by gravitational force, thinner film becomes unstable in some cases due to interfacial interactions which mainly dominates the stability of thin film in disregard of the gravitational force[1]. The dewetting in some films of glycerin-water, polystyrene and polydimethylsiloxane occurred by nucleation and growth[2-4]. In addition, the dewetting by spinodal decomposition has also been reported[5-7]. These dewetting phenomena generally evolved isotropically with round-shape. These existing researches have been investigated for isotropic films such as polystyrene and polydimethylsiloxane. In this study, we investigated the dewetting behavior of an uniaxially-oriented film of polymerizable liquid crystals (PLCs) on a photoalignment layer consisting of silsesquioxane containing citraconimide (SQ-CI). The oriented and random-oriented PLC thin films on the SQ-CI layers showed completely different dewetting behavior. We suggested that anisotropic dewetting of PLC thin film was attributed to the smectic structure in thin film.

5-3. Experimental Section

Materials

Citraconic anhydride, cyclopentanone, n-hexane and toluene were purchased from Tokyo Chemical Industry Co., Ltd. 3-aminopropyltriethoxysilane was obtained from JNC Corp. As a polymerizable liquid crystal (PLC), LC242 and CBHA were obtained from BASF Japan Ltd. and JNC Petrochemical Corp., respectively. As a low molecular

weight liquid crystal, 4-cyano-4'-pentylbiphenyl (5CB) and 4-cyano-4'-octylbiphenyl (8CB) is purchased from Tokyo Chemical Industry Co., Ltd. Acrylic surfactant (Byk361N) was provided from Big Chemie Co. Ltd. As a photo-radical generator, Irgacure 907 was provided from BASF Japan Ltd. These reagents were used without further purification. The chemical structures of PLC were shown in Figure 1.

Synthesis of SQ-CI

As a photoalignment layer, photo-reactive silsesquioxane containing citraconimide (SQ-CI) was synthesized from citraconic anhydride and 3-aminopropyltriethoxysilane as previously reported[8]. The obtained SQ-CI was purified by the three cycles of the dissolution-reprecipitation technique using n-hexane. Weight-average molecular weight of SQ-CI was 3500 as determined by gel permeation chromatography. Chemical structure of SQ-CI is shown in Figure 1 (e).

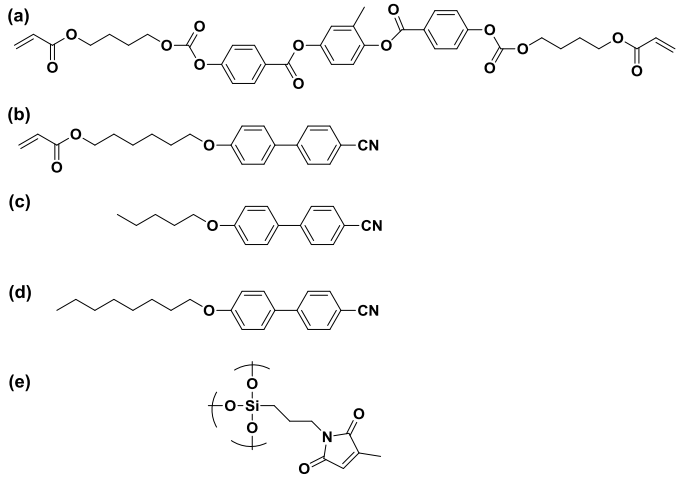

Figure 1. Chemical structures of (a) LC242, (b) CBHA, (c) 5CB, (d) 8CB and (e) SQ-CI.

Preparation of PLC solution

The composition of PLC was LC242 / CBHA / Irgacure 907 / Byk361N (67/33/3/1) in weight. Two PLCs were blended in equimolar ratio. The sample preparation of PLC in detail was as follows. As PLCs, the mixture of 1.000 g of LC242 (1.42 mmol) and 0.4948 g of CBHA (1.42 mmol) was diluted with 13.99 g of toluene and 0.0448 g of photo-radical generator (Irgacure 907) and 0.0149 g of surfactant (Byk361N) were added to the solution. The solution of PLC was finally filtrated through a PTFE membrane filter (average pore size : 0.2 μm).

Measurements

The thin films of the SQ-CI and the PLC were prepared by a spin-coater (1H-DX, Mikasa Co., Ltd.) on glass substrates (40 mm square, 0.7 mm thickness, EagleXG). Film thicknesses of the thin films were measured by an ellipsometer (SA-101, Photonic Lattice Inc.) or a profilometer (alpha-step P-16, KLA-Tencol Corp.). The films after spin-coating were dried off on a hot-plate. Linearly polarized ultraviolet light (LPUVL) obtained by xenon lamp (300W) with a Al wire-grid polarizer and a cutoff filter below 300nm was exposed to the SQ-CI thin film for 60 s, in order to generate an anisotropic surface of the SQ-CI thin film. An ultraviolet-visible-near infrared spectrometer (V-7200, Jasco. Co., Ltd.) was used for evaluation of UV-vis spectra and polarized UV-vis spectra. A polarized optical microscope (POM) (BX60, Olympus Corp.) was used for morphology observation of samples. Morphologies of dewetting pattern were confirmed by scanning electron microscope (SEM) (SM-200, Topcon Corp.). GPC measurements were carried out using SHIMADZU prominence GPC system equipped

with polystyrene gel columns. Tetrahydrofuran was used as eluent after calibration with polystyrene standards.

Calculations

To find optimized molecular structures and determine the transition dipole moment of CBHA, density functional theory (DFT) calculations for model compounds were carried out using Gaussian 09 Revision D.01(Gaussian Inc.)[9]. Geometry optimization was executed using CAM-B3LYP/6-311++G(d,p) and the excited state calculation was carried out by time-dependent DFT[10, 11].

5-4. Results and discussion

As a first step, dewetting behavior of liquid crystalline thin film with random orientation was observed by POM. A 5 wt% of SQ-CI solution in cyclopentanone was spin-coated on a glass substrate and baked at 190 °C for 5 min. The SQ-CI thin film was prepared without the LPUVL-irradiatin, in order not to align the PLC uniformly. The PLC solution was spin-coated on the SQ-CI thin film. The random-oriented PLC thin film was prepared in this way. The PLC layer with random homogeneous alignment was isotropically dewetted on the thin film of SQ-CI with time at room temperature as shown in Figure 2. In the early stage of dewetting, some circular holes formation in the PLC thin film was observed. This dewetting behavior was the same as the isotropic dewetting of polystyrene (PS) or polydimethylsiloxane (PDMS) thin film[4,5]. However, time evolution of isotropic dewetting showed the uniform pattern consisting of minute droplets of the PLC and the behavior was different from the pattern of PS or PDMS.

Dry patches, which is circular dewetting pattern, were formed at an initial period and were not developed with time. This is presumably able to explain that the dry patch was formed by nucleation of hole due to dust or local thinning of the film in the solvent evaporation process.

As the second step, the oriented PLC thin film was prepared as shown below. The photoalignment layer was prepared from 5 wt% of SQ-CI solution in cyclopentanone by

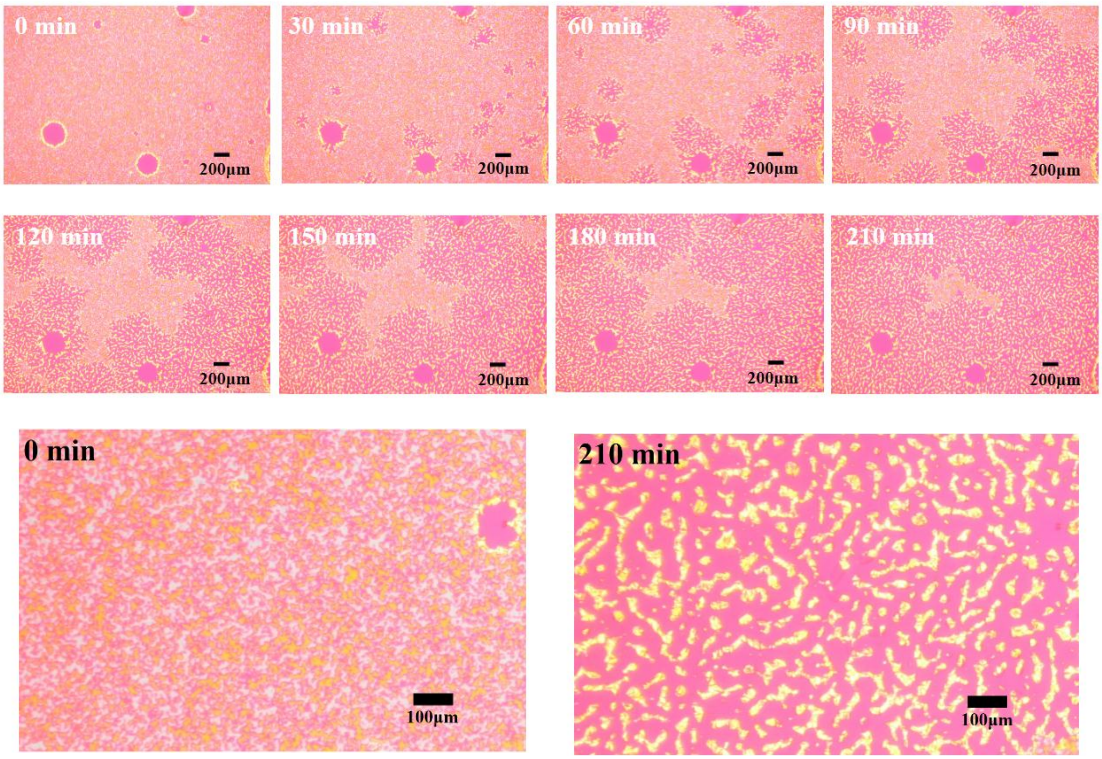

Figure 2. Time evolution of isotropic dewetting for PLC thin film on non-irradiated SQ-CI observed by POM with sensitive tint plate (530 nm). Observation of dewetting is performed at room temperature.

spin-coating on a glass substrate. The SQ-CI thin film was irradiated by linearly polarized ultraviolet light (LPUVL) for 60 s through a cut-filter below 300 nm, after the thermal treatment at 190 °C for 5 min. Subsequently, the PLC solution was spin-coated on the LPUVL-irradiated SQ-CI thin film and dried at 80 °C for 1 min for evaporation of solvent. As shown in Figure 3, the oriented PLC thin film was anisotropically dewetted as distinct from the PLC thin film with random orientation. In the dewetting edge at both side of long axis of dewetting pattern, it appeared that the PLC aggregated and formed rims, which was droplet-like structure of the PLC. The rim at long axis of dewetting pattern enlarged with time until the rims collided each other and ceased to evolve. On the other hand, the edge at short axis of dewetting pattern formed comb-like structures parallel to the short axis of dewetting. Resultingly, the flat film of PLC disappeared and comb-like structures remained on the SQ-CI thin film.

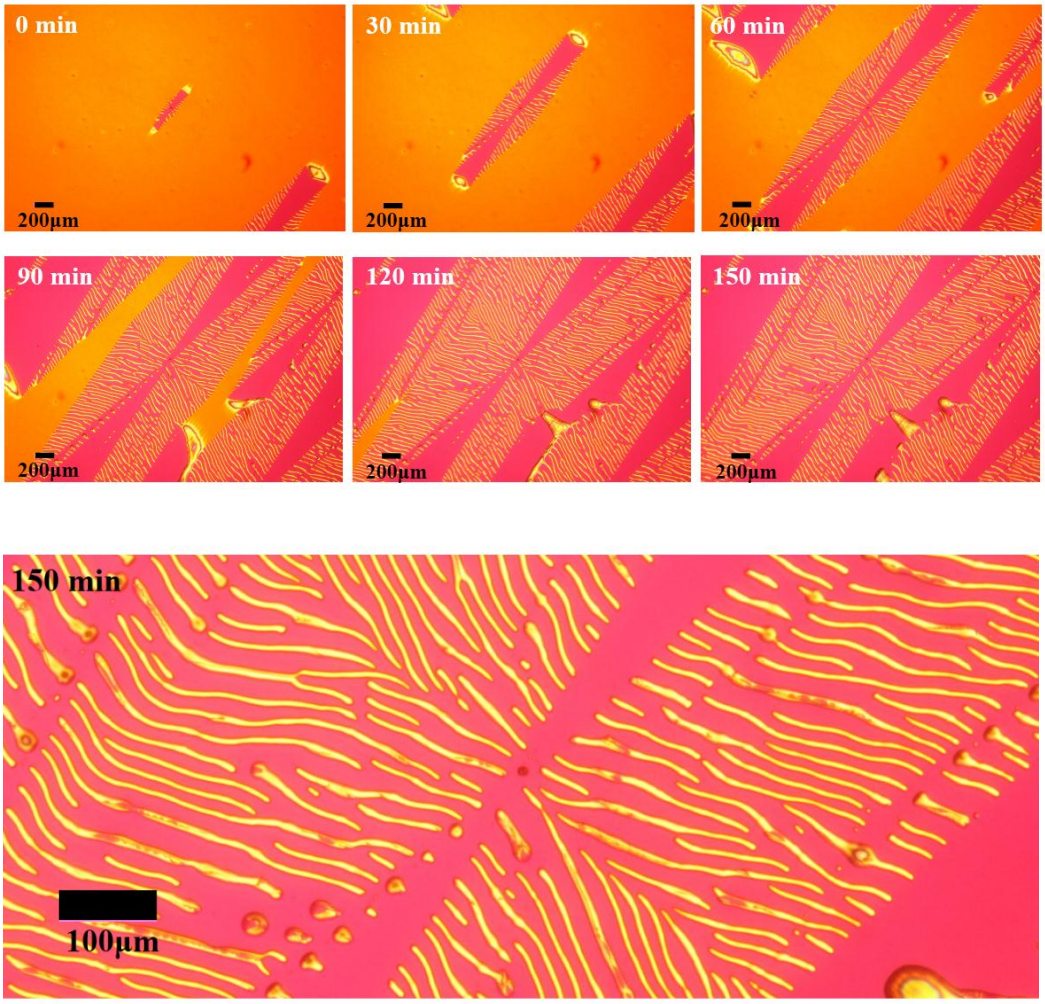

Figure 3. Time evolution of anisotropic dewetting for oriented PLC thin film on SQ-CI observed using POM with sensitive tint plate (530 nm).

The time evolution of anisotropic dewetting was plotted with time as shown in Figure 4. The dewetting length was defined as an entire length of long axis or short axis of dewetting pattern. The dewetting length linearly evolved with time at both long axis and short axis of dewetting pattern. This behavior of linear growth with time is the same as polydimethylsiloxane liquid film[4].

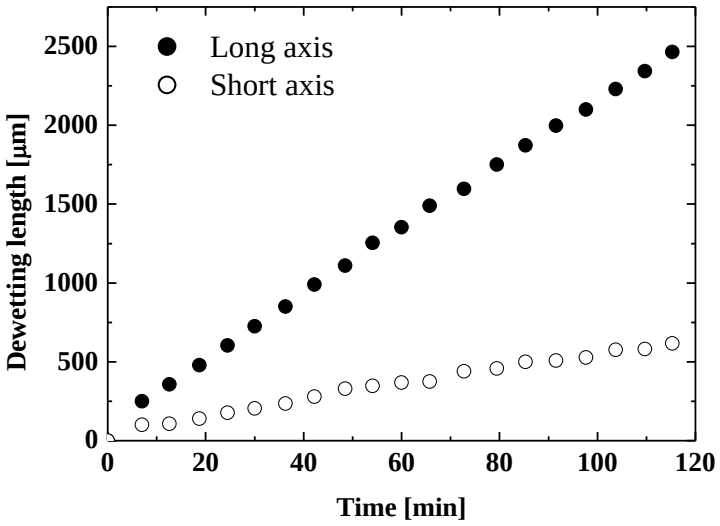

Figure 4. Time evolution of anisotropic dewetting of oriented PLC thin film on SQ-CI thin film. Filled and open circle show long and short axis of dewetting pattern.

An aspect ratio of dewetting pattern was also shown in Figure 5. The aspect ratio was defined by a value of dewetting length at long axis divided by that at short axis. The aspect ratio slightly increased with time.

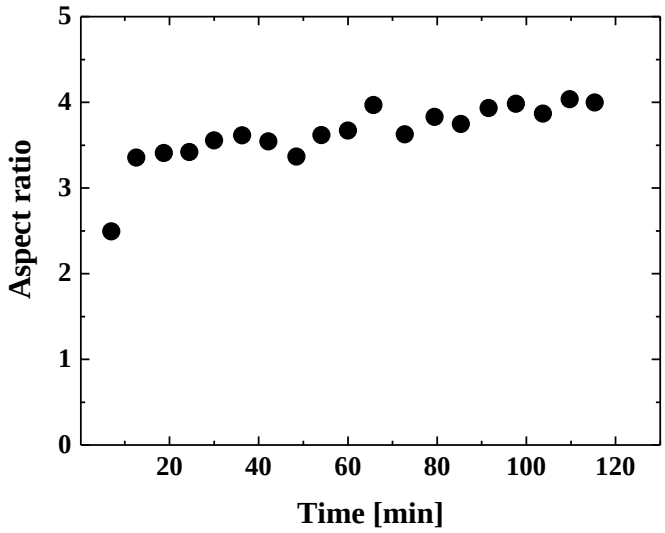

Figure 5 Time evolution of aspect ratio of anisotropic dewetting pattern.

From the observed POM image (Figure 3), white-tinged regions presumably have different film thickness of the PLC from initial film thickness because the tinge of color reflects magnitude of retardation. To reveal the actual image of the dewetting pattern, the sample after the photo-curing to fix the morphology of dewetting was observed using SEM as shown in Figure 6. The edge at long axis of dewetting pattern was apparently thicker than the initial film thickness (Figure 6 (a)). However, the edge at short axis of dewetting pattern appeared as flat without the rim and the comb-like structures were formed (Figure 6 (b)).

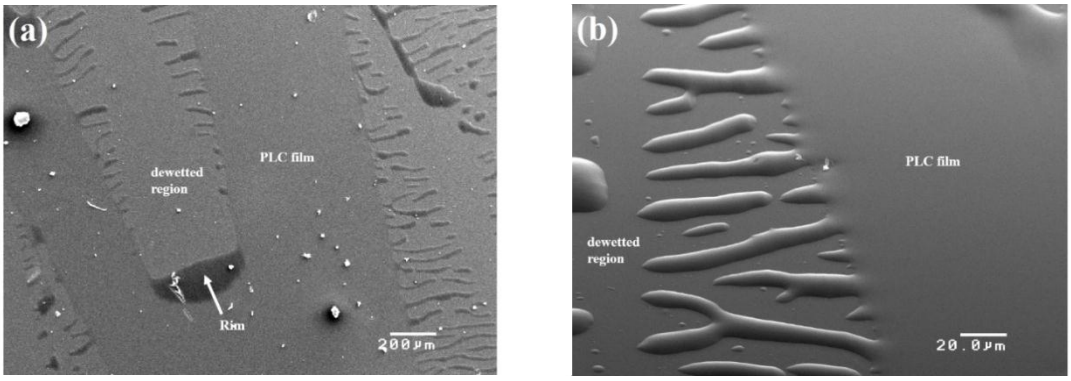

Figure 6. SEM image of anisotropic dewetting patterns;
(a) overall view of anisotropic dewetting and (b) 20 μm scale near edge of short axis of dewetting pattern were shown.

Subsequently, the accurate film thicknesses of anisotropic dewetting pattern were measured by the profilometer after photo-curing of PLC thin film in the process of anisotropic dewetting as shown in Figure 7. Thickness of the rim was approximately 25 μm in this sample (Figure 7 (b)). Therefore, the dewetted volume of PLC aggregated to the rim at the long axis of anisotropic dewetting. However, at the short axis of anisotropic dewetting, the thickness of PLC thin film at the edge was equal to the initial thickness of PLC thin film (Figure 7 (d)). This fact means no rim formation at the short

axis of anisotropic dewetting. Furthermore, we clearly revealed that the dewetting to the short axis proceeded due to the aggregation of dewetted-PLC to the comb-like pattern at the short axis, as shown in Figure 8. From these results, we concluded that the flow direction of PLC molecules was only parallel to the long axis of dewetting pattern. The PLC did not flow to the direction of short axis.

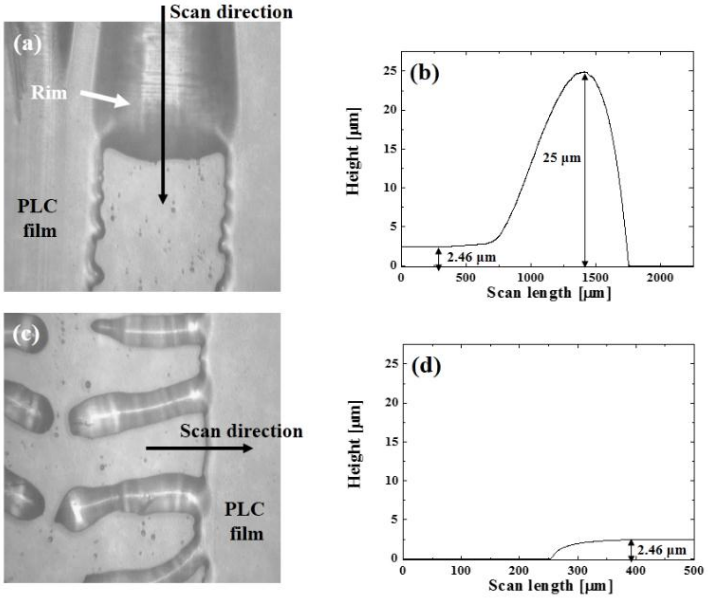

Figure 7. Thickness of anisotropic dewetting pattern;
Image at rim (a), film thickness at rim (b), image at edge of short-axis (c), and film thickness at edge of short-axis (d) were measured by profilometer. In this case, initial film thickness of PLC thin film before dewetting is 2.46 μm.

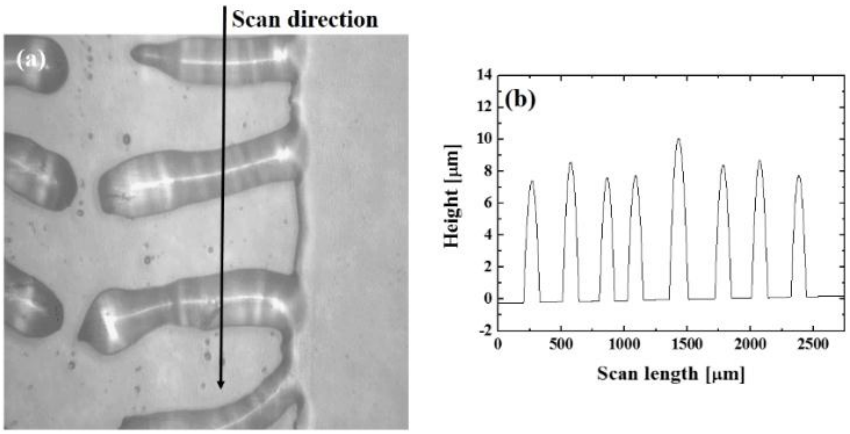

Figure 8. Thickness of comb-like pattern;
Image at comb-like pattern (a), and film thickness at comb-like pattern (b) were measured by profilometer. Initial film thickness of PLC thin film before dewetting is 2.46 μm.

The relationship between the orientation direction of PLC molecules and the dewetting direction was revealed by using polarized UV-vis spectroscopy. As a result of TD-DFT calculation by CAM-B3LYP/6-311++G(d,p) level, transition dipole moment of CBHA was parallel to the long axis of cyano-biphenyl mesogen. Therefore, the direction of higher absorbance in the polarized UV-vis spectra showed the orientation direction of mesogen in the homogeneous alignment of the PLC. As shown in Figure 9, the orientation direction of the PLC mesogens was perpendicular to the long axis of dewetting.

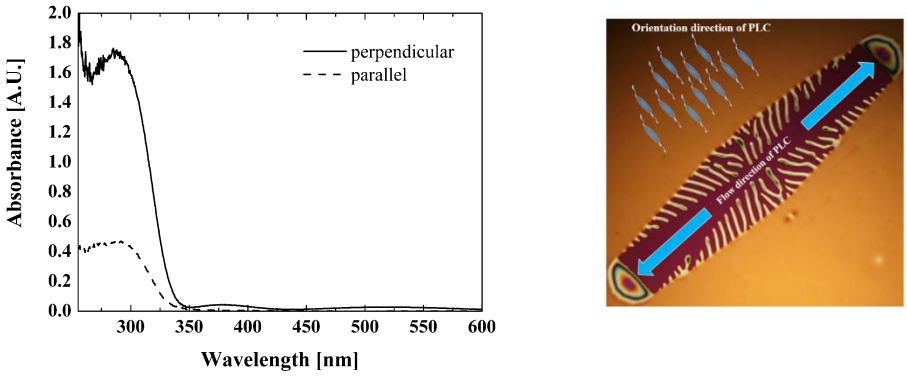

Figure 9. Polarized UV-vis spectra of PLC on SQ-CI thin film. Notation of "parallel" and "perpendicular" show absorbances parallel and perpendicular to long axis of dewetting pattern, respectively (left). Schematic of relation between PLC orientation direction and dewetting direction is shown (right).

In the case of thin film composed of LC242 or CBHA without the blend, the dewetting behavior is isotropic as with the ultrathin film of polystyrene or liquid film of polydimethylsiloxane, even though LC242/CBHA blend was dewetted anisotropically.

To reveal the influence on liquid crystalline phase, 5CB and 8CB which have well-defined phase sequence were evaluated as a model system. 5CB and 8CB show nematic and smectic phases at room temperature, respectively. These LCs were prepared as 10 wt% solution in toluene with 1 phr (parts per hundred resin) of surfactant, and spin-coated on the LPUVL-irradiated or the non-irradiated SQ-CI thin film. Subsequently, the drying was executed at 80 °C for 1 min to remove the solvent. The dewetting behaviors of 5CB and 8CB thin films were observed by POM at room temperature. As shown in Figure 10, 5CB in nematic phase was dewetted isotropically, regardless of homogeneous orientation (Figure 10 (a)) or random orientation (Figure 10 (b)). However, 8CB in smectic A phase was dewetted anisotropically and 8CB with random orientation was dewetted isotropically with minute droplets as shown in Figure

11. This behavior of 8CB is similar to that of LC242/CBHA blend. From these results, we found that anisotropic dewetting of PLC thin film was attributed to smectic phase.

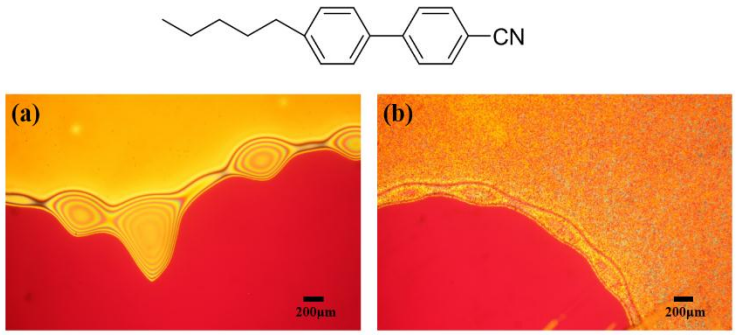

Figure 10. Isotropic dewetting behavior of 5CB thin film observed by POM with sensitive tint plate (530 nm). Oriented 5CB on LPUVL-irradiated SQ-CI (a), and random-oriented 5CB on non-irradiated SQ-CI (b) were shown. Observation of dewetting behavior was performed at room temperature.

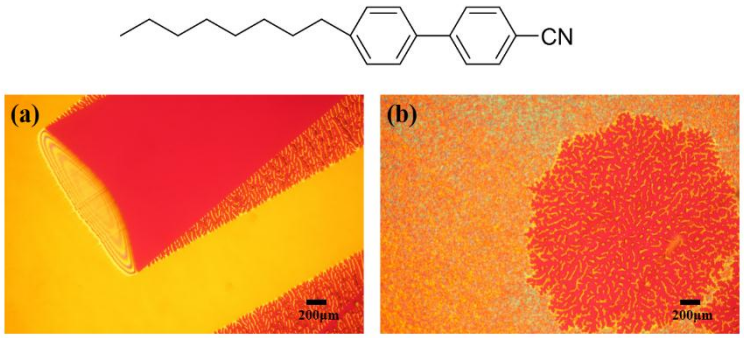

Figure 11. Anisotropic dewetting behavior of 8CB thin film obserbed by POM with sensitive tint plate (530 nm).
Oriented 8CB on LPUVL-irradiated SQ-CI (a), and random-oriented 8CB on non-irradiated SQ-CI (b) were shown. Observation of dewetting behavior was performed at room temperature.

To elucidate the reason of isotropic dewetting of thin film in nematic phase, viscous torque of the oriented PLC molecules was considered as described below. During the dewetting, the flow of PLC molecules and velocity gradient are assumed as described in Figure 12. This is a simple assumption as a shear flow[12, 13]. To specify the orientation

direction of the PLC, the director ***n*** of the PLC is described using θ and ϕ in Cartesian coordinate (Figure 13). Three alignment direction of the PLC for homeotropic alignment (Figure 13 (a)), homogeneous alignment of mesogens parallel to the flow direction (Figure 13 (b)), and homogeneous alignment perpendicular to the flow direction (Figure 13 (c)).

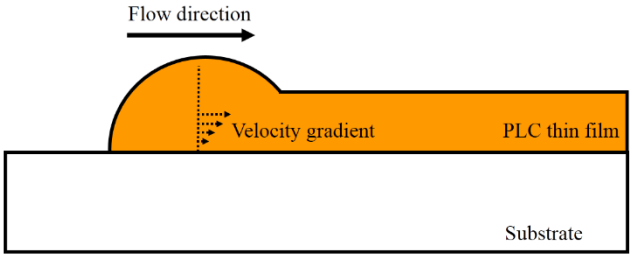

Figure 12. Schematic of dewetting.

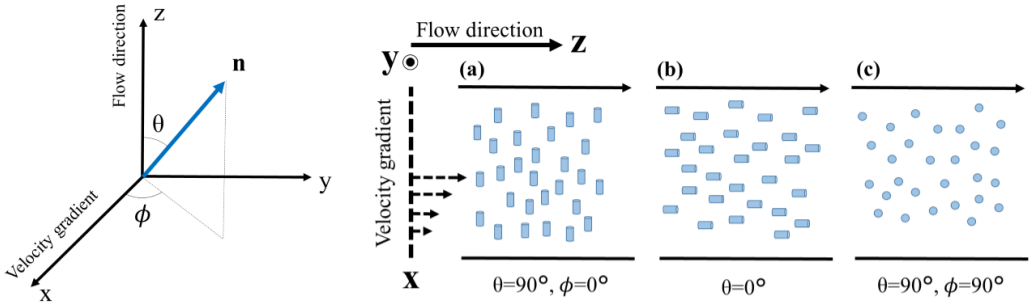

Figure 13. Coordinate of PLC director, flow direction and velocity gradient.

In this situation, viscous torque of liquid crystals is written as follows[14].

$$\Gamma^{\text{visc}} = -\gamma_1 \boldsymbol{n} \times \left(\frac{d\boldsymbol{n}}{dt} - \boldsymbol{\omega} \times \boldsymbol{n}\right) - \gamma_2 \boldsymbol{n} \times A\boldsymbol{n}$$

where γ_1 and γ_2 are viscous coefficient of rotating and nonrotating flow, respectively. $\boldsymbol{n}$ is director for the PLC, and $\boldsymbol{\omega}$ is vorticity. *A* is symmetric tensor component of velocity gradient, which is component of nonrotating flow. In Figure 13, the director $\boldsymbol{n}$ of the PLC is also described below.

$$\boldsymbol{n} = (\sin\theta\cos\phi, \sin\theta\sin\phi, \cos\theta)$$

When the director of PLC exists in xz-plane including the case of Figure 13 (a) and (b), viscous torque in shear plane around y axis is expressed below.

$$\Gamma^{\text{visc}} = -\frac{1}{2}\dot{\gamma}(\gamma_1 + \gamma_2 cos2\theta)$$

In contrast, when the director exists along y axis (Figure 13 (c)), viscous torque in shear plane Γ^{visc} is zero[14]. Therefore, the alignment in Figure 13 (c) do not undergoes viscous torque by shear flow. In addition, Frank free energy density of nematic phase is given below[15].

$$f_d = \frac{1}{2}K_{11}(\nabla \cdot \boldsymbol{n})^2 + \frac{1}{2}K_{22}(\mathbf{n} \cdot \nabla \times \boldsymbol{n})^2 + \frac{1}{2}K_{33}(\boldsymbol{n} \times \nabla \times \boldsymbol{n})^2$$

Where K_{11}, K_{22}, and K_{33} are elastic constants of PLC corresponding to the director deformations of spray, twist, and bend, respectively. Therefore, the deformations of director by viscous torque derived from shear flow increases the elastic free energy of the PLC.

Although the nematic PLC is allowed to flow to the direction of molecular short axis in consideration of the restoring force caused by minimizing the elastic free energy, the

thin film of PLC in nematic phase actually flows isotropically. Therefore, it is considered that the restoring force derived from the deformation of director in nematic phase is sufficiently small and able to be negligible for the dewetting.

On the other hand, free energy density for smectic phase is also written below.

$$f_d = \frac{1}{2}B\left(\frac{\partial u}{\partial z}\right)^2 + \frac{1}{2}K_{11}\left(\frac{\partial^2 u}{\partial x^2} + \frac{\partial^2 u}{\partial y^2}\right)^2$$

where, B and u are an elastic constant and displacement, respectively. The first term shows the contribution by the deformation of layer spacing in smectic phase and the second term indicates the contribution by spray deformation of director which is allowed in smectic phase. In smectic phase, large restoring force works when the layer spacing changes, and then, it is assumed that PLC is able to flow to the direction parallel to the layer because the order of layer direction in smectic phase is liquid-like. Considering this point, anisotropic dewetting in smectic phase presumably occurred by the confinement due to large restoring force derived from the deformation of smectic layer spacing by viscous torque of shear flow, in order to retain smectic layer spacing. In addition, the reason that the minute droplets pattern of PLC was formed in the case of isotropic dewetting (Figure 2) was as explained below. In random orientation of PLC, localized domains were formed and the PLC was aligned in each domain. Although the dewetting direction of PLC in the domain was one direction, the rims of anisotropic dewetting collide with each other because the orientation direction of each domain is random. Therefore, the minute droplets of PLC were formed everywhere on the SQ-CI thin film.

5-5. Conclusions

The dewetting behavior of the PLC thin film on the SQ-CI thin film was investigated. On the non-irradiated SQ-CI thin film, random-oriented PLC was isotropically dewetted and minute droplets were formed. However, on the LPUVL irradiated SQ-CI thin film, the PLC was anisotropically dewetted. The long axis of dewetting pattern formed rims. The rims linearly evolved with time in common with the rim behavior of isotropic dewetting such as polystyrene ultrathin film or polydimethylsiloxane liquid film as already reported by other authors. The rims were formed at edge of long axis of dewetting pattern, while no rims were found at the edge of short axis. At the short axis of dewetting pattern, comb-like structures were also formed along the short axis. This fact indicated that the PLC molecules flowed only to the direction of long axis of dewetting pattern. As a result of dewetting behavior of 5CB and 8CB thin film, which show nematic and smectic phase at room temperature, we found that anisotropic dewetting is attributed to smectic phase of liquid crystals. The flow direction of liquid crystals is confined by large restoring force derived from retaining the layer spacing in smectic phase.

5-6. References

[1] de Gennes, P. G. *Rev. Mod. Phys.* **1985**, 57, 827.

[2] Haroon, S. K.; Scriven, L.E. Dewetting:Nucleation and Growth of Dry Regions. *Chem. Eng. Sci.* **1991**, 46, 519-526.

[3] Sharma, A.; Ruckenstein, E. Dewetting of Solids by the Formation of Holes in Macroscopic Liquid Films. J. Colloid Interface Sci.133, 358 (1989).

[4] Redon, C.; Brochard-Wyart, F.; Rondelez, F. Dynamics of Dewetting. *Phys. Rev. Lett.* **1991**, 66, 715-719.

[5] Reiter, G. Dewetting of Thin Polymer Films. *Phys. Rev. Lett.* **1992**, 68, 75-80.

[6] Reiter, G. Unstable thin polymer films: rupture and dewetting processes. *Langmuir*. **1993**, 9, 1344-1351.

[7] Reiter, G. Dewetting as a Probe of Polymer Mobility in Thin Films. *Macromolecules*. **1994**, 27, 3046-3052.

[8] Kimura, Y.; Kuboyama, K.; Ougizawa, T. manuscript in preparation

[9] Frisch MJ, Trucks G.W, Schlegel HB, et al. Gaussian09, Revision D.01. Gaussian, Inc., Wallingford CT, 2009.

[10] Becke AD. Density-functional thermochemistry. III. The role of exact exchange. J. Chem. Phys. 1993;98:5648-5652.

[11] Yanai T, Tew DP, Handy NC. A new hybrid exchange-correlation functional using the Coulomb-attenuating method (CAM-B3LYP). Chem. Phys. Lett. 2004;393:51-57.

[12] Redon C, Brzoska JB, Brochard-Wyart F. Dewetting and slippage of microscopic polymer films. *Macromolecules.* **1994**, 27, 468-471.

[13] Merabia S, Avalos JB. Dewetting of a Stratified Two-Component Liquid Film on a Solid Substrate. *Phys. Lev. Lett*. **2008**, 101, 208304]

[14] Pieranski P, Guyon E. Instability of certain shear flows in nematic liquids. *Phys. Rev. A.* **1974**, 9, 404-417.]

[15] Frank, F. C. On the Theory of Liquid Crystals. *Discuss. Faraday Soc.* **1958**, 25, 19-28.

Chapter 6

General Conclusions

General Conclusions

In this study, the mechanism of photo-induced alignment of polymerizable liquid crystals (PLCs) based on the axis-selective photoreactions of the photoreactive materials and the orientation behavior of PLCs thin film were investigated.

In Chapter 2, photo-reactive 2,6-bis(4-azidobenzylidene)-4-methyl-1-cyclohexanone (bisABmC) as a bis-azide was blended with a polymer containing acryloyl groups in the side chain (GH-1203). The GH-1203/bisABmC blend was evaluated as a photo-alignment layer for PLCs, and then it was confirmed that it worked well. In this system, in-plane switching of the orientation direction of PLCs was observed, which depended only on irradiation dose of linearly polarized ultraviolet light (LPUVL). The LPUVL irradiation time dependence of FT-IR spectra indicated that the azide group of bisABmC rapidly reacted with the acryloyl group of GH-1203 and gradual reaction of the bisBC unit in the bisABmC also progressed simultaneously. Moreover, the slow axis of retardation of the photo-alignment layer also switched at the same time as the in-plane switching of the orientation direction of PLCs, which means the PLCs aligned along the slow axis of retardation of the photoalignment layer regardless of the in-plane switching. In comparison to the calculated anisotropic polarizabilities of model molecules, it was suggested that photo-reaction of the bisBC led to lower anisotropic polarizability regardless of the photo-isomerization, the photo-dimerization or the other reactions accompanied by the bond cleavage of C=C. Therefore, the reversion of the slow axis of retardation suggested that both the photo-reaction of azide in the early stage of irradiation and that of bisBC unit in the late stage of irradiation dominated the slow axis of retardation.

In Chapter 3, to improve thermal durability of the photo-induced anisotropy in the photo-alignment layer, the photo-reactive polymers containing bisBC unit in the main chain were synthesized by a simple method and evaluated as a photo-alignment layer for the PLCs and a liquid crystalline polymer. These polymers were able to align the PLCs homogeneously and have thermal durability caused by thermal reaction of azide and acrylate at the polymer tail. In these systems, the photodimerization of the bisBC occurred apparently because the polymers after the LPUVL-irradiation was insoluble to cyclopentanone. In addition, the polymers aligned the PLCs perpendicular to the LPUVL eletric field. The orientation direction of the PLCs was also parallel to the slow axis of retardation of the photo-alignment layer and the direction can be explained by the same mechanism described in Chapter 2.

In Chapter 4, to unite photoalignment layer and protection layer by polymer blending for reducing cost and number of processes in manufacuturing, silsesquioxane containing citraconimide (SQ-CI) as a photoalignment material was synthesized and was blended with poly(methyl methacrylate) (PMMA). A photo-aligning material needs to be enriched to the surface of the blend film for aligning the PLCs. In this study, we did not use low surface free energy component for enhancing the surface enrichment because the resultant low surface free energy tends to cause a failure of recoating of PLCs on the film. Thus, we investigated a polymer blend of PMMA and SQ-CI which have similar surface free energy. The blend film of PMMA/SQ-CI prepared from cyclopentanone solution was not able to align the PLCs. However, the blend film prepared from γ-butyrolactone solution enabled to align the PLCs. The SQ-CI was enriched to the surface of the blend film prepared only from γ-butyrolactone solution, although the SQ-CI has higher surface free energy than PMMA. As a result of evaluation for solubility of PMMA into the solvents

and solvent-vapor annealing effect on this system, it was suggested that the difference of affinity between polymer and solvent presumably played important role for surface enrichment of SQ-CI in the blend. This method is simple and useful for surface-segregating any components which do not necessarily show lower surface free energy.

In Chapter 5, a distinctive dewetting phenomenon of the PLCs thin film on the photoalignment layer was found. The thin film of PLCs on the photo-alignment layer anisotropically dewetted at certain film thickness with the shape of elongated ellipse. The edge of long axis of dewetting pattern formed a rim. The rim formation has been also commonly observed in isotropic dewetting of polystyrene and dimethylsiloxane. However, the short axis of dewetting pattern formed comb-like structure. From the polarized UV-vis spectroscopy to determine the orientation direction of PLCs, the PLCs flowed only to the direction of molecular short axis. In the systems of 5CB and 8CB as simple models of nematic and smectic A phase at room temperature, the anisotropic dewetting occurred only in smectic A phase. Based on the dewetting behaviors of 5CB and 8CB, it is considered that the dewetting mechanism of PLC was able to be explained that the flow to the direction perpendicular to the layer spacing in smectic pahse was confined by large restoring force derived from the change of the smectic layer spacing. The spontaneous self-assembly attributed to thin film instability is interesting in fundamental and industrial aspects. Further researches will open the way for controlled anisotropic dewetting available as a bottom-up method for creating fine structures.

Acknowledgments

My warmest and sincere gratitude and appreciation is expressed to Professor Toshiaki Ougizawa for accepting me as his student and for his unfailing assistance, encouragement and guidance given to me throughout my research which led to my successful graduation.

I express my deepest appreciation to Dr. Keiichi Kuboyama, an assistant professor in our laboratory, for his constant assistant in helping with the instrumentation, providing fruitful and constructive discussions and enlightening criticisms.

I wish to thank Professor Shinji Ando and Tomohiro Okada, doctoral course student in Ando laboratory, for their assistance on infrared spectroscopy, and Dr. Wataru Takarada, an assistant professor in Kikutani laboratory, for his assistance on Raman spectroscopy.

I would like to convey my gratitude to all my colleagues of Ougizawa laboratory for their help given to me during my stay at Tokyo Institute of Technology.

I would like to thank JNC petrochemical corporation for giving me this opportunity to undertake my doctoral study at Tokyo Institute of Technology.

Finally, I would also like to thank my wife, Keiko and my daughter, Shisui for their continued supports and encouragement throughout the duration of my study, especially in times of distress.

Tokyo Institute of Technology

February 2016

Yuki Kimura